University of Venda
Creating Future Leaders

International Journal of ENVIRONMENTAL IMPACTS

Management, Mitigation and Recovery

WIT PRESS

Volume 5, Number 4, 2022

Objectives

The **International Journal of Environmental Impacts** provides a forum to discuss the numerous environmental problems present in modern society and their impacts, taking into account scientific, economic and social issues. One important consideration is the way in which they affect the search for sustainability.

The Journal encourages interdisciplinary communication on all issues related to environmental impacts. There is a need to bridge the gap between the broad spectrum of economic and socio-political disciplines and specialists in engineering and physical, biological, environmental and health sciences, amongst others.

The publication discusses whether some forms of development are compatible with environmental protection, particularly in cases of possible serious contamination and toxicity. The management of air, water and soil contamination is one of the most challenging issues facing the international community. A major cause of concern are the impacts of waste on health and the environment.

The Journal provides a platform for researchers and professionals involved in Environmental Impacts to exchange knowledge and gain an insight into the state of the art in the current technologies, methodologies and solutions.

International Journal of ENVIRONMENTAL IMPACTS

Management, Mitigation and Recovery

Volume 5, Number 4, 2022

WIT PRESS
Southampton, Boston

PUBLICATION AND OPEN-ACCESS FEE

WIT Press is committed to the free flow of information to the international scientific community. To provide this service, the Journals require a publication fee to be met by the authors or the research funding bodies for each paper published. The fee in this Journal is US$950 per published article of up to 15 pages (including references and tables) and is payable upon acceptance. Overly long articles, if accepted under peer review, may be subject to an additional US$65 per extra page. Once published the paper will then be Open Access, i.e. immediately and permanently free for everybody to read and download. Discounted publication fee available for journal subscribers.

FREQUENCY AND FORMAT

The **International Journal of Environmental Impacts** will be published in four issues per year in colour. All issues will be supplied to subscribers in paper format (ISSN: 2398-2640).

SUBMISSIONS

The **International Journal of Environmental Impacts** is a refereed journal. In order to be acceptable for publication submissions must describe key advances made in one or more of the topics listed on the right or others that are in-line with the objectives of the Journal.

If you are interested in submitting a paper please contact:

INTERNATIONAL JOURNAL OF ENVIRONMENTAL IMPACTS
WIT, Ashurst Lodge, Southampton, SO40 7AA, UK.
Tel: 44 (0) 238 029 3223, Fax: 44 (0) 238 029 2853
Email: journals@witpress.com

TYPES OF CONTRIBUTIONS

Original papers; review articles; short communications; reports of conferences and meetings; book reviews; letters to the editor; forthcoming meetings, and selected bibliography. Papers essentially of an advertising nature will not be accepted.

AUTHORS INSTRUCTIONS

All material for publication must be submitted in electronic form, in both the native file format and as a PDF file, and be PC compatible. The text area is 200mm deep and 130mm wide. For full instructions on how to format and supply your paper please go to:

www.witpress.com/authors/submit-a-journal-paper

SAMPLE COPY REQUEST

Subscribe and request your free sample copy online at: www.witpress.com/journals

SUBSCRIPTION RATES

2023: **International Journal of Environmental Impacts** Issues 1–4, Print copies US$950.00

- Environmental policies and planning
- Environmental assessment
- Development issues
- Sustainable development studies
- Environmental economics
- Social impact
- Policies and legislation
- Public engagement
- Communications issues
- Extreme events risk studies
- Climate change impact
- Emergency preparedness
- Flood risk studies
- Ecosystem modelling
- GIS and remote sensing applications
- Energy and the environment
- Food production and policies
- Solutions for nature
- Case studies
- Soil contamination
- Industrial waste management
- Hazardous waste
- Agricultural waste
- Waste management
- Water contamination
- Fresh and marine water quality
- Industrial water pollution
- Safety and security
- Air pollution
- Air pollution mitigation
- Industrial air pollution
- Transportation impacts
- Toxicity studies
- Pollution and public health
- Environmental health risk
- Water, sanitation and health
- Remediation
- Recovery and resilience

ISSN: 2398-2659 (on line) and ISSN: 2398-2640 (paper format)

Koji Tamai, Int. J. Environ. Impacts, Vol. 5, No. 4 (2022) 291–305

FOREST MANAGEMENT FOR THE FLOOD MITIGATION FUNCTION OF FORESTS

KOJI TAMAI
Forestry & Forest Products Research Institute, Japan

ABSTRACT

Paired catchment experiments is the method that estimates the change of runoff due to forest change by comparisons between runoff data from two or more adjacent catchments and evaluations the change of their relative relations between two periods when forest changes in catchments.

The increase in volume of maximum daily runoff due to forest degradation was estimated in three treatment catchments in Japan using paired catchment experiments. In one catchment, slope failure occurred and 20% of the catchment area became bare, after which maximum daily runoff increased by approximately 1.1-fold. In the two other catchments, slope failure did not occur, while maximum daily runoff increased by only 6–8 mm day^{-1}. This increase was irrespective of the rainfall volume. Slope failure and the transition to bare land were identified as causes of the degradation of the flood mitigation function.

The causes of slope failure were identified as inadequate forest management, such as clear-cutting in areas with high slope failure risk, simultaneous clear-cutting throughout a catchment, and delayed replanting after clear-cutting. Therefore, forest management strategies for the flood mitigation function of forests could include the avoidance of logging in locations with a high risk of slope failure, limits concerning the amount of logging, and prompt replanting after logging.

Keywords: clear-cutting, maximum daily runoff, paired catchment experiments, replanting.

1 INTRODUCTION

Slope failure prevention is important for maintaining the flood mitigation function of forests. Tamai [6] reviewed studies that used water movement process models to reproduce water movement in forested catchments; the report indicated that the flood mitigation functions of forests originate from forest soil. If forest soil is lost due to slope failure, increased runoff volume during floods can be anticipated. Furthermore, daily runoff was reported to increase due to various types of forest degradation. These conclusions have been obtained with analyses of observational data [8].

Tada [5] demonstrated the importance of the reinforcing effect on slope stability by tree root systems for slope failure mitigation. Based on the reinforcing effect, appropriate forest management strategies for slope failure mitigation have been proposed [7].

The aforementioned previous studies suggest that proper forest management would contribute to the flood mitigation function through the prevention of slope failures. However, the contributions of forest management to the flood mitigation function of forests have not been fully explored. Therefore, this report discusses degradation of the flood mitigation function of forests due to slope failure and suggests the appropriate forest management strategies for this flood mitigation function.

2 METHODS AND SITE DESCRIPTION

2.1 Paired catchment experiments

The runoff volume characteristics from forest catchments varies with many factors such as topography, geology and meteorology, in addition to forest conditions of vegetation and soil.

ISSN: 2398-2640 (paper format), ISSN: 2398-2659 (online), http://www.witpress.com/journals
DOI: 10.2495/EI-V5-N4-291-305

Among these factors, forest vegetation is relatively easy factor to modify artificially. Therefore, with the aim of improving the flood mitigation function by managing forest vegetation, attempts have been made to evaluate changes in flood mitigation function due to the only effects of forest conditions. Paired catchment experiments (Fig. 1) had been developed as the method for it [2]. In paired catchment experiments, runoff data from two or more adjacent catchments are compared to elucidate their characteristics. The influence of forest degradation can be evaluated based on the relative changes of runoff between two periods: a control period, during which forests in two or more catchments share a similar state, and a treatment period, when the forest in a control catchment is healthy while the forest in a treatment catchment has been degraded. Single catchment experiments, which compares the runoff volume from one catchment between a control period and a treatment period, cannot eliminate the effects of different meteorological factors from year to year. In addition, the parallel catchment experiments, which compares the runoff volume observed in the same water year from a control catchment and a treatment catchment, cannot eliminate the effects of different topography and geology between catchments. The paired catchment experiments is a method of excluding the effects of weather, topography and geology, and evaluating only the effects of forest conditions. This report presents the results of analyses of maximum daily runoff during each water year, as an index of the flood mitigation function, and the minimum daily runoff during each water year.

Previous studies (e.g., [2]) demonstrated that the annual runoff volume increases due to forest degradation. Thus, the control and treatment periods are determined from the fluctuations of the ratio Q_{rat}, calculated using eqn (1):

$$Q_{rat} = Q_t/Q_c, \tag{1}$$

where Q_t and Q_c represent the annual runoff volume from the treatment and control catchment, respectively.

Importantly, the annual runoff volume from each catchment varies with the condition of the forest; it also varies in each catchment even in the same water year with factors such as the topography and geology. Therefore, the values of Q_{rat} vary in each catchment, even during the control periods when the forest conditions in the control and treatment catchments are similar. By comparing Q_t and Q_c observed in the same water year, the effects of meteorological fluctuations are excluded from the values of Q_{rat}, but the effects of differences in topography and geology between catchments remain. However, the topography and geology do not change significantly in several decades. It can be considered that the fluctuations of Q_{rat} is not affected by the change of topography and geology. Therefore, Q_{rat} fluctuations represent the

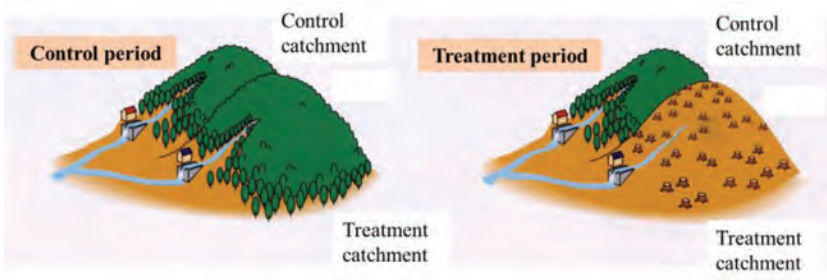

Figure 1: Outline of paired catchment experiments (*Source: [6]*).

effects of only changes of forest conditions. Accordingly, control and treatment periods are determined by fluctuations of Q_{rat}, rather than values of Q_{rat}.

2.2 Forested catchments and cases

This report describes cases in the Tatsunokuchi-yama and Kamabuchi watersheds in Japan, as indicated in Table 1 and Fig. 1. The runoff data used in this report were collected by the Forestry and Forest Products Research Institute.

Table 1: Information on analysis cases by paired catchment experiments (*Source: [8]).*

Case	Experimental site	Control catchment (Area)	Treatment catchment (Area)	Treatment event	Control period	Treatment period
1	Tatsunokuchi -yama	Kitadani (17.274ha)	Minamidani (22.611ha)	Forest fire and Withering of pine trees	1937-1958 1966-1977 1998-2002	1960-1965 1981-1996
2	Kamabuchi	No.1 (3.060ha)	No.2 (2.482ha)	Clear cut	1939-1947 1983-2005	1948-1982
3			No.3 (1,540ha)	Clear cut	1961-1963 1985-2005	1964-1984

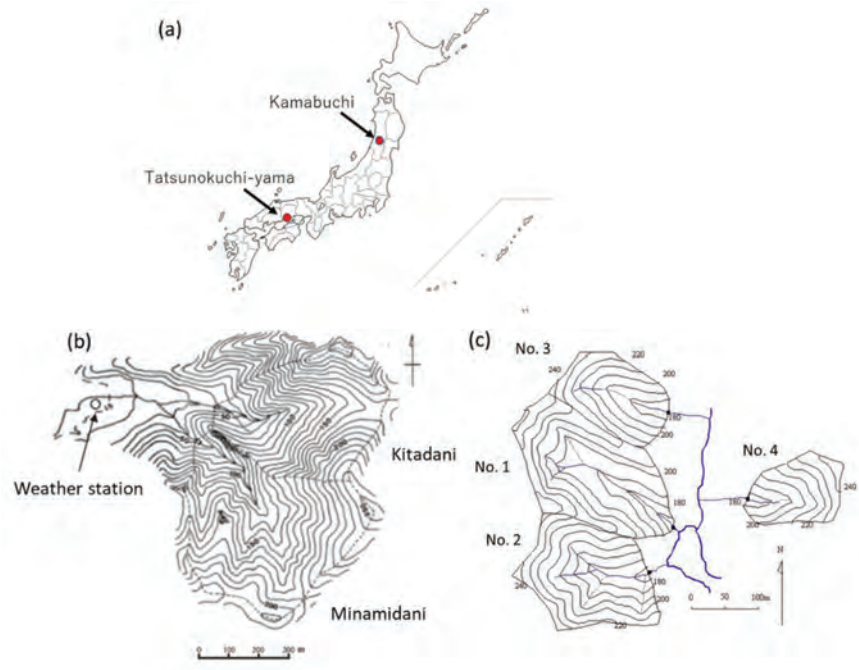

Figure 2: Location of watersheds (a) and topographic map of catchments, (b) Tatsunokuchi-yama Watershed, (c) Kamabuchi Watershed.

Table 2: Forest management history of Tatsunokuchi-yama Watershed (*Source: [8]).*

Year	Kitadani	Minamidani
1937	Observation start	Observation start
1944–1947	Clear cut	Clear cut
1959		Forest fire (Sep.)
1960		Pine replanted (Mar.)
1978–1980		Withering of pine trees

2.2.1 Tatsunokuchi-yama watershed

The Tatsunokuchi-yama watershed (Fig. 2b; located at 34°42′ N, 133°58′ E, with an elevation range of 45–257 m) consists of two catchments: Kitadani (17.27 ha) and Minamidani (22.61 ha). The average air temperature and annual precipitation (1971–2000) are 14.3°C and 1,217 mm, respectively. Snow coverage is rare throughout the year. The geology consists of the Paleozoic Chichibu Formation, and hard sandstone is the predominant lithology [8].

Table 2 presents the forest management history of this watershed. Both catchments were covered with natural Japanese red pine forests in 1937 when observation began. Since then, the Kitadani catchment has grown broad-leaved forests. In contrast, in the Minamidani catchment, forest vegetation has been degraded twice due to forest fire and the withering of pine trees. In this report, the Kitadani and Mimamidani catchments are designated as the control catchment and treatment catchment, respectively, for the paired catchment experiment.

2.2.2 Kamabuchi watershed

The Kamabuchi watershed (Fig. 2c; located at 38°56′ N, 140°15′ E, with an elevation of 162–252 m) consists of four catchments: No. 1 (3.06 ha), No. 2 (2.48 ha), No. 3 (1.54 ha), and No. 4. In this report, the observed runoff data from catchments No. 1, No. 2, and No. 3 are used. Table 3 lists the forest management histories in these catchments. The average annual air temperature and precipitation (1971–2000) are 11.1°C and 2,406 mm, respectively. The period from December to May of the subsequent year is the snow cover season. The geology consists of Tertiary units, with predominant tuff and shale tuff [8].

In 1939, when observation of catchments No. 1 and No. 2 began, all catchments were covered with mixed forests that comprised both coniferous and broad-leaved trees. Since then, the forest in catchment No. 1 has been maintained continually. However, in catchments No. 2 and No. 3, the forests have been clear-cut. In particular, in catchment No. 2, forest soil was lost after clear-cutting due to avalanches and slope failures. Approximately, 20% of the catchment area has become bare [10]. For this report, the control catchment for the paired catchment experiments is catchment No. 1. The treatment catchments are catchments No. 2 and No. 3.

2.2.3 Definition of water year periods

In the Tatsunokuchi-yama watershed, runoff reaches its annual minimum around March. Therefore, the period of April through March of the subsequent year was set as one water year in the Tatsunokuchi-yama watershed. For example, the year 2000 in the Tatsunokuchi-yama watershed represents the calendar period from April 2000 through March 2001.

For the Kamabuchi watershed, daily runoff data for June–November (no-snow period) [8] were used to remove the effects of snow accumulation and melting in the catchments. Therefore, for example, the year 2000 in the Kamabuchi watershed represents the period of

Table 3: Forest management history of Kamabuchi Watershed (*Source: [8]).*

Year	No.1	No.2	No.3
1939	Observation start	Observation start	
1947		Needle tree cut (Dec.)	
1948		Bloard leaves tree cut (-Summer)	
1960		Cedar replanted	
1961			Observation start
1964			Clear cut in lower 50% area (Feb.-Mar.)
1969			Clear cut in Upper 50% area (Dec.)
1970			Cedar replanted (Spring)

June–November 2000. Furthermore, the Q_t and Q_c used in eqn (1) denote the runoff volumes observed between June and November.

3 RESULTS

3.1 Determination of the control and treatment periods

Figure 3a–c shows the fluctuations of Q_{rat} in the three treatment catchments. Q_{rat} values in the three treatment catchments differed from each other at the observation start year when the forest conditions were similar to the conditions of each control catchment. Q_{rat} was less than 1.0 in the Minamidani and No. 3 catchments and less than 1.1 in catchment No. 2 before the forest degradation due to fire and clear-cutting. Thus, the control and treatment periods were determined by the fluctuations of Q_{rat} compared with the values of 1.0 in the Minamidani and No. 3 catchments, and 1.1 in catchment No. 2. In the three treatment catchments, Q_{rat} increased immediately after clear-cutting, forest fire, and the withering of pine trees, it then decreased gradually until returning to its previous level. The duration in years necessary for the Q_{rat} to recover to the previous level (less than 1.0 in the Minamidani and No. 3 catchments, and 1.1 in catchment No. 2) was determined to be a treatment period; all other years were control periods.

In the Minamidani catchment, Q_{rat} was generally less than 1.0 from 1937 to 1958, which was regarded as a control period. Q_{rat} increased to values larger than 1.0 because of a forest fire that occurred in September 1959; it remained larger than 1.0 until 1965. The occurrence of the forest fire was included in water year 1959. Thus, data observed in 1959 were excluded from the analysis, and the period from 1960 to 1965 was regarded as a treatment period. Q_{rat} was again less than 1.0 from 1966 to 1977; this period was regarded as a control period. Q_{rat} became larger than 1.0 in 1981–1996 after the period of 1978–1980, when pines died from wilt disease; the period in 1981–1996 was regarded as a treatment period. Data observed in 1978–1980 were excluded from the analysis because the forest condition was changing in the Minamidani catchment. After 1998, Q_{rat} recovered to less than 1.0, in general, such that

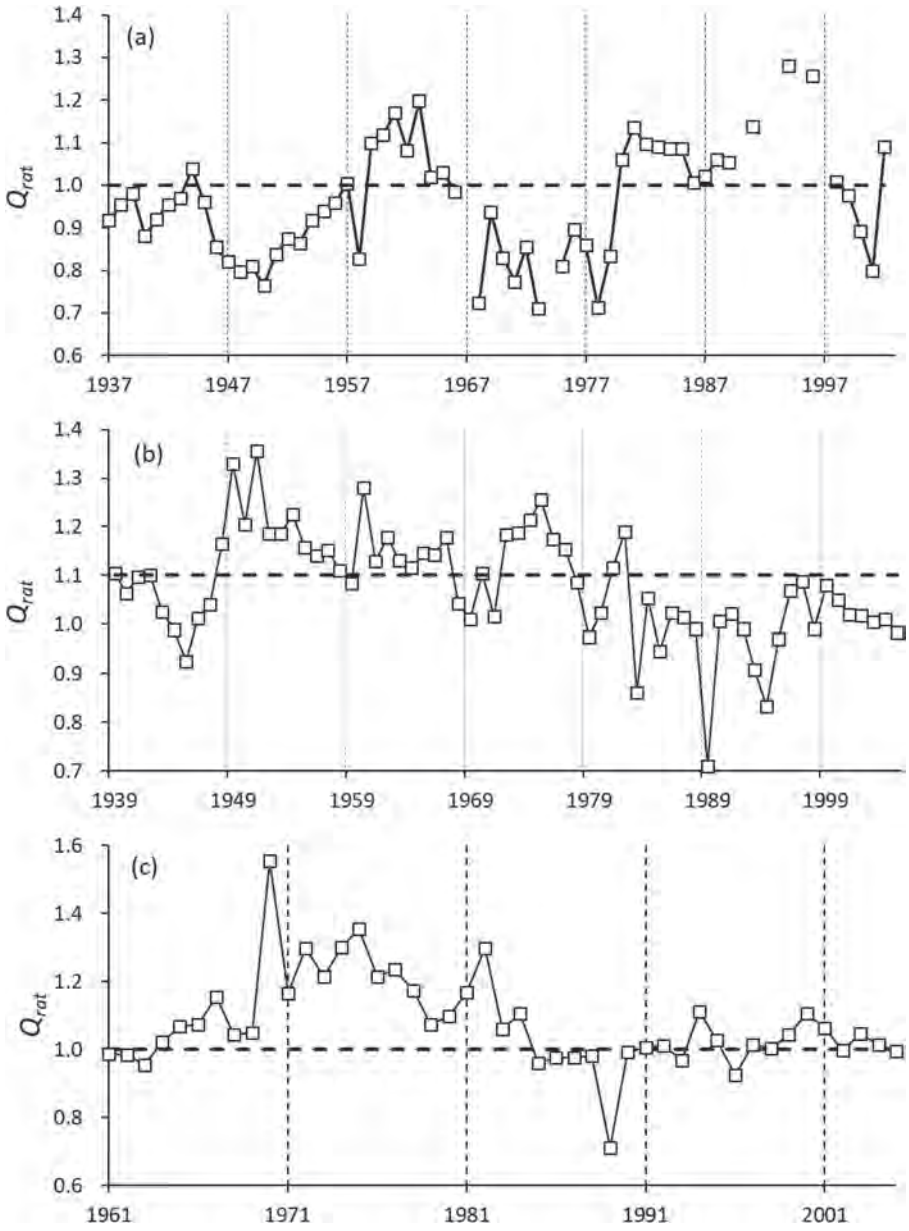

Figure 3: Fluctuation of Q_{rat}: (a) Minamidani catchment, (b) Catchment No.2, (c) Catchment No. 3, (*Source: [8]).*

this period was regarded as a control period. The details of this case (case 1) are summarized in Table 1.

In catchment No. 2, Q_{rat} was less than 1.1 from 1939 to 1947; this period was regarded as a control period. Q_{rat} increased to values larger than 1.1 when clear-cutting was performed

from December 1947 to early summer 1948; it generally remained larger than 1.1 until 1982. Because the period of forest clear-cutting was before water year 1948, the period from 1948 to 1982 was regarded as a treatment period. After 1983, Q_{rat} recovered to less than 1.1; this period was regarded as a control period. This case is summarized as case 2 in Table 1.

In catchment No. 3, Q_{rat} was less than 1.0 from 1961 to 1963, which was regarded as a control period. Q_{rat} increased to values larger than 1.0 because of clear-cutting performed on the lower slope in February and March 1964; it remained larger than 1.0 until 1984. Because the period of forest clear-cutting preceded water year 1964, the period from 1964 to 1984 was regarded as a treatment period. After 1985, Q_{rat} recovered to values generally less than 1.0; this period was regarded as a control period. Case 3 is also summarized in Table 1.

3.2 Influence on minimum daily runoff

Comparisons of the minimum daily runoff from control and treatment catchments in cases 1–3 (Table 1) are presented in Fig. 4a–c, respectively. The liner regression lines for the Minamidani treatment catchment in the control and treatment periods are described by eqns (2) and (3), respectively. They are shown in Fig. 4a as a solid line and a dotted line, respectively:

$$y_c = 0.9078x + 0.0327, \quad \text{RC} = 0.7810, \tag{2}$$

$$y_t = 0.9095x + 0.0746, \quad \text{RC} = 0.5200. \tag{3}$$

where y_c and y_t represent the daily runoff from the treatment catchment in the control and treatment periods, respectively, while x represents the daily runoff from the control catchment. RC represents the regression coefficient.

The linear regression lines for treatment catchment No. 2 in the control and treatment periods are described by eqns (4) and (5), respectively (Fig. 4b):

$$y_c = 0.6445x + 0.0377, \quad \text{RC} = 0.6697, \tag{4}$$

$$y_t = 0.8332x + 0.0579, \quad \text{RC} = 0.6979. \tag{5}$$

The linear regression lines for treatment catchment No. 3 in the control and treatment periods are described by eqns (6) and (7), respectively (Fig. 4c).

$$y_c = 0.5571x + 0.0000, \quad \text{RC} = 0.7348, \tag{6}$$

$$y_t = 0.9621x + 0.0201, \quad \text{RC} = 0.7690. \tag{7}$$

The RC values of eqns (2)–(7) are small, within the range of 0.5200–0.7810. This means that the correlations between the minimum daily runoff in the treatment catchment and control catchment are not strong in either the treatment or control periods for all treatment catchments. Thus, substantial differences in the distributions of data points between the treatment and control periods may not be identified statistically. However, Fig. 4a–c shows that the distribution of dots representing data in the treatment period tends to be clearly higher than the distribution of dots representing data in the control period for all treatment catchments.

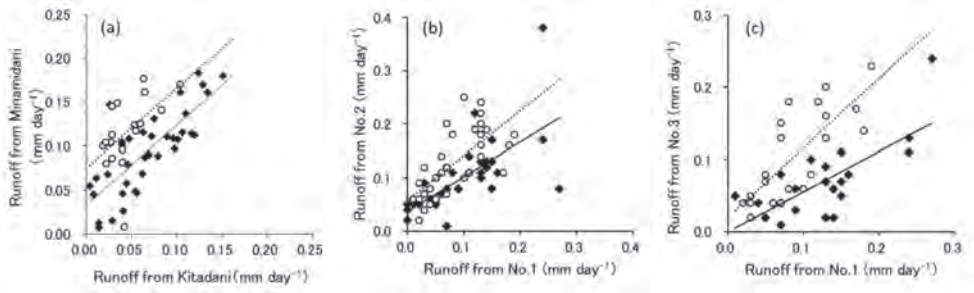

Figure 4: Comparisons of minimum daily runoff from control and treatment catchments and liner regression line (*Source: [8]*). (a) Minamidani catchment, (b) Catchment No.2, (c) Catchment No. 3. Black diamond: control period; white circle: treatment period; solid line: liner regression line for control period; dotted line: liner regression line for treatment period.

This finding suggests that runoff from the treatment catchment is greater during the treatment period than during the control period. Thus, there was a relative increase in minimum daily runoff with forest degradation.

3.3 Influence on maximum daily runoff

Comparisons of maximum daily runoff between the control and treatment catchments in cases 1–3 (Table 1) are presented in Fig. 5a–c, respectively.

The linear regression lines for the Minamidani catchment in the control and treatment periods are expressed by eqns (8) and (9), respectively. They are illustrated in Fig. 5a as a solid line and a dotted line, respectively.

$$y_c = 0.9911x - 4.9877, \quad \text{RC} = 0.9820, \tag{8}$$

$$y_t = 0.9665x + 0.8634, \quad \text{RC} = 0.9600. \tag{9}$$

The linear regression lines for treatment catchment No. 2 in the control and treatment periods are expressed by eqns (10) and (11), respectively (Fig. 5b).

$$y_c = 0.9153x + 6.6388, \quad \text{RC} = 0.9819, \tag{10}$$

$$y_t = 1.0399x + 2.2135, \quad \text{RC} = 0.9872. \tag{11}$$

The linear regression lines for treatment catchment No. 3 in the control and treatment periods are expressed by eqns (12) and (13), respectively (Fig. 5c):

$$y_c = 0.9308x + 3.6910 \quad \text{RC} = 0.9462, \tag{12}$$

$$y_t = 0.9191x + 11.6300 \quad \text{RC} = 0.8784. \tag{13}$$

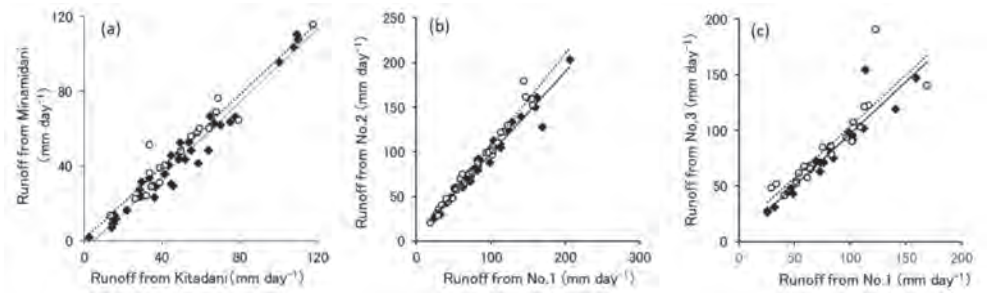

Figure 5: Comparisons of maximum daily runoff from control and treatment catchments and liner regression line (*Source: [8]*). (a) Minamidani catchment, (b) Catchment No. 2, (c) Catchment No. 3. Black diamond: control period; white circle: treatment period; solid line: liner regression line for control period; dotted line: liner regression line for treatment period.

Figure 5a–c shows that the distributions of points representing the data in the treatment and control periods overlap in all cases. Due to this overlap, it is unclear whether runoff from the treatment catchment was larger during the treatment period than during the control period, in contrast to the results for minimum daily runoff shown in Fig. 4a–c. However, the RC values of eqns (8)–(13) are in the range of 0.8784–0.9872; these are much larger than the values of eqns (2)–(7). This finding indicates that the correlations between the maximum daily runoff from the treatment catchment and the control catchment are strong in both the treatment and control periods in all catchments. Thus, eqns (8)–(13) are highly significant. Moreover, the linear regression lines for the treatment period are drawn above the lines for the control period for all treatment catchments (Fig. 5a–c). In summary, the maximum daily runoff from all three treatment catchments increased more in the treatment periods than in the control periods.

3.4 Comparisons of liner regression lines for maximum daily runoff between control and treatment periods

The maximum daily runoff volume varies with the rainfall volume. Points representing the data in the treatment or control periods in the upper-right quadrant in Fig. 5a–c were produced by larger rainfall volumes than were points plotted in the lower-left quadrant. The area between the two linear regression lines can be regarded as the average volume of the runoff increase that is attributable to forest degradation. The linear regression lines reflect the characteristics of water movement in the catchment. Thus, changes in water movement cause changes in linear regression lines. Therefore, the linear regression lines for maximum daily runoff were compared between the control and treatment periods to evaluate the degradation of flood mitigation function in each treatment catchment.

Differing patterns were found among the three treatment catchments. First, catchment No. 3 was explored. In this catchment, the slopes of eqns (12) and (13) are 0.9308 and 0.9191, respectively, which are nearly equal. The intercept of eqn (13) calculated for the treatment period is approximately 8 mm day^{-1} greater than the intercept of eqn (12) for the control

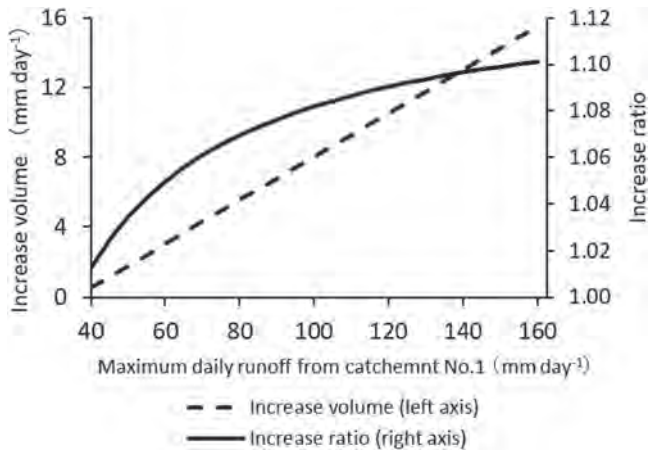

Figure 6: Increase volume (eqn 14) and ratio (eqn 15) of maximum daily runoff from catchment No. 2 against catchment No.1, Kamabuchi watershed during the treatment period (*Source: [8]*).

period. Similar to the case of catchment No. 3, the slopes of eqns (8) and (9) for the Minamidani catchment are approximately equal, at 0.9665 and 0.9911, respectively. Equation (9) for the treatment period has a greater intercept by approximately 6 mm day^{-1} than eqn (8) does for the control period. The two liner regression lines were almost parallel in Minamidani and No. 3 catchments.

In catchment No. 2, the slope increased from approximately 0.9153 in eqn (10) for the control period to approximately 1.0399 in eqn (11) for the treatment period. The difference between eqns (10) and (11) is greater in the upper-right quadrant than in the lower-left quadrant of Fig. 5b. The increase in volume (ΔQ) and increase in ratio (R) can be calculated from eqns (10) and (11), and observed maximum daily runoff (x) from the control catchment No. 1, as defined in eqns (14) and (15):

$$\Delta Q = (1.0399x + 2.2135) - (0.9153x + 6.6388), \quad (14)$$

$$R = (1.0399x + 2.2135) / (0.9153x + 6.6388). \quad (15)$$

ΔQ increased in proportion to the increase in x (Figure 6).

4 DISCUSSION

4.1 Degradation of the flood mitigation function

Two main patterns were observed in the comparisons between the linear regression lines in each treatment catchment. One pattern described the Minamidani and No. 3 catchments, while the other pattern described catchment No. 2. The causes of this difference are discussed below to examine how an increase in maximum daily runoff corresponds to degradation of the flood mitigation function in each treatment catchment.

4.1.1 Minamidani and No. 3 catchments

When the two linear regression lines are nearly parallel, as in the Minamidani and No. 3 catchments, the average increase in maximum daily runoff volume from the treatment catchment is caused by the increase in the intercept from eqns (8) and (12) to eqns (9) and (13), respectively; it can be regarded as constant regardless of the rainfall volume producing the maximum daily runoff.

To discern the mechanism underlying these results, reduction of canopy interception in the treatment catchment during the treatment period must be considered. Iida et al. [3] observed the time courses of rainfall volume outside and within a cedar forest during rainfall events and reported that the difference between these volumes reaches a peak during rainfall events and that the quantity of water that can be contained in tree bark and foliage (7.2 mm) is approximately equal to the maximum interception quantity (6.7 mm). This finding suggests that canopy interception is due to rainwater stored in foliage and tree bark that evaporates after the rain stops. In the Minamidani and No. 3 catchments, as the degraded forest lost foliage and tree bark in the treatment period, the storage quantity was reduced by approximately 6–8 mm per rainfall event. Irrespective of the rainfall volume, the maximum daily runoff increased by 6–8 mm day^{-1} due to the decrease in canopy interception. Based on the above discussion, the increase in runoff volume during the treatment period is presumably attributable to the degradation of forest vegetation alone, rather than forest soil.

When the slopes of the linear regression lines for the control and treatment periods are nearly equal, as in eqns (8) and (9) and eqns (12) and (13), forest soil is maintained. The effects of forest vegetation degradation reduce canopy interception and increase runoff by 6–8 mm day^{-1}, irrespective of the rainfall volume producing the maximum daily runoff, as shown in Fig. 5a and c.

4.1.2 Catchment No.2

As shown in Fig. 6, ΔQ increases in proportion to the increase in x. The value of x can be replaced with the rainfall volume producing the maximum daily runoff. Thus, the increased runoff volume from treatment catchment No. 2 during the treatment period includes components proportional to rainfall volume.

Regarding the mechanism underlying this relationship, a reduction in the soil water holding capacity due to slope failure is one possibility. Thick forest soils with developed pores promote efficient osmosis of rainfall water, hold that water temporarily, and then release it slowly. Arimitsu et al. [1] compared two adjacent forest catchments and reported that runoff volume from a catchment with thin and immature soil was markedly smaller during a drought and larger during a flood period compared with the volume from a catchment with thick and mature soil. In other words, the volume of direct runoff is larger and its outflow is faster in a catchment with a low soil water-holding capacity than one with high water-holding capacity. When water holding capacity is reduced due to forest soil loss associated with slope failure, the ratio of base flow, which is water that penetrates deep into the soil and is released slowly, is expected to decrease. With this reduction in the ratio of base flow, the ratio of direct runoff is expected to increase, becoming proportional to rainfall volume.

In catchment No. 2, bare areas were present due to avalanches and slope failure [10]. The rate of base flow is presumably reduced in such areas due to the loss of forest soil, leading to an increase in direct runoff. In this case, maximum daily runoff increases in proportion to rainfall volume.

4.2 Comparison with model calculations

After using a model to simulate the movement of water in a forested catchment, Tani et al. [9] reported water runoff characteristics calculated under various states of forest soil and vegetation. By comparing the values between calculations under healthy and degraded conditions of forest vegetation with the same soil conditions, the changes attributable to the presence of forest vegetation were determined. No difference in the maximum hourly runoff was found between calculations. The minimum hourly runoff under healthy vegetation is 0.002 mm hour^{-1}, but it becomes 0.04 mm hour^{-1} under the degraded vegetation [6]. This finding agrees with the result showing increased runoff from the treatment catchment during the treatment period, as indicated by the clear increases shown in Fig. 4a and c for minimum daily runoff; the increases are less clear for maximum daily runoff caused by overlap of point distributions representing the data in the treatment and control periods, shown in Fig. 5a and c.

Changes attributable to the presence of both forest soil and vegetation can be evaluated by comparing the results of calculations under healthy and degraded conditions of both forest soil and vegetation. In healthy condition, the maximum and minimum hourly runoff values are 5.0 and 0.01 mm hour^{-1}, respectively. In degraded condition, the maximum and minimum hourly runoff values are 9.3 and 0.04 mm hour^{-1}, respectively [6]. When both forest soil and vegetation are degraded from a healthy condition, both the maximum and minimum values of hourly runoff increase. This finding agrees with the minimum runoff results presented in Fig. 4b for catchment No. 2. For maximum runoff, changes between the control and treatment periods, shown in Figs. 5b and 6, are smaller than the difference between the model calculations mentioned above.

According to the model calculations reported by [9], the maximum hourly runoff under the degraded condition of forest soil and vegetation was 9.3 mm hour^{-1}, which was approximately 1.9-fold greater than the 5.0 mm hour^{-1} rate obtained from calculation under the healthy condition of forest soil and vegetation [6]. Although R increases with increasing rainfall volume, as shown in Fig. 6, the maximum increase is 1.1-fold. Possible reasons for the difference between the 1.9-fold difference reported by [9] and the 1.1-fold difference shown in Fig. 6 might be the percentage of the watershed area degrading forest soil. Tani et al. [9] presented the calculation under the degraded condition of forest soil based on the assumption that no forest soil is present anywhere in the catchment. However, according to a map that shows the forest status of catchment No. 2 in April 1978 [10], bare land occupied only approximately 20% of the catchment area. Changing the percentage of the area without soil in the catchment significantly affects the degree of increase.

4.3 Assessing degradation of the flood mitigation function

For Minamidani and No. 3 catchments, the flood mitigation function of forests was presumably not degraded due to forest fire, withering of pine trees, or clear-cutting; this inference was made because the linear regression lines are nearly parallel (Fig. 5a and c) and the increased volume of the maximum daily runoff was only 6–8 mm day^{-1} in these catchments. It is likely that only the forest vegetation degraded and that the forest soil was preserved.

In contrast, in catchment No. 2, the flood mitigation function of the forest was considered degraded due to clear cutting, avalanche, and slope failure because the slopes of the linear regression lines were larger in the treatment period than in the control period (Fig. 5b); there was an estimated maximum daily runoff increase in proportion to the rainfall volume

producing the maximum daily runoff due to slope failure and transition to bare land in 20% of the catchment area.

The above discussion suggests that forest soil loss associated with slope failures and avalanches causes a degradation of flood mitigation function.

4.4 Forest management

Forest vegetation may be misunderstood as not having a recognized role in the flood mitigation function because degradation of the flood mitigation function may not be identified in treatment catchments where only forest vegetation is degraded while forest soil is preserved, such as the Minamidani and No. 3 catchments in this report. Nevertheless, forest vegetation contributes to flood mitigation by preserving forest soil, reinforcing slope stability with tree root systems. This effect is apparent in degradation of the flood mitigation function caused by slope failure in catchment No. 2 (Fig. 5b and 6).

Among the three treatment catchments assessed in this report, slope failure occurred after clear-cutting in catchment No. 2, while it did not occur after a forest fire and tree withering in the Minamidani catchment or after clear-cutting in catchment No. 3. The reasons for these different outcomes are discussed at the end of this report.

Before that discussion, a forest management system to prevent slope failure [7] is briefly described.

4.4.1 Forest management for prevention of slope failure

Forest tree root systems grow while binding and fixing soil particles. Thus, tree roots reinforce soil connection and slope stability, thereby preventing slope failure. If a forest is clear-cut, this reinforcing effect is reduced as the stump root system decays. The reinforcing effects of planted tree root systems increase with tree growth. Even if replanting occurs immediately after clear-cutting, the reinforcing effects of root systems, including both stumps and replanted trees, decrease for decades after clear-cutting [5].

To maintain the reinforcing effects of tree root systems as completely as possible, the following list of proposals was presented in [7].

(a) Tree cutting should not be conducted in areas where the slope failure risk is high.
(b) When tree cutting is necessary for areas with a risk of slope failure, sites were chosen for tree cutting should be in lower-risk areas or distant from residential areas to prevent damage if slope failure occurs.
(c) The degree and extent of tree cutting should be minimised in areas with a high risk of slope failure. More root systems of trees should be left after cutting.
(d) To shorten the period during which the reinforcing effect of tree root systems is reduced, nursery trees should be replanted promptly after cutting.

4.4.2 Verification of forest management in treatment catchments

In the Minamidani catchment, Japanese black pines were replanted in March 1960, almost immediately after a forest fire that occurred in September 1959 (Table 2). This area was treated similarly to the approach in proposal d). After tree withering occurred in 1978–1980, the area was left to recover naturally. Although all pine trees died, other trees survived. Thus, the slope reinforcing effect by the root systems of the remaining trees was sufficient. Consequently, the effect of proposal c) was also achieved.

In catchment No. 2, trees in the whole catchment area were clear-cut from December 1947 through summer 1948; cedar trees were replanted more than 10 years later, in 1960 (Table 3). Stumps stabilized the snow on the slopes, prevented avalanches, and preserved the soil through their root systems in some years after clear-cutting [10]. Subsequently, as stumps and their root systems decayed, they became unable to resist the movement pressure of snow. In 1959, more than half of the catchment area experienced frequent avalanches. Moreover, some areas were transformed into bare land due to slope failure. Clear-cutting performed in whole areas within the catchment with a high risk of slope failure is counter to the approaches in proposals (a) and (c). Replanting was not performed immediately after clear-cutting in this case, which is counter to the approach in proposal (d).

In catchment No. 3, clear-cutting was conducted for 50% of the catchment area on the lower portion of the slope during February–March 1964. Cedar trees were replanted in the spring of 1970. Although cedar replanting occurred approximately 6 years after the clear-cutting of the lower slope, it occurred immediately after clear-cutting of the upper slope area (Table 3). During 1964–1969, no trees were present on the lower slope, whereas trees remained on the upper slope. The movement pressure of snow was thus suppressed, allowing the stumps remaining on the lower slope to conserve the forest soil. Additionally, the remaining tree root systems on the upper slope reinforced the stability of the upper slope. The range of clear-cutting was limited to 50% on the lower slope, in accordance with proposal (c). The replanting of cedars immediately after 50% clear-cutting of the upper slope aligns with the approach in proposal d).

5 CONCLUSIONS

The increased volume of maximum daily runoff and degradation of the flood mitigation function of forests due to forest degradation was estimated using paired catchment experiments. In the two treatment catchments where forest soil was preserved and only forest vegetation was degraded, the flood mitigation function of the forest was judged not to be degraded because the volume increase was estimated to be only 6–8 mm day^{-1}, irrespective of the rainfall volume producing the maximum daily runoff. Based on [3], it was discussed that the decrease of canopy interception with degradation of only forest vegetation causes the small runoff increase independent of rainfall volume. On the other, in the one catchment where forest soil was not preserved, the flood mitigation function of the forest was judged to be degraded because the estimated maximum daily runoff increased approximately 1.1-fold in proportion to the rainfall volume producing the maximum daily runoff. Based on [1] and [9], it was discussed that the increase of direct runoff with degradation of forest soil causes the increase of runoff in proportion to rainfall volume.

By examining the forest management histories of the three treatment catchments, the causes of slope failure were assessed to identify inappropriate forest management activities, as follows: clear-cutting in areas with high slope failure risk, clear-cutting simultaneously across the whole catchment area, and delayed replanting after clear-cutting.

The above findings imply that prevention of slope failures is necessary to maintain the flood mitigation function of forests. Therefore, several forest management strategies for utilizing reinforcing slope stability with tree root systems [5] are recommended for the flood mitigation function of forests: avoid logging in places with a high risk of collapse, limit the amount of logging, and promptly plant trees after logging.

REFERENCES

[1] Arimitsu, K., Araki, M., Miyakawa, K., Kobayashi, S. & Kato, M., Water holding capacities estimated by soil pore capacities of Takaragawa Experiment Station; Comparison of No. l and No. 2 experimental watersheds (in Japanese with English summary). *Japanese Journal of Forest Environment*, **37**, pp. 49–58, 1995.

[2] Bosch, J.M. and Hewlett, J.D., A review of catchment experiments to determine the effect of vegetation changes on water yield and evapo-transpiration. *Journal of Hydrology*, **55**, pp. 3–23, 1982.

[3] Iida, S., Levia, D., F., Shimizu, A., Shimizu, T., Tamai, K., Nobuhiro, T., Kabeya, N., Noguchi, S., Sawano, S. & Araki, M., Intrastorm scale rainfall interception dynamics in a mature coniferous forest stand. *Journal of Hydrology*, **548**, pp. 770–783, 2017.

[4] Kitamura, Y. & Namba, S., Tree roots upon landslide prevention presumed through the uprooting test (in Japanese). *Bulletin of the Forestry and Forest Products Research Institute*, **313**, pp.175–208, 1981.

[5] Tada, Y., Historic transition of natural disaster and land, forest-use in Japan (in Japanese). *Water Science*, **62(4)**, pp. 121–137, 2018.

[6] Tamai, K., The evaluation of forest functions of flood control and water resources conservation. *International journal of environmental impact,* **3**, pp.304–313, 2020.

[7] Tamai, K., Forest management to mitigate disasters caused by heavy rain, *WIT Transactions on Ecology and the Environment,* **251**, pp. 57–63, 2021a.

[8] Tamai, K., Deforestation effects on maximum and minimum daily runoff (no-snow season) – cases of Kamabuchi and Tatsunokuchi-yama experimental watersheds (in Japanese). *Journal of Japan Society of Hydrology and Water Resources*, **34**, pp. 243–253, 2021b.

[9] Tani, M., Fujimoto, M., Katsuyama, M., Kojima, N., Hosoda, I., Kosugi, K., Kosugi, Y. & Nakamura, S., Predicting the dependencies of rainfall-runoff responses on human forest disturbances with soil loss based on the runoff mechanisms in granite and sedimentary rock mountains. *Hydrological Processes*, **26**, pp. 809–826, 2012.

[10] YAMAGATA Experiment Site, TOHOKU Branch Station, Statistical Reports of Hydrological Observation at KAMABUCHI Experimental Watershed, No. 1 and No. 2 Experimental Watersheds (January 1959–December 1978), *Bulletin of the Forestry and Forest Products Research Institute*, **311**, pp. 129–188, 1980.

CLIMATE CHANGE IN CHILE, STRATEGIC PLAN AND CIRCULAR ECONOMY

VALERIA SCAPINI[1] & PRISCILLA BERRIOS[2]
[1]Centro de Investigación en Innovación, Desarrollo Económico y Políticas Sociales (CIDEP) – Universidad de Valparaíso, Chile
[2]Universidad de Valparaíso, Chile

ABSTRACT

Environmental problems have been increasing at a disproportionate rate, contributing to global warming, one of humanity's greatest challenges. As stated in the latest report of the Intergovernmental Panel on Climate Change 'climate change is widespread, rapid and intensifying' and there is certainty that this is a result of human activity. In this context, environmental social responsibility is fundamental to prevent, mitigate or repair the environmental damage generated by productive activity. This obliges us to take concrete actions and thus move from a linear economy approach to a circular economy approach that allows for sustainable development, where waste and pollution are eliminated from the design stage and materials are used for as long as possible. Chile must implement actions that allow it to meet the commitments obtained in its Nationally Determined Contribution of 2020, and move towards sustainable development. The Chilean case is interesting to study because it is a highly exposed and fragile country in the face of climate change. The purpose of this publication is to highlight the current problem of climate change and the threat it poses to our planet, to understand that the circular economy approach as a business model allows for a long-term solution to this problem, to understand the consequences of climate change in Chile and to know the current situation in terms of strategic planning at the country level in relation to the circular economy.

Keywords: circular economy, climate change, greenhouse gases, recycling, sustainable development.

1 INTRODUCTION

Environmental problems have increased considerably, contributing to global warming by 1.02°C due to the increase of greenhouse gas (GHG) emissions and their accumulation in the atmosphere [1]. Globally, GHGs have increased since the post-industrial period, reaching a total of 49.36 billion tonnes in 2016 [2]. Among these gases are mainly carbon dioxide (CO_2), methane (CH_4) and nitrous oxide (N_2O), the former being the major contributor to global warming because the burning of fossil fuels (oil, coal and gas) causes more heat to be trapped in the atmosphere. In July 2021, the ambient concentration of CO_2 was 416.96 ppm [3, 4] and the countries/regions emitting the most CO_2 are China (30.7%), the United States (13.8%), the European Union (7.9%), India (7.1%) and Russia (4.6%) [5].

Due to all the environmental problems, the Conferences of the Parties (COP), annual international meetings of the United Nations in which the countries of the world meet to discuss environmental issues, have been held since 1995 and carried out by the United Nations Framework Convention on Climate Change (UNFCCC). Specifically, during the COP No. 21 held in Paris in 2015, a historic milestone known as the Paris Agreement was reached, which establishes the commitment of countries to 'keep the average temperature increase well below 2°C above pre-industrial levels and to pursue efforts to limit this temperature increase to 1.5°C above pre-industrial levels, recognising that they would significantly reduce the risks and impacts of climate change' [6]. Thus, following the signing of this agreement, each country indicates voluntary commitments to reduce its GHG emissions through Nationally Determined Contributions (NDCs), which are an instrument for measuring the real contributions of each nation in relation to its committed environmental efforts. These must be reviewed and updated every 5 years in the hope that there will be ever greater ambition in terms of their realisation [7, 8].

ISSN: 2398-2640 (paper format), ISSN: 2398-2659 (online), http://www.witpress.com/journals
DOI: 10.2495/EI-V5-N4-306-315

In August 2021, the Intergovernmental Panel on Climate Change (IPCC) published its 6th report stating that 'climate change is widespread, rapid and intensifying' and is certain to be a result of human activity [9]. In relation to the Paris Agreement, the report states that 'unless greenhouse gas emissions are reduced immediately, rapidly and on a large scale, limiting warming to around 1.5°C or even 2°C will be an unattainable goal'. Experts indicate that we are in a climate emergency and that urgent global action is needed, as failure to act could have catastrophic and irreparable global consequences [9].

Chile is a country that is highly exposed to and fragile in the face of climate change [10,11]. In this context, in December 2020, the Ministry of the Environment launched the 'Climate Risk Atlas (ARClim)', which features maps showing Chile's risks to climate change so that this information can be made available and support decision-making in relation to the changes that need to be faced in the country [12]. The effects include increased temperatures, droughts, precipitation, coastal erosion and increased heat waves, among others [10,11].

The purpose of this study is to highlight the current problem of climate change and the threat it poses to both the planet and Chile, to understand that the circular economy approach as a business model allows for a long-term solution to this problem, and to learn about the current situation in terms of strategic planning at the national level in relation to the circular economy. Finally, some examples that have promoted solutions in this line of work are shown. This paper is an extension of the work found in Scapini and Berríos [13], where a bibliographic review of the concept of circular economy and the state of progress of the laws in the country is carried out. The paper is structured as follows. Section 2 contains a literature review on the concept of climate change and the importance of the circular economy as a solution to this problem; section 3 presents the methodology; section 4 shows the result of the research describing the effects of climate change in Chile and the strategic planning at the country level in relation to the circular economy; and finally, section 5 concludes on the subject.

2 LITERATURE REVIEW

Sustainable development is development that 'meets the needs of the present generation without compromising the ability of future generations to meet their own needs' [14]. This definition involves a number of aspects, all of them very important, that must be considered: resource scarcity, population growth, clean production and pollution. The growing needs and the limited resources that allow us to satisfy these needs allow us to understand that our planet has a limited capacity and that we are approaching the destruction of the ecosystem. This forces us to rethink an approach that can be sustained in the long term.

In 1990, David Pearce and Kerry Turner first used the term circular economy when they mentioned that materials in an economy flow in a closed loop [15] and since then the concept has become increasingly important. In order to accelerate the transition to a circular economy model, the Ellen MacArthur Foundation was established in 2010 to promote the concept as an alternative to economic growth that reduces environmental impact. It implies a radical change in current production and consumption, as the value of products and materials must be maintained for as long as possible from the design stage. This concept seeks to decouple economic growth and development from the consumption of finite resources [16].

2.1 Climate change and its effects

The IPCC defines climate change as a change in the state of the climate that is due to changes in the mean or variability of characteristics and that lasts for an extended period, usually more

than ten years [14]. Causes include internal or external natural processes such as volcanic eruptions and anthropogenic changes. The Framework Convention on Climate Change (UNFCCC) defines it as a change in climate that is due directly or indirectly to human action that alters the composition of the atmosphere. Climate change generates a range of negative consequences that affect natural ecosystems, socio-economic systems, or human health and well-being [17].

Climate change is making the hydrological cycle more intense, resulting in heat waves, droughts, fires, melting ice, sea level rises, and at the same time, higher temperatures lead to more evaporation from the oceans into the atmosphere, resulting in increased precipitation (monsoons, typhoons, hurricanes), floods and landslides. These events are increasing in frequency in all areas of the world and with them, the impacts on ecosystems, flora, fauna and societies [9].

3 METHODOLOGY

The methodology used is mainly based on a literature review. Firstly, the current problem of global climate change is studied, the challenge it represents for humanity, and the importance of the circular economy approach as a business model that allows for a long-term solution to this problem. Subsequently, information is compiled on the main effects that climate change will have on the economic sectors in Chile in the medium and long term. Subsequently, information is collected regarding the current situation of strategic planning at country level in relation to the circular economy. Finally, some examples of sustainable initiatives are mentioned. The inclusion criteria were articles, in Spanish and English, on the topics indicated in the diagram below. On the other hand, all information available on the website of the Ministry of the Environment was included, and articles whose text was not available or those that were not related to the topic studied were excluded.

4 RESULTS

4.1 Climate change in Chile

In the case of Chile, GHG emissions in the country have increased by 129.4% between 1990 and 2018 [18]. Although Chile is responsible for only 0.24% of the planet's GHGs, it is one of the countries most vulnerable to the harmful effects of climate change, due to its long coastline and the diversity of climates across the country [18].

To determine a country's vulnerability in relation to the climate crisis, the United Nations Framework Convention on Climate Change has set nine criteria, as follows: (1) low-lying coastal areas, (2) arid and semi-arid areas, (3) forested areas, (4) territory susceptible to natural disasters, (5) areas prone to drought and desertification, (6) urban areas with air pollution, (7) mountainous ecosystems, (8) low-lying and island countries, (9) landlocked and transit countries. In the particular case of Chile, the country meets 7 of the 9 vulnerability criteria, while criteria 8 and 9 are not met [19].

This means that the country is more exposed to increases in temperature, droughts, precipitation, coastal erosion and heat waves, among others. Because of this, and because we are also in a global climate emergency, Chile needs to address these effects immediately [11].

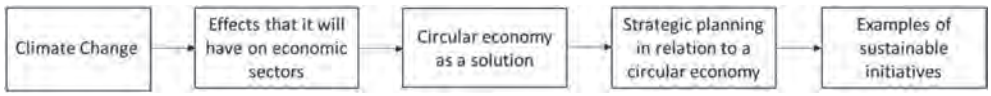

Figure 1: Diagram of the literature review.

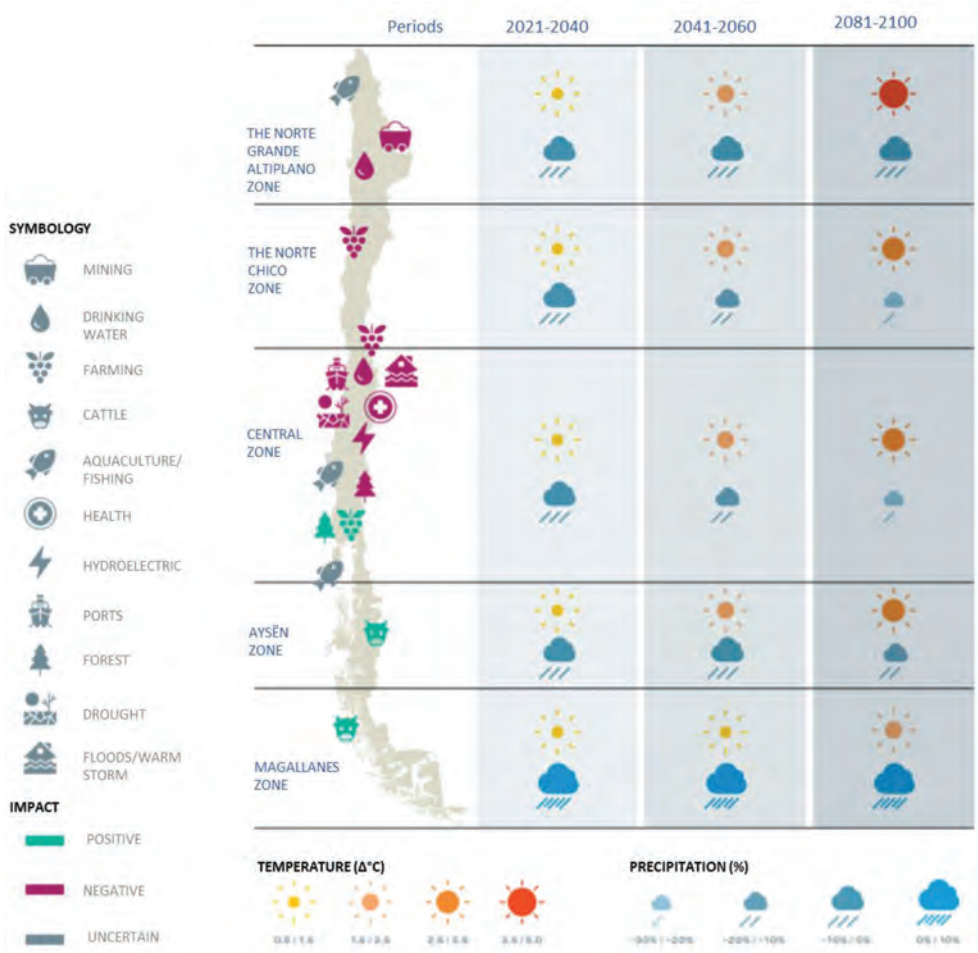

Figure 2: Climate change in Chile [18].

Figure 2 shows that the effects of climate change affect the entire country. Precipitation will increase only in the southern part of the territory, specifically in the Magallanes region, while the rest of the country will see a decrease in precipitation. Temperatures will increase throughout the country, with the most affected areas being the north and centre of the country. Among the economic impacts, we can see that the northern and central areas will be negatively affected by all economic activities (see purple symbology), while in the extreme south of the country there will be positive impacts related to forestry, agriculture and livestock activities (see green symbology). Finally, aquaculture and fishing activities throughout the territory will have an uncertain impact (see grey symbology).

4.2 Chile's strategic planning in the long term

Chile, in its international commitments in relation to environmental issues, signed on to the Paris Agreement since 2015 through the NDC in which it establishes reaching carbon neutrality by 2050 and sets targets to reduce these emissions progressively over time [20, 21].

Currently, in order to promote a circular economy model, the Circular Economy office of the Ministry of Environment is working on two main areas of action. The first is the implementation of Law No. 20.920, which establishes the framework for Waste Management, Extended Producer Responsibility and the Promotion of Recycling (REP Law); while the second seeks to stimulate an environment of innovation, a regulatory framework and other instruments [22].

The lines of work and their state of progress are as follows [22]:

1) The implementation of the REP Law: This law aims to reduce waste generation and encourage reuse and recycling, forcing producers of priority products to finance the collection and recycling that their products generate.
2) Circular Economy Roadmap: It is a strategic planning instrument with a long-term vision of environmental management, which aims to achieve a regenerative circular economy by 2040 with medium (2030) and long-term (2040) goals. This was done through collaborative work with different national stakeholders as well as an international advisory committee. The targets included in the Roadmap are: 'more jobs, less waste/person, less waste/GDP, more material productivity, more recycling, more municipal recycling and more recovery of sites affected by illegal disposal' [23].
3) Recycling Fund: This fund finances municipal and municipal association projects aimed at preventing waste generation, promoting separation, reuse and recycling.
4) Policy for the Inclusion of Grassroots Recyclers: This policy aims to promote the social, economic and environmental inclusion of grassroots recyclers through proper waste management.
5) Action Plan Against Plastic Pollution: This is one of the biggest challenges worldwide and therefore seeks to minimise the consumption of single-use plastics in commerce and to create labels for products that provide information to consumers regarding the recyclability of containers and packaging.
6) Organic Waste Management Strategy: Aims to prevent organic waste from being turned into rubbish and ending up in sanitary landfills or dumps, causing pollution.
7) Construction and Demolition Waste (CDW): The purpose is to provide solutions to problems generated by the construction sector, since it is considered one of the most polluting economic activities and one of those that emits the most GHGs globally, and, on the other hand, represents 35% of the country's inert waste (only considering the construction process) that often end up in illegal landfills since most regions do not have legal landfills to dispose of this type of waste [23, 24].
8) Transboundary Movement of Waste: Its purpose is to comply with the Basel Convention on the 'Control of Transboundary Movements of Hazardous Wastes and their Disposal'.

4.3 Some initiatives with a sustainable approach

The REP Law will start to apply from 16 September 2023, where producers will be obliged to finance the collection and recovery of waste, packaging and packaging. Some companies have already committed to the environment by transforming their products and processes to adopt a circular economy approach. Examples include:

4.3.1 AZA, sustainable steels

They have removed thousands of polluting wood-burning stoves, each representing about 27 kilos of scrap metal, and replaced them with less polluting heaters. The scrap has been

Figure 3: The circular route of recycled steel: from old stove to renewable energy [25].

transformed into new steel products, such as support towers for wind power plants, which has allowed them to apply circular economics to transform polluting material into clean energy through the recycling chain [25].

4.3.2 Revaloriza, new life for waste

Revaloriza is the first company in Chile and South America that reuses construction and demolition waste to be recycled and converted into new secondary raw materials. The relevance of this company is that it solves an environmental problem related to the fact that waste from this sector is usually not properly disposed of in a sanitary landfill, but rather becomes debris that ends up in ravines, streets, beaches, or illegal dumps [26].

4.3.3 Recovery and recycling of fishing nets

Fishing nets are very commonly used by the fishing sector. They are made of plastic and end up as polluting waste that is not easy to dispose of. That is why Sonapesca generated an agreement with the company Bureo who created the programme 'Net Positive' where new products are generated with recycled materials and donated by fishermen. In this way, the oceanic ecosystem is protected and the economy is boosted with the generation of recycled products [28].

5 CONCLUSIONS

The indiscriminate consumption of resources worldwide has brought the issue of sustainability into discussion. This, together with pollution and GHG emissions, has contributed to global warming, currently one of humanity's greatest challenges. This forces us to rethink an economic model that can be sustained in the long term. This leads us to consider the concept of a circular economy as an alternative to economic growth that reduces environmental impact and decouples economic growth and development from the consumption of unlimited resources.

Climate change in Chile is scientifically evidenced and its vulnerability is proven. It is a country that is highly exposed and fragile in the face of climate change, which obliges us to

Figure 4: Revaloriza, new life for waste [27].

Figure 5: Recovery and recycling of fishing nets [28].

transform all economic sectors and move towards sustainable development. In this sense, Chile has established the goal of carbon neutrality by 2050, articulated with the draft Framework Law on Climate Change that is currently being processed in the Senate.

To promote a circular economy model, legislation has made progress in reducing waste generation and promoting reuse and recycling, through the enactment of the REP Law, the Roadmap for a Circular Chile 2040, the National Organic Waste Strategy, the fight against plastic, and the RCD Roadmap for a Circular Economy in Construction. Among the challenges are the development of circularity indicators that allow the country to measure the progress of its commitments. Some companies are already committed to the environment, transforming their products and processes to adopt a circular economy approach.

However, the unexpected arrival of the worldwide Covid-19 pandemic has generated many questions regarding the circular economy that would be interesting to study in the

future. The closure of the borders and the long periods of quarantine have led to a shortage of products, rise in prices, and an increase in home delivery services, among others. The long periods of quarantine have reduced the impacts on the environment, however, we have seen an increase in the amount of garbage that is generated with the use of safety items (such as disposable masks, face shields, chests, sanitization, etc.) and the packaging of delivery products, among others. It is unknown whether these changes have allowed progress or regression in the implementation of the 2040 Circular Economy Roadmap in the country.

REFERENCES

[1] NASA, *Global climate change: Global Temperature*, available at https://climate.nasa.gov/vital-signs/global-temperature/ (accessed 06 January 2022).

[2] Ritchie, H., & Roser, M., *COz and Greenhouse Gas Emissions*, Our world in data, available at https://ourworldindata.org/greenhouse-gas-emissions, 2022 (accessed 09 January 2022).

[3] NOAA Global Monitoring Laboratory, *Trends in Atmospheric Carbon Dioxide*, available at https://gml.noaa.gov/ccgg/trends/, 2022 (accessed 06 January 2022).

[4] WHO, *The State of Greenhouse Gases in the Atmosphere Based on Global Observations through 2020*, WMO Greenhouse Gas Bulletin, available at https://library.wmo.int/doc_num.php?explnum_id=10904, 17, 2021 (accessed 15 December 2021).

[5] Mena, M., *Emisiones de CO2. Los países que más contaminan*, available at https://es.statista.com/grafico/23395/paises-regiones-con-mayor-volumen-de-emisiones-de-dioxido-de-carbono/, 2021 (accessed 20 December 2021).

[6] Nations Unies, *Conferencia de las Partes. Vigésimo primera sesión. FCCC/CP/2015/L.9. París, 30 de noviembre al 11 de diciembre de 2015*, Convention-cadre sur les changements climatiques, París: ONU, available at https://unfccc.int/resource/docs/2015/cop21/spa/l09s.pdf, 2015 (accessed 18 December 2021).

[7] United Nations, *Framework Convention on Climate Change*, NDC Registry, available at http://unfccc.int/focus/ndc_registry/items/9433.php, 2016 (accessed 06 Januay 2022).

[8] Boletín 13.191-12, *Proyecto de ley, iniciado en mensaje de S. E. el Presidente de la República, que fija Ley Marco de Cambio Climático*, available at https://leycambioclimatico.cl/wp-content/uploads/2020/07/ProyectoLeyCC_13012020.pdf (accessed 06 January 2022).

[9] Allen, M., Dube, O.P., Solecki, W., Aragón-Durand, F., Cramer, W., Humphreys, S. & Mulugetta, Y., *Global warming of 1.5° C. An IPCC Special Report on the impacts of global warming of 1.5° C above pre-industrial levels and related global greenhouse gas emission pathways, in the context of strengthening the global response to the threat of climate change, sustainable development, and efforts to eradicate poverty. Sustainable Development, and Efforts to Eradicate Poverty*, available at https://www.ipcc.ch/site/assets/uploads/sites/2/2019/06/SR15_Full_Report_High_Res.pdf, 2018 (accessed 15 December 2021).

[10] Naciones Unidas. Comisión Económica para América Latina y el Caribe (CEPAL), *La economía del Cambio Climático en Chile*, available at https://repositorio.cepal.org/handle/11362/35372, 2012 (accessed on: 15 Dec. 2021.

[11] Vivanco, E, *Cambio Climático: Conceptos e impactos. Asesoría Técnica Parlamentaria*. Biblioteca del Congreso Nacional de Chile, available at https://obtienearchivo.bcn.cl/obtienearchivo?id=repositorio/10221/27848/1/CC_Conceptos_e_impactos_Website_CC_2019.pdf, 2019 (accessed 06 January 2022).
[12] Ministerio del Medio Ambiente (MMA), *Atlas de Riesgos Climáticos*, available at https://arclim.mma.gob.cl (accessed 15 January 2022).
[13] Scapini, V. & Berrios, P., Circular economy in Chile: Background, law and opportunities. *WIT Transactions on Ecology and the Environment*, **253**, WIT Press, 2021. doi:10.2495/SC210161.
[14] ONU, *Nuestro futuro común*, Alianza: Madrid, 1987.
[15] Pearce, D.W. & Turner, R.K. *Economics of Natural Resources and the Environment*, JHU press, 1990.
[16] Ellen MacArthur Foundation, available at https://www.ellenmacarthurfoundation.org/ (accessed 13 December 2021).
[17] PROGRAMA DE LAS NACIONES UNIDAS PARA EL MEDIO AMBIENTE (UNEP), *Convención Marco de las Naciones Unidas para el Cambio Climático*, Ginebra, available at https://unfccc.int/resource/docs/convkp/convsp.pdf, 1992 (accessed 15 January 2022).
[18] Ministerio del Medio Ambiente (MMA), *Resumen del Estado del Medio Ambiente para la Ciudadanía*, available at https://sinia.mma.gob.cl/wp-content/uploads/2021/01/Resumen-Ejecutivo-IEMA2020.pdf, 2020 (accessed 17 December 2021).
[19] Olivares, I, *El país cumple siete de nueve criterios de vulnerabilidad frente al impacto del cambio climático*, available at https://www.latercera.com/que-pasa/noticia/pais-cumple-siete-nueve-criterios-vulnerabilidad-frente-al-impacto-del-cambio-climatico/428539/, 2018 (accessed 17 December 2021).
[20] Benavides, et al., *Opciones para lograr la carbono-neutralidad en Chile*, available at https://halshs.archives-ouvertes.fr/halshs-03410019/file/Opciones-para-lograr-la-carbono-neutralidad-en-Chile-una-evaluacion-bajo-incertidumbre.pdf, 2021 (accessed 17 December 2021).
[21] Rojas, M., Aldunce, P., Farías, L., González, H., Marquet, P. A. & Vicuña, S., *Evidencia científica y cambio climático en Chile: resumen para tomadores de decisiones*, available at https://www.cr2.cl/wp-content/uploads/2019/12/Evidencia-cient%C3%ADfica-y-cambio-clim%C3%A1tico-en-Chile.pdf, 2019 (accessed 15 January 2022).
[22] Ministerio de medio ambiente (MMA), *Economía circular*, available at https://mma.gob.cl/economia-circular (accessed 14 February 2021).
[23] Ministerio de medio ambiente (MMA), *Hoja de Ruta para un Chile Circular al 2040*, available at https://economiacircular.mma.gob.cl/wp-content/uploads/2021/07/HOJA-DE-RUTA-PARA-UN-CHILE-CIRCULAR-AL-2040-ES-VERSION-ABREVIADA.pdf (accessed 14 December 2021).
[24] Ministerio de medio ambiente (MMA), *Hoja de Ruta RCD Economía Circular en Construcción 2035*, available at https://construye2025.cl/download/187/documentos-de-interes/6321/hoja-de-ruta-rcd-economia-circular-en-construccion.pdf (accessed 14 December 2021).
[25] AZA, *Aceros AZA recicla más de 6 mil estufas en la Región Metropolitana*, available at https://www.aza.cl/noticias/aceros-aza-recicla-mas-de-6-mil-estufas-en-la-region-metropolitana/ (accessed 15 December 2021).

[26] Revaloriza, available at https://revalorizachile.cl/ (accessed 14 January 2022).
[27] Gonzalez, C., *País Circular, Industria/Centro de tratamiento de RCD, 2021 abre con un hito en economía circular: así será la primera planta de valorización de residuos de la construcción en Chile*, available at https://www.paiscircular.cl/industria/2021-abre-con-un-hito-en-economia-circular-asi-sera-la-primera-planta-de-valorizacion-de-residuos-de-la-construccion-en-chile/ (accessed 15 January 2021).
[28] Aqua, *Economía circular: Recuperación y reciclaje de redes de pesca*, available at https://www.aqua.cl/reportajes/economia-circular-recuperacion-y-reciclaje-de-redes-de-pesca/# (accessed 15 January 2022).

ASSESSING DOWNSTREAM FLOOD RISK UNDER CHANGING CLIMATE FOR BAKUN DAM IN SARAWAK

JERRY BETIE CHIN[1,2], HUSNA BINTI TAKAIJUDIN[1] & SITI HABIBAH BINTI SHAFIAI[1]
[1]Departmental of Civil and Environmental Engineering, Universiti Teknologi PETRONAS, Malaysia
[2]Hydro Department, Sarawak Energy Berhad, Malaysia

ABSTRACT

Rajang River Basin (RRB) comprise about 40% of the Sarawak State area in Malaysia. Any extreme storm event in the Upper RRB may cause a flood, affecting the downstream communities and infrastructures of the Rajang River. There are two large dams in a cascade scheme at upper RRB, Murum Dam and Bakun Dam. With the concern of changing climate impact, the future peak precipitation and peak river discharge are analysed in this study to assess the potential flood impact along the Rajang River. This study focused on developing flood modelling for downstream of Bakun Dam down to Belaga Town. The peak rainfall analysis was carried out to generate peak discharge for the return period of 1 in 50 and 1 in 100 years of historical and projected future storm events. The corresponding floodplains map pre- and post-Bakun Dam operations were generated using GeoHECRAS software. The study results show that the projected peak rainfall and peak discharge under future changing climate are increased between 6–27% and 7–30%, respectively, and this warrants attention from the relevant authorities and parties to access the flood risk downstream Bakun Dam continuously. The generated maps of pre- and post-Bakun Dam operation show that Bakun Dam can mitigate the flood from impacting the downstream structures and communities. The outcome from this study can be useful information to educate the local people and public about the benefit of having a Dam, not only for the source of power generation but also for flood mitigation.

Keywords: Bakun Dam, climate change impact, flood mapping, GeoHECRAS, peak flood discharge, peak rainfall, rainfall frequency analysis, Rajang River Basin, reservoir flood routing, RORB.

1 INTRODUCTION

Floods are a natural disaster and occur almost yearly in Sarawak, including the Upper Rajang River Basin (RRB). RRB constituted about 40% of the Sarawak state area and is located at the central of Sarawak. Due to its topography, RRB's climate is a mixture of wet and dry throughout the year. During the wet season, the rainfall intensity. Therefore, any heavy storm event upstream of the Rajang River will possibly cause a flood to the downstream communities. The flood event is commonly caused damage to properties, loss of economies and even loss of lives.

There is always a high possibility that flood events will occur again in the future. A study by Mubasher et al. [1] suggests increased annual precipitation in RRB by the end of the 21st century. In addition, logging activities and forest clearance for development upstream of RRB have caused significant sedimentation issues [2], further increased water levels during extreme precipitation, and led to flood events downstream of Rajang River.

With more hydrology and topography data available and increased concern on future precipitation impact under changing climate, the Rajang River's flood risk needs to be continuously assessed downstream [3]. Flooding is often unavoidable and unexpected; however, it can be controlled through appropriate measures to minimise losses and damage [4]. Therefore, the study of floodplains is necessary to assist Sarawak Energy and local authorities in ensuring proper mitigation measures, emergency response planning, and potentially limiting the potential destruction downstream of Rajang River communities and infrastructures [5].

ISSN: 2398-2640 (paper format), ISSN: 2398-2659 (online), http://www.witpress.com/journals
DOI: 10.2495/EI-V5-N4-316-330

A hydrology study was carried out using RunOff Routing on Burroughs (RORB) software. Thiessen Polygon method estimates the spatial distribution of six (6) rainfall stations within the Bakun catchment. The peak rainfall for 1 in 50 and 1 in 100 year return period were derived using the rainfall statistical analysis; Pearson Type III, Log-Normal and Gumbel distribution. Rainfall-runoff routing modelling was undertaken with the RORB tool to estimate peak flood discharge (PFD) for 1 in 50 and 1 in 100 year return period.

For future precipitation under changing climate, the projected rainfall data from [1] is used for this study. The peak for rainfall and discharge are analysed using RORB, and the result becomes the input for hydraulic modelling using GeoHECRAS software. GeoHECRAS is a useful tool in floodplain mapping studies because of its capabilities in performing flood routing, hydraulic modelling and surface profile analysis in a single platform.

Reservoir flood routing through Bakun spillway and power station was carried out based on the data and operation rules from [6]. Reservoir capacity, inflow hydrograph and spillway discharge capacity were the input to generate inflow–outflow hydrograph. In addition, the flood mapping pre and post Bakun Dam operations were generated to see the impact of Bakun Dam in flood mitigation.

This study aims to (1) Analyse peak rainfall and PFD at Murum-Bakun Catchment for 1 in 50 and 1 in 100 years return period based on (i) historical rainfall and (ii) future projected precipitation under changing climate and (2) generate a flood map pre and post Bakun Dam operation for 1 in 50 and 1 in 100 year return period of historical and future projected flood event using GeoHECRAS software. The study areas extent includes the upper Rajang River reach until Belaga Town. It will also be a platform for assessing the capability of GeoHECRAS for flood mapping exercises in Sarawak.

2 STUDY AREA AND DATA DESCRIPTION

2.1 Study area

Rajang River is the longest river in Sarawak, Malaysia and extends approximately 565 km in length. Major towns located downstream of the Rajang River are Belaga, Kapit, Song, Kanowit and Sibu. This study maps Rajang River's floodplain to Belaga Town, and selection was made due to Belaga Town's vulnerability to the flooding risk.

Belaga is one of the districts in the Kapit division. Its centred area is Belaga Town, with a population of 44,500 people. The Town has a maximum elevation of 73 m above sea level and a minimum of 51 metres above sea level. It is also located in a tropical area with high temperatures and high rainfall experienced throughout the year.

Due to its location in the tropical area, the rainfall in Belaga Town is generally evenly distributed throughout the year as they are more sheltered from the influence of the monsoon, with an average annual rainfall of about 2,286 mm.

Being equatorial, the temperature is generally uniform throughout the year, with an annual variation of less than 2°C. Daily temperature variations can be large; however, extreme hot or cold temperatures are rare. Seasonal and spatial temperature variations are relatively small.

Mean monthly relative humidity is 70%–90%, depending on location and time of year. Daily variations can be significant, with mean daily minimums as low as 42% during dry months and as high as 70% during wet months. In 2010, Belaga had 20.3 Mha of natural forest, extending over 87% of its land area.

A locality map of the study area and rainfall stations in Murum-Bakun catchment is presented in Fig. 1.

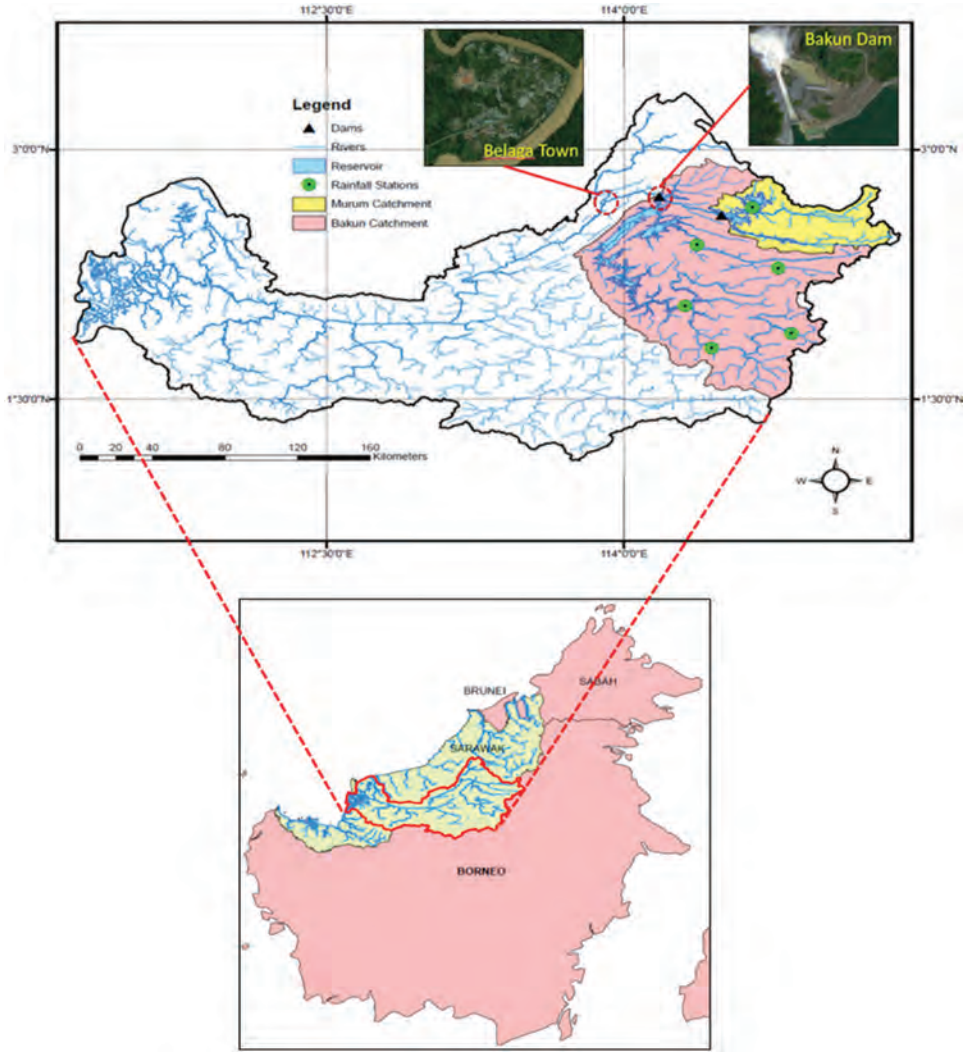

Figure 1: Locality map of the study area and rainfall stations in Borneo.

2.2 Data description

2.2.1 Rainfall and inflow data

The historical rainfall data from the 6 rainfall stations from 1976 to 2020 within the Murum-Bakun catchment were used to generate the peak rainfall for 1 in 50 and 1 in 100 year return period. These two return periods are selected as the flood boundary of the 50- and 100-year flood are often used in flood mitigation programs in high-risk flooding areas.

Climate change will impact the seasonal and annual precipitation over the RRB. Climate models are widely used for assessing climate changes impact that includes precipitation, temperatures and sea level. A global climate model simulation was referred to as the Climate Model Intercomparison Project (CMIP) [7]. The future rainfall data for this study was

generated using Climate Model Intercomparison Project Phase 5 (CMIP5). This selection is because CMIP5 is the most up-to-date set of widely used climate models [7] and is widely used for assessing the global flood risk based on the multiple atmosphere-ocean general circulation model (AOGCM) [8].

In 2014, the RCPs were first used in the Fifth Assessment Report of the Intergovernmental Panel on Climate Change (IPCC) as part of the final reports to deliver the findings. The RCPs use to encapsulate future trends. It predicts the changes in the concentrations of greenhouse gases in the atmosphere in future. The four RCPs range from very high (RCP8.5), average (RCP4.5) and (RCP2.6) are, representing the concentrations in 2100.

For this study, two Representative Concentration Pathway (RCP), representing 'medium' (RCP 4.5) and 'high' (RCP 8.5) scenarios to generate data in [1], were used to project precipitation for the year from 2022 to 2081.

2.2.2 Streamflow and outflow data

Sarawak Energy Berhad (SEB) has hydrometric stations at Murum Dam, Bakun Dam and downstream of Belaga Town. The hydrometric stations at Murum and Bakun dams record water level and inflow, and the data are stored in the centralised hydrological database. A hydrometric station downstream of Belaga Town is recording the water level. In addition, the river discharge was manually recorded from time to time to provide a rating curve for the elevation against discharge. All the inflow data has been checked for calibration and validation of the hydrological model exercise in RORB.

The required input for the Bakun reservoir flood routing calculation was obtained from Table 1 and the Bakun spillway operating manual [6].

The controlled release discharge parameters were incorporated into the reservoir routing model using the following information:

- Discharges from the Bakun Dam of 1,314 m^3/s have been assumed for normal operating conditions for electricity generation.
- The minimum operating water level of the reservoir is 195 m ASL. If the water level falls below this limit, it is assumed that normal operations will cease, and dam discharge will be limited to 150 m^3/s.
- The full supply level is 228 m ASL. If the water level exceeds this limit, it is assumed that the spillway will be opened to lower reservoir water levels. The spillway has a crest level of 209 m ASL and consists of 4 radial gates of 15 m width.

Table 1: Characteristics of Bakun HEP.

Reservoir parameter	Bakun HEP	Units
Catchment area	14,750	km^2
Full supply level (FSL)	228	m ASL*
Crest level	235	m ASL*
Minimum operating level (MOL)	195	m ASL*
Reservoir volume at FSL	35,895	Mm^3
Reservoir area (maximum flood level)	625	km^2
Active storage volume	16,466	Mm^3

* ASL – above sea level.

- Bakun releases water through the power station, via release valves or over the spillway to ensure a minimum combined release of 800 m^3/s when the reservoir level reaches EL 216 m and above to enable downstream express boat navigation.
- The reservoir application into the hydraulic model was partly conceptual, based on available topographic data and adjusted to include the specified depth-volume curves. Flow through the Bakun plant was described using two control structures in GeoHECRAS.

2.2.3 Topographic data

The delineation of catchment sub-basins and stream reaches was sourced from Interferometric Synthetic Aperture Radar (IFSAR) with a resolution of 3 m. For the river stretch from Bakun Dam to Belaga Town, Light Detection and Ranging (LiDAR) survey data were used. Both topography data are available within Hydro Department in Sarawak Energy Berhad.

3 METHODOLOGY

This study's two major components are (1) hydrology modelling – analysis for the historical and future precipitation to generate the peak rainfall and peak discharge under 50 and 100 years event and (2) hydraulic modelling – generating the flood plain mapping using GeoHECRAS, pre- and post-Bakun Dam operation for output of the first component.

3.1 Hydrology modelling

3.1.1 Areal catchment rainfall

There are six rainfall stations within the Bakun catchment. The rainfall recorded at each station represents only a specific catchment area. So naturally, the rainfall distribution is not uniform over the entire catchment, and there is a need to obtain average rainfall that can represent the entire catchment. Limin et al. [9] mentioned three conventional methods used to generate average areal rainfall: arithmetic, the Thiessen Polygon and the Isohyetal method.

Qing et al. [10] mentioned that Thiessen Polygon is one of the important methods for quantifying area rainfall. This method is also widely used because of its high accuracy on better-distributed rainfall stations, and the computation process is fast.

The Thiessen Polygon approach determines average precipitation over a Murum-Bakun catchment area. This approach was selected as it is suitable for the non-uniform distribution of rainfall stations in the Murum Bakun catchment area, which also factored in the weightage area for each gauge [11]. The World Meteorological Organisation [12], in the report, mentioned that the Thiessen polygon method was acceptable to be used for non-uniform rainfall station areas. In their research, Bruce and Clark [13] identify that the Thiessen Polygon method possesses value points for areas with fewer rainfall stations and non-uniform distributed areas. Ward and Robinson [14] view that the method has some spaces for non-uniform distribution of rainfall station and allow adjacent areas data to be incorporated in the average areas. Ahmed et al. [15] mentioned that the Thiesson Polygon method is more accurate for the non-uniform network of rainfall stations than the arithmetic method. The method is acceptable if the differences between the rainfall data are not significant. For this study, the result of average rainfall generated using the Thiessen Polygon method was not compared with other methods due to the constraint of time. Refer to Fig. 2 for the Sub-catchment area divided into polygons for the Thiessen Polygon method.

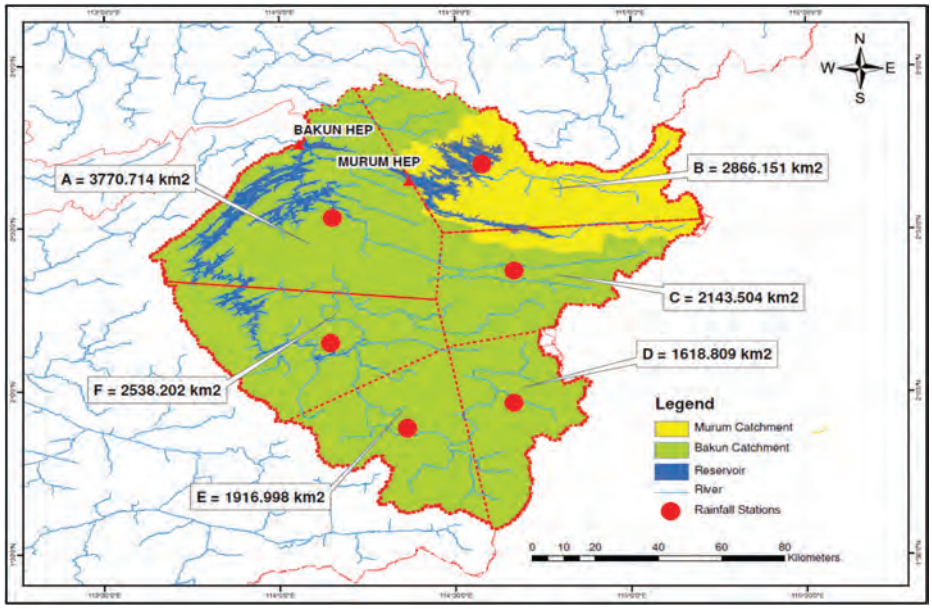

Figure 2: Sub-catchment area divided into polygons for Thiessen Polygon method.

3.1.2 Storm temporal pattern

There is a temporal pattern for the Sarawak region developed by the Department of Irrigation and Drainage (DID) through the publication of "Estimation of Design Rainstorm in Sabah and Sarawak" [16].

There are five regions in Sarawak with different Temporal Patterns, and the Bakun catchment is located in Region 3. Therefore, the temporal pattern data for Region 3 in the report was adopted for the rainfall analysis; refer to Fig. 3.

3.1.3 Analysis for peak rainfall based on historical data and future precipitation projection

Probability distribution and annual peak rainfall are commonly used to analyse the historical rainfall to manage better water resources, including flood mitigation [17]. Khudri et al. [18] stated that selecting the best fit for probability distribution to assess the extreme rainfall estimates depends on the rainfall characteristics and the selected area. Authors [19], [20] and [21] reported that normal, log-normal, log-Pearson type-III and Gumbel distributions commonly analyse peak annual rainfall. Authors [22] and [21] mentioned that Log Pearson Type III (LPIII) is the overall best fit for probability distribution for one (1) day storm events. Baghel et al. [23] consider Log-Normal (LN) and Gumbel (GBL) distribution as the best fit in their study.

For this study, Log Pearson Type III, Log-Normal and Gumbel were adopted and compared to fit maximum rainfall values in the Bakun catchment. Analyses were performed for storm periods of 1-day. Daily rainfall data from six stations for the 44 years (1976–2020) provided the basic data for the study.

3.1.4 Analysing peak discharge using RORB

There are many methods for estimating peak runoff or discharge in a catchment. One of the methods is through runoff routing technique using a network of storages like runoff routing on burroughs (RORB) model [24].

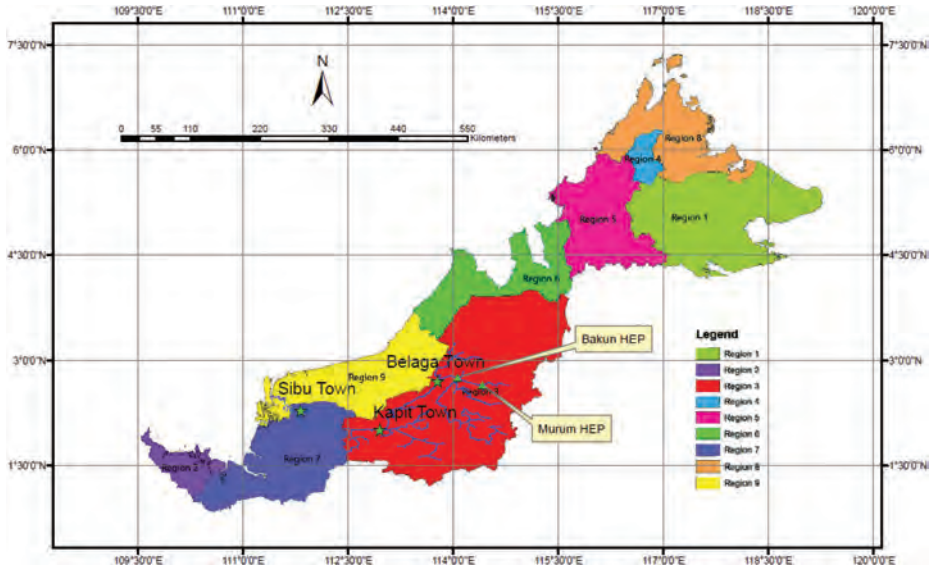

Figure 3: Region maps in Sabah and Sarawak, Malaysia.

RORB is an interactive, non-linear distributed runoff and inflow routing model. This software was chosen because of its widely recognised capabilities in flood routing. URS Australia [25] has used RORB in assessing the peak rainfall and flood routing to determine the peak discharge from 1 to 2 AEP to 1 to 2000 AEP for rivers in Bowen Basin, Australia. A similar exercise has been performed by a SMEC consultant using RORB to develop Baleh and Baram Hydro Electric Project (HEP) in Sarawak, Malaysia [26, 27]. The catchment area for these two projects carried by SMEC consultants is comparable to the Murum Bakun catchment.

The software is relatively easy to use and only require two inputs, K_c and m, for the user to determine. It has also been widely used in many catchments studies in the Asia Pacific and Malaysia for flood risk assessment. For example, Selvalingam et al. [28] found that the RORB model was able to simulate the runoff hydrograph and the result is well fitted with the recorded hydrographs in their study in Singapore. The step by step using RORB is detailed in sections 3.1.5–3.1.7.

3.1.5 Catchment delineation and reaches and nodes

RORB model setup begins with the catchment modelling. The catchment was divided into 114 sub-catchments, river links and nodes were connected utilising a combination of LiDAR and IFSAR survey data of the Murum–Bakun catchment [3]. The formed series of links and nodes represent the reaches of flow and the nodes of each sub-catchment, as shown in Fig. 4. Parameters like river length and sub-catchment area were defined and determined. The storage discharge relationship in the RORB model is:

$$S = 3{,}600 * K_c * K_{cri} * Q^m, \quad (1)$$

where S = storage in reach (m^3), Q = discharge (m^3/s), K_c and m are main catchment parameters that can be obtained through trial and error fitting, known as a fit run in RORB model setup, while K_{ri} = relative routing lag parameter for the specific reach and storage [25].

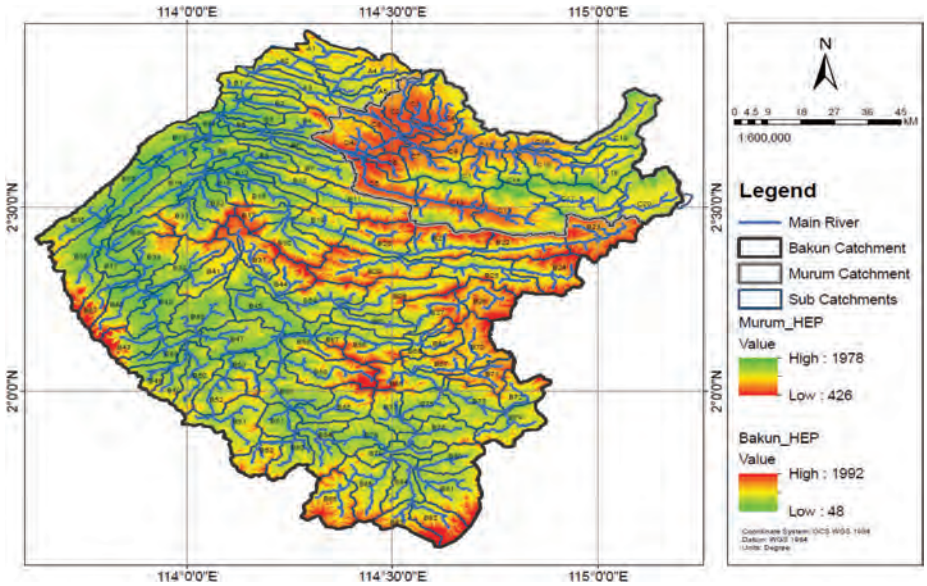

Figure 4: RORB model layout.

3.1.6 K_c and m values in RORB

In the RORB model, catchment lag and non-linearity are controlled by K_c and m, respectively. The selection of K_c and m values was performed through the fit run. A wide range of peak discharges of the recorded inflow was selected to estimate the K_c and m values. Trial and error methods were performed by adjusting the K_c and m values range to obtain the best fit of the recorded inflow hydrograph. The selected K_c and m values were tested against other peak discharge graphs and provided an acceptable fit with accuracy within +/-15% [24], which is considered good accuracy. Among all the fit runs, the m value of 0.75, K_c value of 152 and 0 for initial loss were adopted as the best fit for all the storm events in the study area.

3.1.7 Reservoir flood routing

Reservoir routing is an arithmetical process to determine the magnitude changes over time and shape of a transitioned flood wave passed dam structure. The flood wave travels from the reservoir's surface level to the outflow structures such as spillways, low-level outlets and turbines at the power station. Complex calculations are made factoring in the elevation storage and elevation-discharge data of the reservoir.

There are two common methods used in flood routing; hydraulic and hydrological. A hydrological method is selected for this study as it is simpler and only requires an inflow hydrograph to generate outflow. One of the hydrological methods used is Modified Puls. It was selected for this study because the reservoir eliminates its suitability in flood wave impact.

A study by Ogbonna et al. [29] stated that the prediction for outflow and measured outflow are close and have low standard error compared to other models. Modified Puls routing also is typically used for reservoir routing where a unique storage-outflow relation is available [30]. Reservoir flood routing will be performed based on a relationship between reservoir storage and outflow. The continuity form for each time step will be calculated using equation (2):

$$\left(\frac{S_t}{\Delta t}+\frac{O_t}{2}\right)=\left(\frac{I_{t-1}+I_t}{2}\right)+\left(\frac{S_{t-1}}{\Delta t}-\frac{O_{t-1}}{2}\right), \quad (2)$$

where S_t = storage for each increment, I_t = inflow, O_t = outflow and t = time step.

3.2 Hydraulic modelling

3.2.1 Generate flood using GeoHECRAS

GeoHECRAS is a useful tool in floodplain mapping studies because of its capabilities in performing food routing, hydraulic modelling and surface profile analysis in a single platform [5]. In addition, it saves much time compared to a more standard approach using HEC-RAS coupled with Geographic Information System (GIS) tools.

Digital elevation map of the study area was obtained from LiDAR data and processed using GeoHECRAS to get the elevation grid. A downstream of Rajang River reach until Belaga Town was selected to cover resettlements along the river and assess the flood risk to Belaga Town.

A river centreline was drawn along the river alignment displayed on the base map layer using the Draw River Reach tools in GeoHECRAS software. Then, the next step is to draw cross-sections on the pre-determined intervals. Finally, Manning's *n* values were assigned for the main channel and over banks based on the software's default values.

The boundary condition for downstream and upstream river reach was selected, and the software calculated the boundary slope. Flood flows under 1 in 50 and 1 in 100 years return periods were specified in steady-state flow data, and analysis was performed using a computed steady function in GeoHECRAS.

The rating curve for Pelagus gauging station was selected for calibration as it has the most actual discharge measurement compared to other gauging stations downstream of Bakun Dam. The observed water surface level (WSL) of the peak discharge at the Pelagus gauging station was obtained from the available rating curve of elevation-discharge data. It was then compared with the simulated WSL in the software. This is done in a steady flow calibration function. If these two data were found to have a significant difference in value, the model needs to be calibrated by adjusting Manning's n values for both the main channel and the over banks. Once the model is calibrated, flood maps under different return period floods were generated for visualisation in a GIS map.

4 RESULT AND DISCUSSION

4.1 Current and future rainfall analysis

The peak rainfall for 1 in 50 and 1 in 100 years return period was analysed as per Section 3.1.3. Figure 5 shows the rainfall depth at different return periods computed using statistical analysis methods. The maximum rainfall for Bakun catchment for 1 in 50 years return period is 148 mm, and 171 mm for 1 in 100 years return period based on the historical rainfall. The same would be expected for the projected rainfall under RCP 4.5 and RCP 8.5. However, looking at Fig. 5 for 1 in 100 years event. The peak rainfall for the RCP4.5 2022–2051 is higher than RCP4.5 2052–2081. The result does not behave as expected and does not align with the result for RCP4.5 under 50 years event. The difference could be due to some errors in input for perturbation exercise in CMIP5 modelling. The next study on this subject will reassess and fix the difference mentioned above.

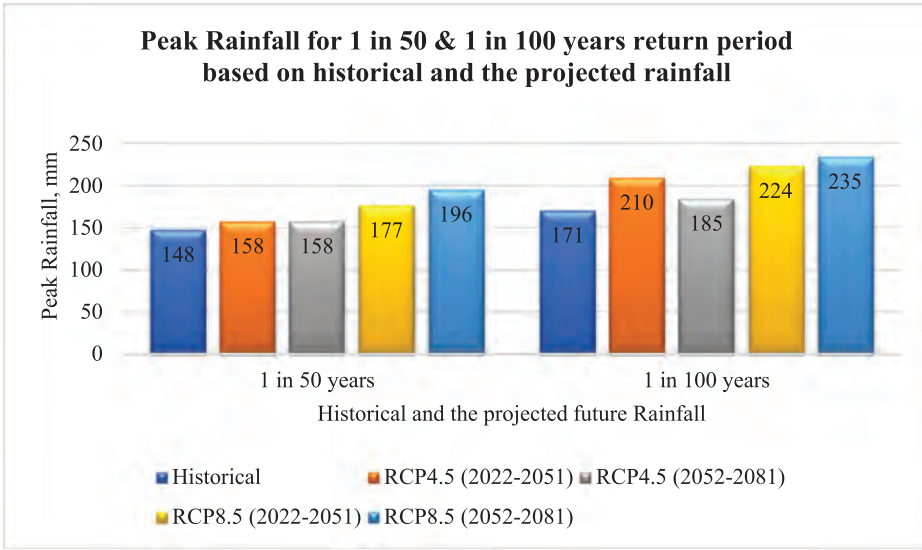

Figure 5: Peak rainfall for 1 in 50 and 1 in 100 years return period based on historical and projected rainfall.

There are increases in precipitation observed for the latter part of the 21st century, under RCP4.5 and RCP8.5 for 2022–2051 and 2052–2081. For RCP4.5 2022–2051 and 2052–2081, the peak rainfall is increased about 6–22% each under 1 in 50 years return period and 1 in 100 years return period. Meanwhile, for RCP8.5 2022–2051 and 2052–2081, the peak rainfall is increased about 16–27% each under 1 in 50 and 1 in 100 years return period.

4.2 Peak flood analysis under historical and future precipitation

Methods employed to evaluate peak discharge in the upper RRB have produced a range of estimates of peak design discharge, as in Fig. 6. The peak discharge value is higher in the more significant return period and increases toward the 21st century. For example, the peak discharge for 1 in 100 years return period from historical data, 8,714 m³/s, is higher than 7,358 m³/s, a peak discharge for 1 in 50 years return period. The peak discharge values under RCP4.5 and RCP8.5 for 2022–2051 and 2052–2081 are higher, about 7–31%, than peak discharge from historical data. Again, the peak discharge for RCP4.5 under 100 year events of 2022–2051 compared to 2052–2081 are directly affected by the peak rainfall from the same parameter.

4.3 Flood mapping for pre- and post-Bakun Dam operation

The WSL (m) for the peak discharges of 1 in 50 and 1 in 100 return periods for the Pelagus gauging station was generated using the available rating curve of average discharge (m³/s) against the WSL (m) graph for Pelagus gauging station. These levels were categorised as observed WSL. In addition, the WSL generated from the simulation of steady flow simulation was categorised as calculated WSL.

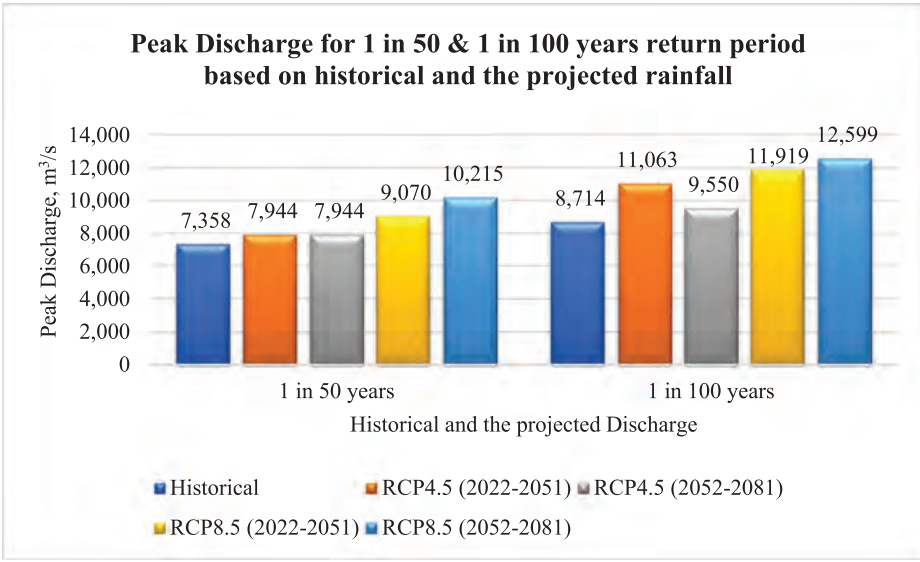

Figure 6: Peak discharge (m³/s) in 1 in 50 & 1 in 100 years return period based on historical and the projected future discharge.

The first step for calibration involves assigning default Manning's value, *n*, for the river cross-section [31]. The default value of 0.032 was used for the main channel and 0.045 for the over banks in the steady flow analysis step. Next, the observed WSL will be compared against the calculated WSL. There are differences at the first analysis run, and the model needs to be calibrated. The calibration was completed with *n* values of 0.032 and 0.040 for the main channel and river overbank.

The peak discharge recorded at Pelagus gauging station was 4,390 m^3/s with a WSL of 21.55 m. The calculated WSL for 4,390 m^3/s using GeoHECRAS was 20.94 m, and these two figures are quite close to each other.

The calibration model was evaluated using Nash-Sutcliffe efficiency (NSE) for model performance. Moriasi et al. [32] mentioned that NSE rating can be categorised as NSE = 1.0 is the perfect fit, NSE > 0.75 is a very good fit, NSE = 0.64–0.74 is a good fit, NSE = 0.5–0.64 is a satisfactory fit and NSE < 0.5 is an unsatisfactory fit. In general, an NSE of more than 0.5 is considered satisfactory in performance rating. The NSE formula has calculated NSE value was 0.88, which falls under a very good fit category. The observed and calculated WSL for different return period floods for the river reach at Upper Rajang River are presented in Table 2.

Figure 7 shows the Belaga Town condition impacted by the flood under 1 in 50 years and 1 in 100 years return period based on peak discharge data from historical RCP4.5 and RCP8.5 pre-Bakun Dam operation. The figure shows that more than 50% of the Belaga Town area is inundated or submerged under the water under these flood events.

However, Fig. 8 shows that with Bakun Dam is in operation, the potential flood impact at Belaga Town is mitigated. This is because the extreme discharge upstream due to storm events is contained by Bakun reservoir. When the reservoir level reaches full supply level (FSL) of 228 mean above sea level (masl), the water will be released through spillway and

Table 2: Observed and calculated WSL at Pelagus gauging station for different return period floods

Flood event (year)	Discharge (m^3/s)	Observed WSL (m)	Calculated WSL without reservoir routing (m)	Calculated WSL with reservoir routing (m)
Calibration	4,390	21.55	20.94	Not Applicable
1 in 50	7,358	23.94	23.72	16.88
1 in 100	8,714	24.76	24.83	16.88
RCP4.5 (1 in 50)	7,944	24.31	24.22	16.89
RCP4.5 (1 in 100)	11,063	25.95	26.59	16.89
RCP8.5 (1 in 50)	10,215	25.55	25.98	17.09
RCP8.5 (1 in 100)	11,919	26.61	27.59	17.09

Figure 7: Flood plain map for Belaga Town under 1 in 100 years return period for historical, RCP4.5 and RCP8.5 pre-Bakun Dam operation.

turbines. Figure 6 also shows that with Bakun Dam's existence, the simulated water level at Pelagus gauging station is about the normal water level, showing the efficiency of Bakun Dam in mitigating the extreme flood under 1 in 50 and 1 in 100 years event.

5 CONCLUSIONS AND RECOMMENDATION

This study analyses the peak rainfall under historical data (1976–2020) and projected future precipitation of 2022–2081 for Murum Bakun catchment from the Coupled Model Intercomparison Project Phase 5 (CMIP5). Figures 4 and 5 observed that peak rainfall and peak discharge are increased between 6–27% and 7–30%, respectively, compared to peak rainfall

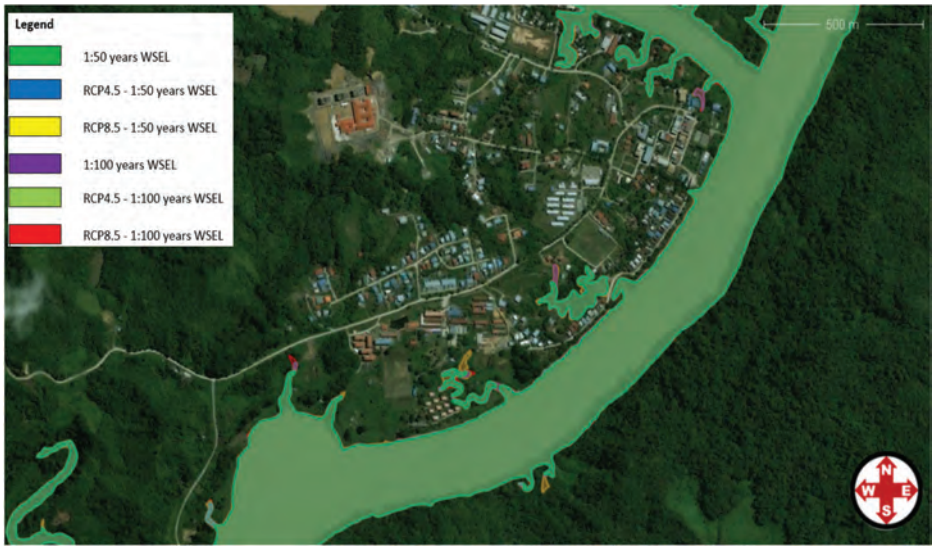

Figure 8: Flood plain map for Belaga Town under 1 in 100 years return period for historical, RCP4.5 and RCP8.5 post Bakun Dam operation.

and peak discharge based on historical data. The increase in future precipitation projection warrants the relevant authorities and asset owners' attention to assess the flood risk continuously in the future toward the structures and communities downstream of Bakun station.

Figures 7 and 8 shows the flood plain mapping under 1 in 50 years and 1 in 100 years return period for Belaga Town pre and post-Bakun Dam operation. Post Bakun Dam operation, the flood risk is reduced significantly as the Dam collects and holds the reservoir waters until the level reaches FSL at 228 m ASL. When they reach 228 m ASL, the reservoir waters will be released back to the downstream river at a controlled speed through the spillway. Therefore, with Bakun Dam in operation and with a properly planned and controlled release of water downstream of the Dam, it was concluded that the flood occurrence to the downstream communities would be further minimised, especially in Belaga Town.

With frequent flood events in the past at upper RRB and the increased precipitation projection, this study's findings will provide useful information for flood mitigation and preparation for emergency action plans. Therefore, the recommendation for the next steps of the study are summarised as follows:

1. To extend flood plain mapping under the peak discharge up to Probable Maximum Flood (PMF) for historical and future precipitation of RCP4.5 and RCP8.5 for 2022–2081 to assess Belaga Town susceptibility toward the most extreme flood risk.
2. To generate the flood mapping post-Bakun operation for item 1 to assess the functionality of Bakun station in mitigating flood to the downstream river.

Floodplain mapping is crucial in development planning, sustainable water resource management and advanced emergency action plans. The software used for this study, GeoHECRAS, demonstrates a useful and user-friendly tool in hydraulic modelling and flood mapping exercise. The software also is capable of performing flood routing, hydraulic modelling

and surface profile analysis in a single platform. All the hydraulic modelling and flood plain mapping process is done in a single software and has saved much time compared to the most commonly used method, a combination of HEC-RAS and GIS tools.

ACKNOWLEDGEMENTS

This study is funded by Sarawak Energy Berhad, Malaysia (SEB), under a Master research program. The authors would like to thank SEB for approving a research grant and using the data for hydro Dams for this study. The authors are also thankful to the Department of Irrigation and Drainage, Sarawak, to provide the relevant rainfall data for the RRB.

REFERENCES

[1] Hussain, M., Climate change impact on water resources availability and hydropower production in Sarawak, Malaysia: Universiti Tecknologi Petronas, Malaysia, 2018.

[2] Ling, T.Y., Soo, C.L., Sivalingam, J.R., Nyanti, L, Sim, S.F., Grinang, J., Assessment of the Water and Sediment Quality of Tropical Forest Streams in Upper Reaches of the Baleh River, Sarawak, Malaysia, Subjected to Logging Activities. *Journal of Chemistry*, 2016, 8503931, 2016.

[3] Chin, J., Yusof, W., Hussain, M., Estimation of frequent peak flood discharge for the upper Rajang river basin in Sarawak, Malaysia. WIT Transactions on the Built Environment: WIT Press, p. 8, 99–106, 2020.

[4] Wang, Z., Lai, C., Chen, X., Yang, B., Zhao, S., Bai, X., Flood hazard risk assessment model based on random forest. *Journal of Hydrology*, 527, 1130-41, 2015.

[5] Bhandari, R., Parajuli, R., Lamichhane, G., Alyami, A., Kalra, A., Ahmad, S., et al. Utilizing Civil Geo-HECRAS Capabilities for Floodplain Mapping of Colorado River in Texas during Hurricane Harvey, 387-97 p, 2018.

[6] Hidro, S., Spillway – Operation, Surveillance and Maintenance Manual of Civil Works 2012.

[7] Schramm, P.J., Uejio, C.K., Hess, J.J., Marinucci, G.D., Luber, G., Climate models and the use of climate projections: a brief overview for health departments.

[8] Hirabayashi, Y., Tanoue, M., Sasaki, O., Zhou, X., Yamazaki, D., Global exposure to flooding from the new CMIP6 climate model projections. *Scientific reports*, 11(1), 3740, 2021.

[9] Limin, S., Oue, H., Takase, K., Estimation of Areal Average Rainfall in the Mountainous Kamo River Watershed, Japan. Journal of Agricultural Meteorology. 2015;71:90-7.

[10] Qing, Z., Gang, L., Zhiting, Z., editors. Improvement and optimization of Thiessen polygon method boundary treatment program. 2009 17th International Conference on Geoinformatics; 2009 12–14 Aug. 2009.

[11] Kadhim, Y., Allami, A., Al-Shamarti, H., Calculation of the mean annual rainfall in Iraq using several methods in GIS, 1156-60, 2020.

[12] Guide to hydrometeorological practices Geneva, World Meteorological Organization, 1965, Fr.S. 30. (WMO Report no 168. TP.82.). *Journal of Hydrology*, 4, 354, 1966.

[13] Bruce, J.P, Clark, R.H., CHAPTER 1 – INTRODUCTION. In: Bruce JP, Clark RH, editors. Introduction to Hydrometeorology: Pergamon, p. 1-4, 1966.

[14] Ward, R.C., Robinson, M., Principles of hydrology/R.C. Ward, M. Robinson. Third edition. ed. London: McGraw-Hill, 1990.

[15] Ahmed, K.F., Wang, G., Silander, J., Wilson, A.M., Allen, J.M., Horton, R., et al. Statistical downscaling and bias correction of climate model outputs for climate change

impact assessment in the U.S. northeast. *Global and Planetary Change*, 100, 320-32, 2013.

[16] Malaysia DoIaD. HP 26: Hydrological Procedure. Estimation of Design Rainstorm in Sabah and Sarawak (Revised and Update 2018). 2018.

[17] Ng, J.L., Yap, S., Huang, Y., Noh, N., Al-Mansob, R., Razman, R., Investigation of the best fit probability distribution for annual maximum rainfall in Kelantan River Basin. *IOP Conference Series: Earth and Environmental Science*, 476, 012118, 2020.

[18] Khudri, M.M., Sadia, F., Determination of the Best Fit Probability Distribution for Annual Extreme Precipitation in Bangladesh. *European Journal of Scientific Research*, 103, 391-404, 2013.

[19] Singh, B., Rajpurohit, D., Vasishth, A., Singh, J., Probability Analysis for Estimation of Annual One Day Maximum Rainfall of Jhalarapatan Area of Rajasthan. *Plant Archives*, 12, 1093–100, 2012.

[20] Aksoy, H., Use of gamma distribution in hydrological analysis. *Turkish Journal of Engineering and Environmental Sciences*, 24, 419-28, 2000.

[21] Amin, M., Rizwan M., Alazba, P., A best-fit probability distribution for the estimation of rainfall in northern regions of Pakistan. *Open Life Sciences*, 11, 2016.

[22] Nithiyanantham S., Probability analysis for consecutive-day maximum rainfall for Tiruchirapalli City (south India, Asia). *Applied Water Science*, 2015.

[23] Baghel, H., Mittal, H.K., Singh, P.K., Yadav., K.K., Jain, S., Frequency Analysis of Rainfall Data Using Probability Distribution Models. *International Journal of Current Microbiology and Applied Sciences*, 8, 1390–6, 2019.

[24] E.M., Laurenson, RGM, and R.J., Nathan., RORB Version 6 – Runoff Routing Program User Manual, Monash University and Hydrology and Risk Consulting Pty Ltd, January 2010. 2010.

[25] BM Alliance Coal Operations Pty Ltd A., Flood Hydrology Technical Report, Red Hill Mining Lease EIS. 2013.

[26] SMEC, Baleh Hydroelectric Project – Hydrology review and update, Sarawak Energy Berhad, July 2013. 2013.

[27] SMEC., Baram Hydroelectric Project – Hydrology review and update, Sarawak Energy Berhad, June 2014. 2014.

[28] Selvalingam, S., Liong, S.Y., Manoharan, P., Application of RORB model to a catchment in Singapore. JAWRA *Journal of the American Water Resources Association*, 23, 81-90, 2007.

[29] Ogbonna, D., Okoro, B., Osuagwu, J., Application of flood routing model for flood mitigation in Orashi River, South-East Nigeria. *Journal of Geoscience and Environment Protection*, 05,31-42, 2017.

[30] Hussain, A., Flood Routing in Reservoir using Modified Puls Method. *International Journal of Science and Research (IJSR)*, 2018.

[31] Chow, V.T., *Open-channel hydraulics*, New York: McGraw-Hill, 1959.

[32] Moriasi, D., Arnold, J., Van Liew, M., Bingner, R., Harmel, R.D., Veith, T., Model evaluation guidelines for systematic quantification of accuracy in watershed simulations. *Transactions of the ASABE*, 50, 2007.

DIFFUSION OF INNOVATION – IMPLEMENTATION OF CONSTRUCTED WETLANDS IN THE KATHMANDU VALLEY, NEPAL

Z. BOUKALOVÁ[1,2], J. TĚŠITEL[2,4] & B. D. GURUNG[3]
[1]VODNÍ ZDROJE, a. s.; Czech Republic.
[2]METCENAS o. p. s.; Czech Republic.
[3]University of Life Sciences, Faculty of Tropical and Subtropical Agriculture, Czech Republic.
[4]AMBIS, Czech Republic.

ABSTRACT
Constructed wetlands (CW) can be considered an efficient municipal wastewater treatment technology, suitable to be used on a local level in both rural and urban environments. This technology is popular and normally used in Europe having the attributes of a success story – cheap in investment and simple in operation. Nevertheless, the transfer of this technology to developing countries is a challenge of some kind, the main reason being a different technological and cultural context there. The paper discusses the implementation process of CWs in the Kathmandu Valley, Nepal, the East. The concept of diffusion of innovation is used as the guideline, namely two of its perspectives – motivation of end-users to implement the technology, and the way the information about the technology is spread. Empirical data were obtained by use of semi-standardized interviews with the three types of stakeholders involved, the end-users themselves, local authorities, and pertinent NGOs. On this basis, three main reasons (motivations) to implement CWs for municipal sewage water treatment were found, which can appear in a combination – environmental-religious, pragmatical and prestigious. In parallel, three communication channels were identified which can be metaphorically named professional enlightenment, peer influence (or exempla trahunt) and direct external aid.
Keywords: communities, constructed wetlands, diffusion of innovation, land management, Nepal, pollution control, water management.

1 INTRODUCTION

In Nepal, as in other Southeast Asian countries, the urban areas are spontaneously expanding. Regional and urban planning is obviously not enough to keep up, including the design of infrastructure for wastewater management [1].

As to the Kathmandu Valley, the major sources of wastewater are domestic, industrial, commercial, agricultural and storm waters [2]. The High-Powered Committee for Integrated Development of Bagmati Civilization (HPCIDBC) was established in 2009 to work with the objective of keeping the Bagmati River and its tributaries clean by preventing, or at least minimizing, the direct discharge of solid and liquid wastes into the river and conserving the river system within the Valley. The Committee planned to construct a trunk sewer pipeline along either bank of the river, secondary sewer pipelines and wastewater treatment plant (WWTP), along with the river training works [2]. Subsequently, five centralized municipal WWTPs were constructed within the Kathmandu Valley [3].

However, considering the volume of wastewater production, the volume of treatment is not satisfactory [4]. In 2013, a comprehensive solution to the situation was proposed: The Kathmandu Valley Wastewater Management Project (KVWMP) of the government of Nepal, which, however, was still not completed in 2019 (in December 2019, testing of its part, the newly reconstructed Guheshwori WWTP, was launched) and during the COVID pandemic stagnated. This project was aimed at improving wastewater services in Kathmandu

ISSN: 2398-2640 (paper format), ISSN: 2398-2659 (online), http://www.witpress.com/journals
DOI: 10.2495/EI-V5-N4-331-341

Valley through extensive investment in rehabilitating and expanding the sewerage networks, modernizing, and constructing WWTPs, and supporting operational and financial improvements and capacity building. The work included the rehabilitation and construction of new WWTP at Kodku (Patan), Sallaghari (Bhaktapur), Dhobighat (Kathmandu) and Guheshwori (Kathmandu). All WWTPs designed under this project were supposed to be rehabilitated or constructed on the land area owned by the government. This should have ensured their proper operation, continuous specialist supervision as well as sufficient electric power supply [5].

Nevertheless, the centralized wastewater treatment systems appeared to be questionable, mainly due to the high cost of operation, discontinuous power supply, lack of proper maintenance and lack of proper technical workforce to address the problem [3]. Instead of the centralized municipal wastewater treatment systems, decentralized systems (DEWATs) that imitate the purification function of natural wetlands, started to be promoted in Kathmandu at varied levels, including households, institutions and communities [2]. The systems are designed to treat the greywater from the household through a well-designed and aesthetically pleasing wetland, pond and water fountain systems. The treated water is reused for gardening, agriculture, or domestic use. The efficiency of the system is measured from 80% to 98% removal of both biological oxygen demand and chemical oxygen demand [6]. In addition to its efficiency in removing pollutants, this technology is cheap in investment and simple in operation. As such it can be considered appropriate for application in Nepal, as these attributes seem to help in overcoming obvious obstacles new high-tech technologies face when implemented in situations that do not meet the European standard.

The pilot-scale constructed wetland (CW) technology was implemented in Nepal in 1997, by the Environment and Public Health Organization (ENPHO), in collaboration with the Institute for Water Provision, University of Agricultural Sciences, Vienna, Austria. Local government units, UN-Habitat, ENPHO and users' community groups supported the use of CW technology [1].

The CW technology is popular and normally used in Europe. Although it has the attributes of a success story – cheap in investment and simple in operation – its transfer to developing countries is a challenge of some kind, the main reason being a different cultural context there. It can be documented, among others, by experiences the ENPHO obtained when evaluating the first decade since the technology had been introduced into the country. They found that this simple and cost-effective system can be used to treat various types of wastewaters, ranging from greywater to leachate and septage. However, despite the enormous potential for the use of CWs for wastewater treatment, there are still some challenges that slow down the process of the practical application of this technology in Nepal. These challenges can be found discussed at length in the pertinent professional literature [7], [8], [9], [10], and many others, and simply listed in the following way:

- The CW technology is relatively new to Nepal, and thus, it is unknown to most of the population. Due to the lack of awareness of this technology, it is often difficult to convince people that it will work;
- although CWs are cheaper than centralized wastewater treatment systems, the CW technology still can be expensive for low-income populations. Hence, it is still difficult to convince people to invest in the technology instead of just discharging effluent into the river;
- it is a low maintenance system, nevertheless, people often think it is a no-maintenance system. This sometimes leads to carelessness in operation and maintenance requirements such as checking for blockage in the pipes, harvesting the plants, etc;

- wastewater treatment is not a priority for the city governments, private industrialists, or institutions, due to the lack of strong legislation and standards; and
- on the individual level, one of the biggest challenges is the lack of land for CW construction since land is very expensive in city areas and people occupy land only for house building construction, and no open free space is available.

The present situation does not differ from the picture drawn above, the practical implementation of CW technology into practice sustains still a challenge.

The problem of the application of new technologies, obviously called the application of innovations, is a more general theme, however. The process of adopting new technologies has been studied for over 30 years, one of the most popular adoption models being explained by Rogers [11]. Much research from a broad variety of disciplines has used the model as an explanatory framework. The papers [12] and [13] mention several of these disciplines as political science, public health, communications, history, economics, technology and education, and define Rogers' theory as a widely used theoretical framework in technology diffusion and adoption. In fact, much diffusion research involves technological innovations, so Rogers usually used the words "technology" and "innovation" as synonyms and defines diffusion as the process in which an innovation is communicated through certain channels over time among the members of a social system [11]. As can easily be derived from the definition, the nature of innovation, communication channels, time and social system can be considered the four key components that form the process by which the new technology is supposed to spread out.

In the context discussed here, it is important to point out that for Rogers, the technology is composed of two parts: hardware and software. While hardware is "the tool that embodies the technology in the form of a material or physical object", software is "the information base for the tool" [1]. The "software", in our case, can be interpreted as the social and cultural context in which the technology is discussed and interpreted, and, consequently, decided to be or not to be implemented. The paper addresses the two components of Rogers model, namely communication channels and social system in terms of the motivation of users with the aim to understand ways by which the technology is promoted, and reasons that led users to apply this technology in practice.

2 METHODS USED

The aim of the research was to understand the situation; therefore, qualitative methods were preferred for information gathering and processing [14] and [15]. The identification of the unit of analysis was based on the theoretical presumption that refers to the Thomas theorem [16] and early works of the Chicago School [17], namely that social reality is dynamic, and socially constructed by all actors involved in a particular situation. Based on that, a particular CW, either functioning or out of operation, was used as the unit of analysis, defined as a situation in which three actors participate:

- Users, i.e. local communities, institutions (both governmental and non-governmental), and private owners,
- local authorities, that set the political and economic context, i. e. mayors, regional politicians, etc., and
- NGOs (from local to internationally recognized) that mediate financing, building and operation of the CW.

The basic set was defined as the CWs in the Kathmandu Valley, identified by the list elaborated by the ENPHO. In total, it was comprised of 60 CWs existing within the Kathmandu Valley operated by a variety of users. Having the list at disposal, the next step was the try to contact the persons responsible and arrange a meeting in situ. It appeared, however, that out of the total 60 CWs, only 23 responded in some way which enabled us to visit these respondents and consider them as the sample (see Table 1).

The field campaign was realized in the form of semi-structured interviews with key informants in situ, i.e. next to the CW, or in the office of a pertinent authority or an NGO (Fig. 1). The narration was structured primarily along with the following themes, the scheme however was flexible enough to cope with local peculiarities:

Table 1. The structure of the sample.

Type of the user	State of the constructed wetland			
	Fully functioning	Partly functioning	Not functioning	In total
Schools	1	1	3	5
Communities	1	1	3	5
Private houses	1	1	1	3
Research institutions	2	0	4	6
Hospitals	1	0	1	2
Monasteries	0	0	1	1
Industry	1	0	0	1
In total	7	3	13	23

Figure 1: The interview in Sunga Thimi village.

- "Ownership" of the CW and stakeholders involved, as well as the reasons to decide for choosing the technology, and
- conditions of the system maintenance, and the prospect of the future (more details about the narratives can be found in [18].

Being there enabled us to combine interviewing with observation. We were fully aware of the fact, that Nepal is "another world" distant from our understanding both in terms of language and, particularly, in terms of culture. To cope with the challenge, three interviewers were present in situ together, two Czech, and one Nepali, the latter playing the role of "interpreter" mediating the questions asked in English to fit the local context. All the interviews were then ultimately held in Nepali, audio-recorded, subsequently transcribed verbatim, and translated into English. The short films and photo documentation of the terrain research were made. Finally, all the texts became the subject of thematic analysis.

3 RESULTS

3.1 Channels of communication

As said earlier, the technology was installed for the first time in the Kathmandu Valley in 1997. Since it started to spread out in various ways. Behind the variability, however, three more general patterns can be identified.

3.1.1 ENPHO – interested end-user

National NGO named ENPHO (Environment and Public Health Organisation) appeared to play a pivotal role in the process of CW technology propagation both in terms of direct construction and promotion among the public, including capacity building, as it can as well be documented by their webpage, where these activities represent an important part of their portfolio [19].

This to some extent unique position can be explained by the fact that "ENPHO was there" when the technology was for the first time introduced into the country. The external professional assistance provided by BOKU at that time, and further even pronounced the chance of the ENPHO to take the almost monopolistic position at the market or at least the position of the indispensable actor operating there. ENPHO identifies the potential user and addresses it with the offer that it (ENPHO) can mediate the whole process, i.e. establish the consortium of financing the project, including co-financing by the end-user, organize the building of the CW, and assist in monitoring the CW operation. The alternative variant is that the interested potential user addresses the ENPHO with the request. The other steps are identical to the above. This channel can be metaphorically called a "professional enlightenment with the business aspect" since ENPHO partly lives from this money. Over time, as well other NGOs, such as e.g. LUMANTI, entered the market, however as cooperating institutions only, without any factual effect on the leading role of the ENPHO in this field of activities.

3.1.2 Exempla trahunt

Meaning replication of the technology based on "following already existing and proved example". The information on the (somewhere) functioning CW is crucial in this case. Hence the publicly accessible CWs seem to play a pivotal role, or the information spread in the hearsay mode. The story of the CW designed by the Shreekandphur community is somewhere in the middle and can serve as a typical example. The community in fact replicated the model

existing in the Dhulikhel Hospital. The chef of the community saw the CW when visiting the hospital and was inspired. As he was in very good personal relations with the manager responsible for the hospital wastewater treatment, he was explained informally about the pros and cons of this kind of wastewater cleaning and, consequently, provided by the appropriate contacts which in the end enabled to build and operate the CW in the Shreekandphur.

3.1.3 Direct foreign aid

This model represents initiatives realized and funded by international projects and can be applied not only to CWs but more generally. It is a matter of fact, that these projects follow their own logic dictated by donor agencies. It is not surprising then, that their objectives are defined to meet requests of particular calls, rather than local conditions and needs. Only afterward they are negotiated with local or regional potential end-users with the aim to find the compromise – to fulfil the project main objectives and satisfy local needs. It, in some cases, may lead to the situation when the end-user does not feel to be the "owner" of the project output and cease to take care of it immediately after the project life is over. There are of course success stories, usually in the cases, where the historical and cultural role of a community is placed at the centre of the process via 'community-led' planning [20]. Horizontal CW, combined with rainwater harvesting for the Dhapakhel municipality can be mentioned, realized under the EUREKA BIORESET project, as the solution of the water scarcity in the area, and the Nala CW, financed by UN-HABITAT, Nepal, as demonstration projects for community-based wastewater treatment. CW in Nala addresses the problems experienced in the previous examples of Sunga and Sreekhandapur and adopts alternative solutions accordingly [21].

3.2 Motivation

As the channels of communication, the motives as well represent a relatively broad array of reasons to be found behind the building and operating of CWs. These categories or classes, however, exist in a non-exclusive way. In fact, the classification is arbitrary in the sense that reasons named below exist, however in the case of particularly CW they can appear in combination, with one motivation obviously prevailing.

3.2.1 Environmental religious

This category represents the viewpoint merging two dimensions "expert" and spiritual, both addressing, in fact, the same issue – humility. The expert dimension is based on the conviction, that pollution negatively affects the river and that only clean water should be released to the watercourse to keep the river living. The community of Sano Kokhana can be used as an example of this approach. With the comment, they made that it is a pity, that they are the only village on the Bagmati riverbank that goes this way and others, either up or downstream, do not follow this way.

The spiritual dimension addresses the same issue but uses different "language". Assessed from this standpoint, any pollution of water, regardless underground or in the river, is a transgression, a sin against God's will (Fig. 2). In the case of Satya Sai Sikshya Sadan ecclesiastic school, the care of water adopted as well educational aspects, as the CW as an appropriate system of wastewater treatment is used for demonstration in teaching as can be illustrated by Fig. 3.

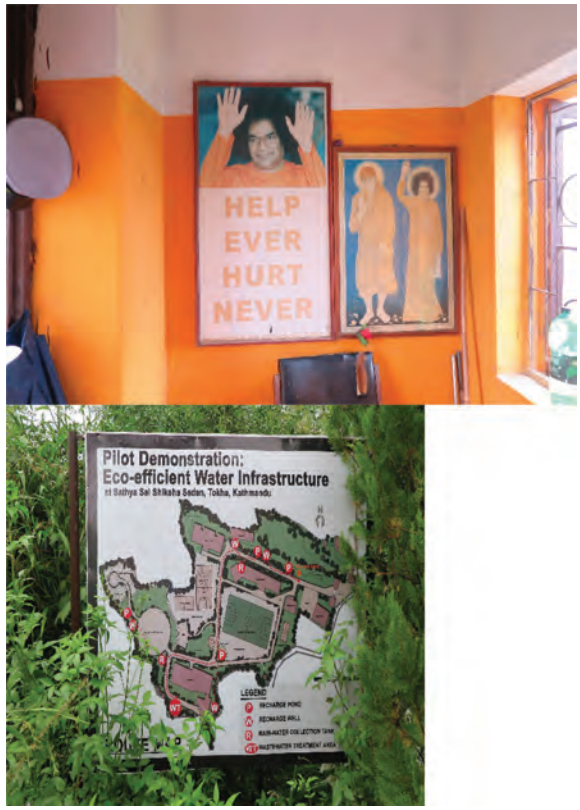

Figure 2 and 3: Satya Sai Sikshya Sadan.

3.2.2 Utilitarian

This type of motivation prevails in terms of the frequency in which appears. As in the Kathmandu Valley, the water supply is a challenge for most of the inhabitants, it is not surprising, that people try to use the treated wastewater for irrigation. This source of utility water is frequently combined with rain harvesting as is the case of Dhapakhel.

The utility of CWs is, in the situation when it is possible, enhanced by producing biogas from solid parts of the wastes. Such a combination is seen as a good investment and often becomes a subject of local business – especially selling gas for heating and cooking for community members. This kind of utilization of a CW was found when analysing the situation in the Sano Kokhana and the Shreekandphur communities (see Fig. 4 and 5).

3.2.3 Image-making (prestige)

Unlike the two previously mentioned motivations that can be attributed mainly to local communities and institutions, image-making is the dominating reason for implementing CWs in places oriented outwards. Two types of such places were identified during the analysis – prestigious schools and tourist-oriented places. Shuvatara International School in Lalitpur, the private boarding high school, trying to attract rich clientele can be used as an example to

Figure 4: Shreekandphur.

Figure 5: Sano Kokhana.

document the statement. The school uses the "environment-friendly" way of treating wastewater as a "trademark" to demonstrate its exceptionality to attract rich students.

Tourist-oriented places are in our sample represented by the Namo Buddha Resort and Chandra Ban Eco tourist localities. They are examples of private investment that builds on the image of Nepal as a spiritual country (sometimes referring to the hippie era). And the indispensable attribute of such an image is environment-friendly behaviour. Nature-based technology, as the CW is, serves to manifest this standpoint with the aim to attract (rich) clientele. As in many other businesses, the image, the pretending, is more important than reality. Having it in mind, you cannot find surprising the fact, that the nicely looking basin with flowering water plants is situated in the front. However, this basin is used for cleaning the

Figure 6 and 7: Namo Buddha Resort.

water from the kitchen only, while the black water is being freely released to nature through non-functioning wetland by pipelines in the back (Fig. 6 and 7).

4 CONCLUSIONS

Based on the information obtained by the research we suggest stating that CWs as a technology for household wastewater treatment is getting recognition within the Kathmandu Valley, slowly but continuously. It is despite the fact, that the government support is still not adequate both in terms of direct (financial) support for building CWs and missing legislation as to the environmental standards.

Given the situation, the process of diffusion cannot be seen as a top-down, officially supported process. It can rather be interpreted as network-based diffusion using personal contacts, sometimes based on the peer model.

The array of motivation to use this technology is relatively broad, spanning from the very pragmatical reasons induced partly by the lack of other utility water available up to purely spiritual arguments. The tendency to pretend environment-friendly behaviour can be hypothesized to be related to the opening of Nepal to globalization trends, misusing to some extent the image of Nepal as a trademark of "spirituality" on the global market.

We are fully aware of the fact, that the sample we used for our research was limited as any other sample, hence outputs derived from the data gathered can be seen as contingent. Nevertheless, they represent a probe of some kind to the value system of the Nepali society. It would be then challenging to conduct such research in European conditions for comparison.

ACKNOWLEDGEMENTS

This paper was developed thanks to the EUEKA project E! 12219 BIORESET, co-financed by the Ministry of Education, Young and Sports, Czech Republic (50%) and organization VODNÍ ZDROJE a.s. and thanks to the activity COST 17133: CIRCULAR CITY RE.SOLUTION, the project "Natural Based Solutions for Water management in cities", financed by the Ministry of Education, Young and Sports, Czech Republic

REFERENCES

[1] Shrestha, R. R., Application of constructed wetlands for wastewater treatment in Nepal – Dissertation Thesis, University of Natural Resources and Life Sciences (BOKU), Vienna, Austria. 1999.

[2] Roka, R. B., Dongol, R., Kalavrouziotis, I. K., Historical Development of Wastewater Management in Kathmandu Valley. *Conference paper: 4th IWA International Symposium on Water and Wastewater Technologies in Ancient Civilization*, Coimbra, Portugal, 2016.

[3] Green, H., Poh, S. C., Richards, A., *Wastewater treatment in Kathmandu, Nepal*, Master Thesis: Massachusetts Institute of Technology, Cambridge: USA, 2003.

[4] Shrestha, N., Lamsal, A., Regmi, R. K., Mishra, B. K. (2015): Current Status of Water Environment in Kathmandu Valley, Nepal. Water and Urban Initiative Working Paper Series, United Nations University Institute for the Advanced Study of Sustainability. Available online: http://collections.unu.edu/view/UNU:2852

[5] Boukalova, Z., Těšitel, J. & Gurung, D. B., Nature-based water treatment solutions and their successful implementation in Kathamndu Valley, Nepal. WIT Transactions on Ecology and the Environment, vol. 242, WIT Press: Southampton and Boston, pp. 121–132, 2020.

[6] Shrestha, J., Kalu, S., Performance of DEWATS in Nepal. Journal of Environment and Public Health, 1(1): 21-26, 2017. Online available: https://www.scribd.com/document/458266773/ENPHO-Journal-V1-I1.

[7] Tuladhar, B., Shrestha, P., Shrestha, R., Decentralised wastewater management using constructed wetlands. Online available: https://es.ircwash.org/sites/default/files/Tuladhar-2008-Decentralised.pdf, 2008.

[8] WaterAid, *Decentralised wastewater management using constructed wetlands in Nepal*. WaterAid in Nepal, Kathmandu: Nepal, 2008.

[9] Gurung, A. and Oh, S-E., An overview of water pollution and constructed wetlands for sustainable wastewater treatment in Kathmandu Valley: a review. *Scientific Research and Essays,* 7(11), 1185-1194, 2012.

[10] Gurung, S. B., Geronimo, F. K. F., Lee, S., Kim, L. H., Status of constructed wetlands in Nepal: recent developments and future concerns. *Journal of Wetlands Research*, 19(1), 45-51, 2017.

[11] Rogers, E. M., *Diffusion of innovations (5th ed.)*. New York: Free Press, 2003.

[12] Dooley, K. E., Towards a holistic model for the diffusion of educational technologies: an integrative review of educational innovation studies. *Educational Technology & Society, 2*(4), 35-45, 1999.
[13] Stuart, W. D., *Influence of sources of communication, user characteristics and innovation characteristics on adoption of communication technology*. Dissertation Thesis, University of Kansas: Kansas, USA, 2000.
[14] Charmaz, K., *Constructing grounded theory – A practical guide through qualitative analysis*. SAGE Publications: London, Thousand Oaks, New Delhi, 2006.
[15] Kielmann, K., Cataldo, F., Seeley, J., Introduction to qualitative research methodology: a training manual, produced with the support of the Department for International Development (DfID), UK, under the Evidence for Action Research Programme Consortium on HIV Treatment and Care (2006–2011), 2012.
[16] Thomas, W. I., Thomas, D. S., The child in America: Behavior problems and programs. New York: A. A. Knopf, 1928.
[17] Park, R. E., Burgess, E. W., *Introduction to the Science of Society*, University of Chicago Press: Chicago, USA, 1921.
[18] Boukalová, Z., Těšitel, J. & Gurung D. B., Constructed wetlands implementation in Kathmandu Valley, Nepal. *International Journal of Environmental Impacts*, 4(4), 363-374, 2021. Online available: https://www.witpress.com/elibrary/ei-volumes/4/4/2849
[19] https://enpho.org/
[20] https://doi.org/10.1177/000271629956600105
[21] Arnstein, S. R., A ladder of citizen participation. *Journal of the American Institute of Planners,* 35(4), 216–24, 1969.

CH_4, CO_2 AND SO_2 EMISSIONS FROM THE HULENE DUMP, MUNICIPALITY OF MAPUTO

AMAD H. A. GANI[1,3], FARISSE J. CHIRINDJA[2], ANTÓNIO G. J. DIAS[3] & ANTÓNIO A. R. MONJANE[1]
[1]Universidade Pedagógica de Maputo, Faculty of Natural Science and Mathematics – Moçambique.
[2]Universidade Eduardo Mondlane, Faculty of Science, Department of Geology – Moçambique.
[3]University of Porto, Faculty of Science, Department of Geosciences, Environment and Spatial Planning, Portugal

ABSTRACT

The objective of this work is to evaluate the amount of CH_4, CO_2 and SO_2 that is currently emitted by the Hulene dump into the atmosphere. The work consisted in measuring these three gases using an S360 multigasometer that simultaneously measures eight gases. Measurements were made in April, May, June, July, August and September, which are considered the dry season in Maputo city. Measurements were made at 18 points of gas release pipes installed by the Municipality of Maputo. Point P10, presents the highest value of 2.56 and 2.59 (% vol of CH_4), respectively in the months of April and May. Point P14 had the highest value of 2.95 (% vol of CH_4) in April and 2.28 (% vol of CH_4) in May. Point P15 presented values of 2.78 and 2.72 (% vol of CH_4), respectively in the months of August and September. Points P10, P14 and P15 showed higher values of CH_4 in April, May, August and September. Points P9 to P13 showed marked variations of CO_2 in the months of July, August and September. Point P10 presented the highest value of 2.56 and 2.59 (ppm of CO_2), respectively in the months of April and May. Point P14 showed the highest value of 2.95 (ppm CO_2) in April and 2.28 (ppm CO_2) in May. Point P15 presented the highest value of 5,000 ppm of CO_2 in August and September. In April, points P1 to P6 showed values above 100 ppm of SO_2 and dropped drastically from point P7 to 3 ppm of SO_2. In April, P6 reached 137 ppm of SO_2. In August and September, the values gradually increased, reaching 178 ppm of SO_2 at point P18.

Keywords: biogas, emission, greenhouse effect

1 INTRODUCTION

The Hulene dump is a place where Maputo city's MSW has been deposited in the open for 30 years. The Hulene dump underwent improvement works to increase its solid waste receival capacity, increasing from 17 to 23 ha, after the tragedy that killed nineteen people, caused by the swelling of gases produced by the anaerobic digestion of the organic fraction of urban solid waste deposited. When the waste is deposited, the biodegradable fractions decompose through a complex series of microbial and chemical reactions, in addition to physical changes, with the result being the production of biogas [1]. Biogas basically consists of methane (CH_4), carbon dioxide (CO_2) and other gases in very low concentrations, such as several non-methane volatile organic compounds, which can be toxic [2]. In the sanitary landfill, the biodegradation of urban solid waste occurs through physical, chemical and biological processes, producing leaching water and gases. These processes occur over time and in aerobic, anaerobic non-methanogenic and methanogenic phases. CH_4 and CO_2 are the main gases inducing the increase in the greenhouse effect on the planet [3]. According to [4], landfills emit 18% of CH_4 and it is estimated that 35 to 69 tons of CH_4 are emitted annually into the atmosphere worldwide. In 2020, the Hulene dump received a total of 577,848.90 tons of urban solid waste, according to data provided by the Municipality of Maputo [5]. The Municipal Solid Waste Management Regulation (MSWMR) of Maputo City defines MSW as originating from domestic and commercial activities in urban settlements [6]. Methane (CH_4)

ISSN: 2398-2640 (paper format), ISSN: 2398-2659 (online), http://www.witpress.com/journals
DOI: 10.2495/EI-V5-N4-342-349

and carbon dioxide (CO_2) reach the atmosphere during the deposition of waste, through percolation processes in the cover layers and through gas release pipes, the latter represents the places where biogases were measured. According to [7], [8], the production of gases in landfills starts from the first three months of solid waste compaction and extends until approximately 15–20 years after the deactivation of the area.

2 MATERIALS AND METHODOLOGY

To carry out this research, an S360 multigasimeter was used (Fig. 1), capable of measuring eight biogases by suction simultaneously, namely CH_4, CO_2, CO, NO_2, SO_2, O_2, H_2S and H_2. The S360 series equipment is a portable multi-gas detection instrument with high sensitivity for industrial use. It can detect different gases according to different types of sensors, with rich functions, simple operation, easy to carry and good shock resistance. This product uses high resolution touch LCD technology, the screen is more intuitive, clear, and more convenient to operate. The multigasimeter is equipped with a high temperature detector, suitable for high temperature gas occasions. In this work, only three gases are treated. The gases were measured at 18 points previously defined and installed by the Municipality of Maputo, through a project in partnership with the Japanese government, as part of the requalification of the dump. The 18 points are distributed in 3 lines of 6 points each and spaced 20 m apart on the line and 5 m high, with gabion protection at the end of each bench (Fig. 2). The choice of measurement points considered the existing points where pipes for continuous release of biogas were installed, which passes through a network of pipes installed at the bottom of the dump, allowing the circulation of biogas inside the dump, and releasing it through the pipes (Fig. 3). Measurements were taken in the last week of each month during a 6-month period of the dry season, starting in April and ending in September 2021.

Figure 1: Multigasimeter S360.

Figure 2: Bench with gas release pipes.

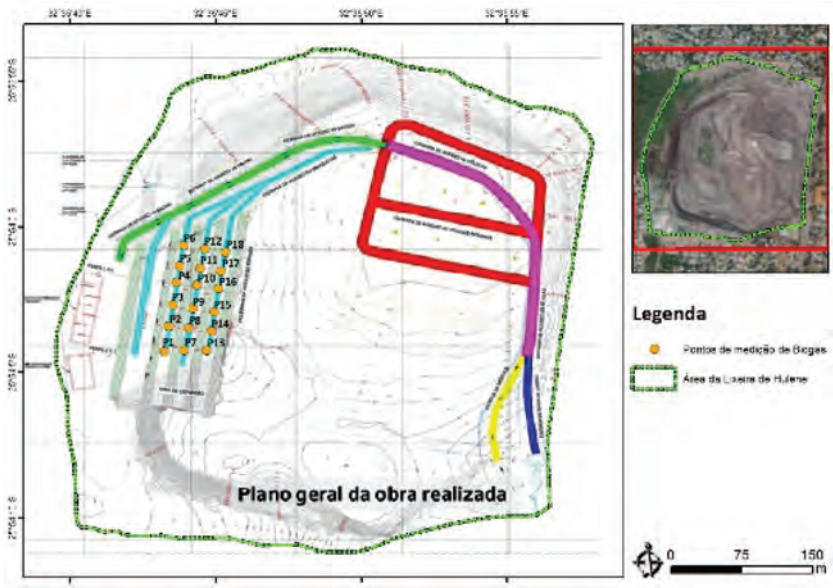

Figure 3: Biogas measurements points (adapted from [9]).

3 FRAMEWORK OF THE STUDY AREA

The city of Maputo is in Mozambique on the west bank of Maputo Bay in the extreme south of the country, close to the South African border and Swaziland's border. The limits of the municipality of Maputo are between latitudes 25º49′09″S and 26º05′23″S and longitudes 33°00′00″E (on the island of Inhaca) and 32°26′15″E, at an average altitude of 47 m. The municipality has an area of about 346.77 km^2 and a population density of 35 hab/km^2. About 60% of the population of this municipality works in the informal sector, with the remaining 40% of the population in the formal sector, divided into the areas of fishing, agriculture, manufacturing, tourism and services. Throughout the year, the temperature varies from 16°C to 29°C and is rarely below 14°C, often exceeding 40°C in the rainy season. The Hulene dump is located about 7 km from downtown Maputo, in the KaMavota district, covering an area of 23 ha (Figs. 4 and 5). The municipality of Maputo is made up of seven municipal districts, namely: KaMavota, KaMaxaquene, KaMpfumo, KaMubukwane, KaNlhamakulo, KaTembe and KaNyaka. Waste produced in KaTembe and KaNyaka districts is not deposited into the Hulene dump. The KaTembe district is located on the southernmost bank of Maputo Bay while the KaNyaka district is an island, which means that its waste does not reach the Hulene Municipal dump. The dump has been exploited since 1972, reaching the end of its useful life in 2016 and extended in 2018 for another 10 years due to compaction work. The dump has an extension of 17 ha and a maximum height of accumulated waste of about 30 m. Commerce is characterized by two types of markets: the formal, which comprises the retail and wholesale trade network, and the informal, comprising fixed and mobile resellers scattered throughout the city streets and in the formal and informal markets. In the green belt of Infulene, a variety of vegetables are produced. In many suburban neighbourhoods, poultry, rabbits and swine are raised. In urban neighbourhoods, the sanitation of the environment is served by a public drainage system of domestic wastewater and conventional rainwater built in the colonial era and in the older and emerging peri-urban neighbourhoods, it consists essentially of septic

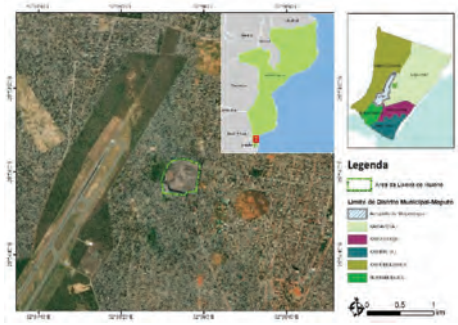

Figure 4: Hulene municipal dump location.

Figure 5: Hulene municipal dump.

tanks, generally without connection to the public system of drainage. In terms of environmental legislation, the municipality has legal and regulatory instruments for GRSU in which each of them complements each other in the absence of a more adequate policy, namely:

- Decree No. 94/2014, of 31 December: Regulation on Urban Waste Management [6]; and
- Resolution No. 86/AM/2008, of 22 May, Cleaning Posture of Urban Solid Waste in the Municipality of Maputo [10].

4 PHYSICAL COMPOSITION OF MSW AND MANAGEMENT STRUCTURE

Pursuant to article 14 of the Regulation on GRSU of the municipality of Maputo, waste must be segregated according to the following categories: paper/cardboard, organic matter, rubble, plastic, glass, metal, textiles, rubber, bulky household waste and special waste. The annual deposition of municipal waste in the Hulene dump increased from 127,385 tons in 2007 to 365,000 tons in 2017 [5]. In that period, the collection capacity increased from 39.93% to 84.10%. Peri-urban neighbourhoods, with about 75% of the population, are responsible for the average production of 73% of organic matter against 64% generated in urban neighbourhoods [5]. The MSW produced in the city of Maputo are the following: paper/cardboard, textiles, glass, metals, plastic, organic matter and others. Bulky household waste, which includes construction waste, is used in foundation landfills for new construction works. The Hulene dump does not receive this type of waste. Waste pickers essentially collect waste

such as cardboard and cover boxes, plastics, pet bottles, glass bottles and metals and sell them to companies that export them to South Africa. The Municipal Council of Maputo City is responsible for cleaning municipals streets and collecting waste produced in the city. According to [5], the per capita rate of MSW generation in the city of Maputo is 1 kg/inhabitant/day in urban areas and 0.56 kg/inhabitant/day in suburban areas. Gani et al. [5] also states that the average capitation rate in the city is 1.06 kg/inhabitant/day. The Municipality of Maputo engaged, in a public-private partnership (PPP), two companies for the collection of MSW in the city of Maputo, namely Ecolife, which collects waste in the urban area and Envioroserv, which collects waste in the suburban area, then deposits them in the Hulene dump [11]. Micro-enterprises that collect waste at specific locations and that can collect, whenever requested for this purpose, upon payment of amounts to be agreed between the parties, have been licensed, but these companies do not deposit the waste in the Hulene dump, these being the wastes that are selected for recycling.

5 RESULTS AND DISCUSSION

Table 1 shows the results of measurements of meteorological conditions, temperature and humidity, for the days in which the biogas measurements were made in each of the indicated months. It was observed that the lo west temperature value was measured in May and August and the highest temperature was measured in April. In turn, the lowest value of humidity was registered in the month of June and the highest value was registered in the month of August.

The graph in Fig. 6, illustrates the methane measurements taken at the 18 sampling points. Point P10 has the highest value of 2.56 and 2.59 (% vol of CH_4), respectively in April and May, compared to the remaining points in other months. Point 14 has the highest value of 2.95 (% vol of CH_4) in April and 2.28 (% vol of CH_4) in May. Point P15 presents values of 2.78 2 2.72 (% vol of CH_4), respectively in the months of August and September. Points P10, P14 and P15 present higher values than the other points in the months of April, May, August and September. The month of April presents itself simultaneously with higher values of temperature and humidity.

The graph in Fig. 7 illustrates the CO_2 measurements taken at the 18 sampling points. Points P9, P10, P11 have higher values, ranging from 3,000 to 5,000 ppm of CO_2, respectively in the months of June, August and September. Point P13 has the highest value in July, reaching 3,000 ppm. Point P15 has the highest value of 5,000 ppm of CO_2 in the months of August and September. The month of August has the highest humidity.

Table 1: Characteristics of Bakun HEP.

Month	**Temperature (°C)**	**Humidity (%)**
April	25	77
May	20	66
June	22	45
July	21	47
August	20	85
September	23	52

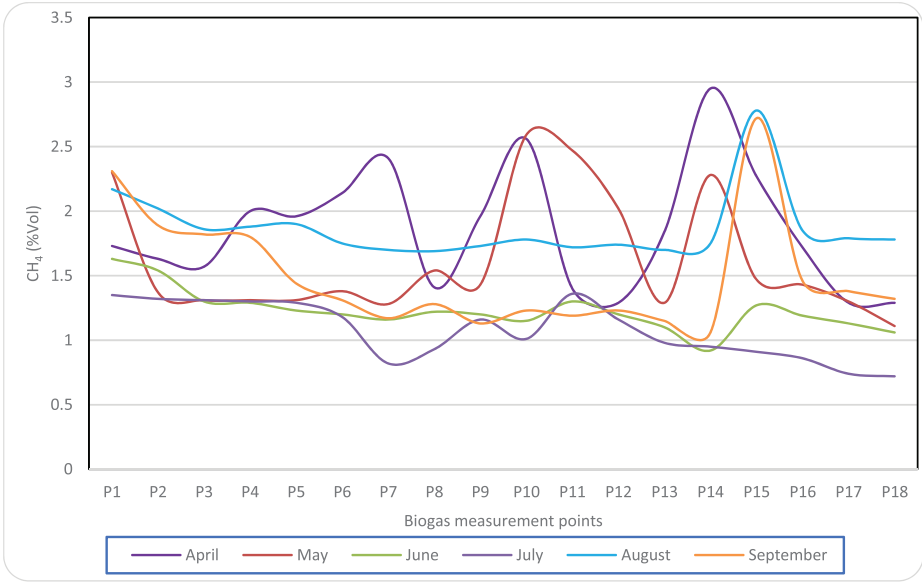

Figure 6: Results of CH_4 measurements.

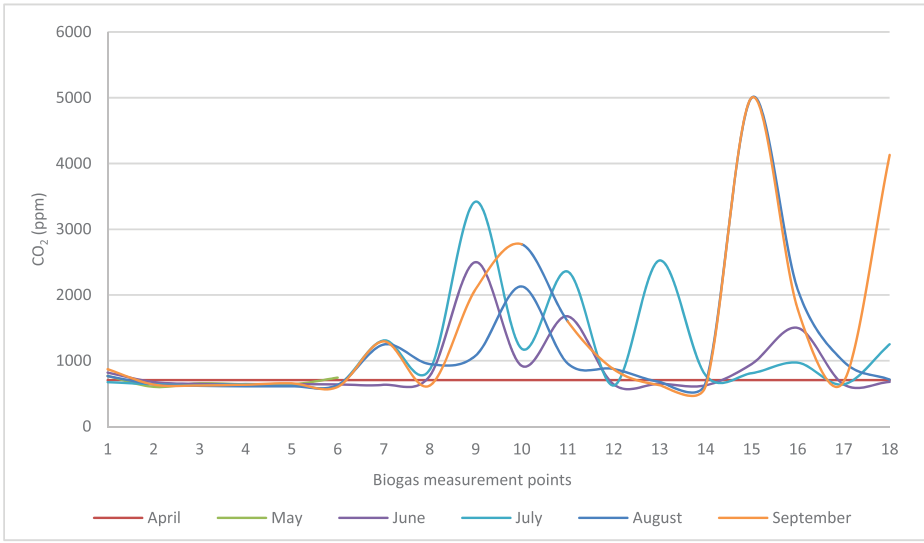

Figure 7: Results of CO_2 measurements

The graph in Fig. 8 illustrates SO_2 measurements taken at the 18 sampling points. In the month of April, points P1 to P6 showed values above 100 ppm of SO_2, which dropped drastically from point P7 to 3 ppm of SO_2. In the same month of April, P6 reached 137 ppm of SO_2. In the months of August and September, the values gradually increased, reaching 178 ppm of SO_2 in P18. There is no data registered in May.

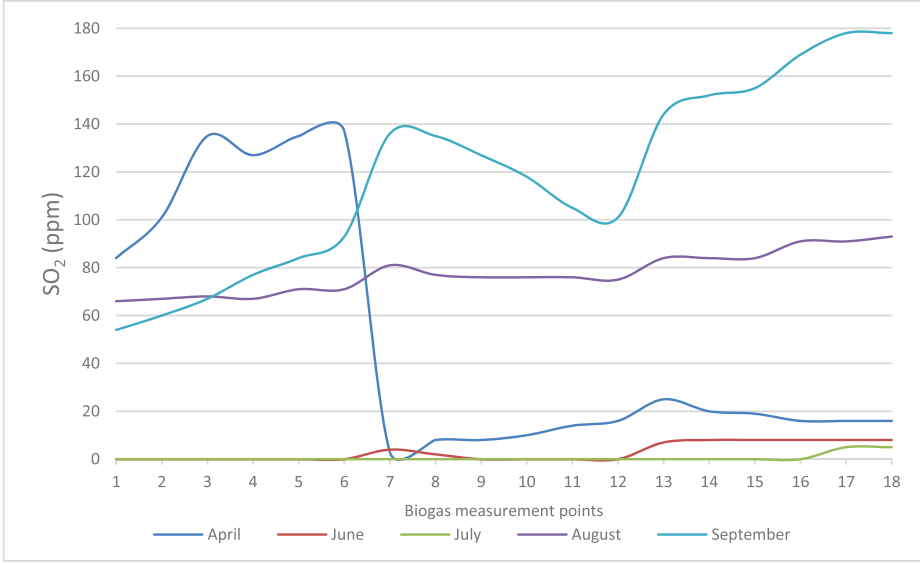

Figure 8: Results of SO_2 measurements.

6 CONCLUSIONS

According to the results obtained, it is concluded that the points P7, P10 and P14 presented higher values of methane emission in the month of April compared to the other months studied in this work. These points, according to the location of the biogas metering points in the Hulene dump, are on the highest quota lines where the waste deposited is relatively more recent. In July, points P7 and P8 had the lowest methane emissions values. The months of April, May, August and September had the highest methane emissions values at points P10, P14 and P15. The point P10, presented the highest value of 2.56 and 2.59 (% vol of CH_4), respectively in the months of April and May. Point P14 had the highest value of 2.95 (% vol CH_4) in April and 2.28 (% vol CH_4) in May. Point P15 presented values of 2.78 and 2.72 (% vol of CH_4), respectively in the months of August and September, showing that methane production is higher in the most recently deposited wastes. Points P9, P10 and P11 showed higher values of carbon dioxide in the months of June, July, August and September, ranging from 2,500 to 3,500 ppm. The months of August and September presented high values of CO_2 that reached 5,000 ppm. Point P15 presented the highest value of 5,000 ppm of CO_2 in the months of August and September. The sulphur dioxide values showed a variation between the points of the measurement lines over the months. These results show that there is greater production of CO_2 in the most recently deposited wastes compared to the older and temperature-influenced waste in the hottest months of August and September than April and May. In the month of April, the first line of metering points presented higher values, decreasing considerably in the second and third lines, showing that the production of SO_2 is higher in wastes with longer deposition time than recent deposited wastes. In April, points P1 to P6 showed values above 100 ppm of SO_2 and dropped drastically in the point P7 to 3 ppm.

ACKNOWLEDGEMENT

Our thanks go to the Director of the Faculty of Natural Sciences and Mathematics of the Pedagogical University of Maputo, Mozambique for his technical support and opportunities, to the support provided by the Director of the Faculty of Sciences, Department of Geosciences,

Environment and Spatial Planning – Porto, Portugal and to the Municipal Direction of Environment and Health of the Municipal Council of the City of Maputo, for the support provided in the collection of field data that culminated in the completion of this work.

REFERENCES

[1] Spokas, K., Bogner, J., Chanton, J.P., Morcet, M., Aran, C., Graff, C., Golvan, Y.M.L., Hebe, I., Methane mass balance at three landfill sites: what is the efficiency of capture by gas collection systems? *Waste Management*, 26(5), p. 516-525, 2006.

[2] Hrad, M., Huber-Humer, M., Wimmer, B., Reichenauer, T.G., Design of top covers supporting aerobic in situ stabilization of old landfills – an experimental simulation in lysimeters. *Waste Management*, 32(12), p. 2324-2335, 2012.

[3] Aronica, S., Bonanno, A., Piazza, V., Pignato, L., Trapani, S., Estimation of biogas produced by the landfill of Palermo, applying a Gaussian model. *Waste Management*, 29(1), p. 233-239, 2009.

[4] Bogner, J., Pipatti, R., Hashimoto, S., Diaz, C., Mareckova, K., Diaz, L., Kjeldsen, P., Monni, S., Faaij, A., Sutamihardja, R.T.M., Gregory, R., Mitigation of global greenhouse gas emissions from waste: conclusions and strategies from the Intergovernmental Panel on Climate Change (IPCC) Fourth Assessment Report. Working Group III (Mitigation). *Waste Management Research*, 26, p. 11-32, 2008.

[5] Gani, A., Monjane, A., Guerner Dias, A., Impact of Gross Domestic Product (GDP) Change in Municipal Solid Waste (MSW) Generation in Maputo. *WIT Transaction on Ecology and Environment*, 247. p.15-24, 2020. UK.

[6] Decree No. 94/2014. Regulation on Municipal Waste Management. Maputo, 31 Dec 2014.

[7] Mclennan, D., Aterros Sanitários. Revista JB Ecológico. *Rio de Janeiro: jornal do Brasil*, 2(17), 2003.

[8] Korhonen, M. R., Dahlbo H., Reducing Greenhouse Gas Emissions by Recycling Plastics and Textiles into Products. Finnish Environment Institute/Research Department. 62p, 2007. Available at: http://www.ymparisto.fi/download.asp?contentid=74073. Accessed: May 2010.

[9] CMCM/JICA Projecto Piloto para a Melhoria da Segurança na Lixeira de Hulene. Município de Maputo, 2020.

[10] Resolution No. 86/AM/2008. Posture of Cleaning of Solid Municipal Waste in the Municipality of Maputo. Maputo, 22 May 2006.

[11] Gani, A., Monjane, A., Guerner Dias, A., Olaide, A., Improving the Attitude and Reation Towards Municipal Solid Waste Management in Mozambique. *WIT Transaction on Ecology and Environment*, 247, p 47-56, 2020. UK.

[12] Maputo, C.M.C., Solid Waste Management Master Plan (SWMMP). Maputo, Available on: https://www.giz.de/en/downloads/giz2012-en-economic-instruments mozambique. pd,_2008.

Harsho Sanyal & Joseph Cataldo, Int. J. Environ. Impacts, Vol. 5, No. 4 (2022) 350–361

LABORATORY EXPERIMENTS AND MODELLING TO DETERMINE THE PROFILES OF THE JAVITS CENTER GREEN ROOF

HARSHO SANYAL & JOSEPH CATALDO
The Cooper Union for the Advancement of Science & Art, New York, USA

ABSTRACT

Climate change has led to triple digit temperatures globally, notably along the western coast of the United States. These changes have produced intense weather-related events such as fires and landslides. Green roofs are one strategy to mitigate these high temperatures. For this report, several studies were compiled, using data found from physical green roof models as well as on-site data from the Javits Center Green Roof. At the Javits Green Roof, an infrared camera was used to collect thermal images at various parts of the roof, to determine its effectiveness for thermal buffering. Off site, a rain simulator was used on model green roof and a control roof, to determine change in retention and peak runoff rate. The green roof was able to retain 2%–22% of rainfall and reduce peak runoff by 19%–28%. From the graph comparing roof temperatures, there were higher temperatures on the black top roof in comparison to the green roof, and the slopes of the lines indicated the mitigating effect of the green roof on heat waves. These models were also analysed with an infrared camera, which showed that green roofs can be, as much as 25°F cooler than their standard roof counterparts, providing valuable evidence for the usefulness of green roofs to combat heat waves. Runoff quality was experimentally measured using a green roof model, where nitrogen concentration is measured before and after to determine change in runoff quality. This concept is based on studies which claim that the addition of wood mulch to soil can reduce nitrogen content. This experiment revealed a 23% reduction in runoff nitrates for the wood-mulch treated soil, in comparison to a 6.5% reduction for the control roof. Furthermore, a mathematical model was used to determine the ceiling temperature of the Javits Center within 3%.
Keywords: green infrastructure, green roof, infrared camera, thermal buffering, runoff.

1 INTRODUCTION

The world is currently entering a period of rapid and significant change. The past 5 years alone have been the hottest 5 years recorded since major weather and climate agencies began to track global temperatures in the 1880s. July 2021 has been the hottest month ever recorded in history [1]. Scientists estimate that upon the conclusion of the 21st century, the average global temperatures will increase by at least 3°C [2]. To contextualize this rate of change, global temperatures have risen by a little over 1°C in the past 141 years [3]. An increase as projected would correspond with triple the number of weather-related events such as hurricanes, wildfires and heat waves. A multitude of regions are heavily affected by the shift in climate. Rising sea levels and worsening hurricane seasons are a threat to the Mississippi River Delta [4]. Many areas along the eastern coast of the United States are directly impacted by flooding from sea level rise. In Alaska, global warming and longer summers have caused the Arctic permafrost to melt [5]. The Amazon rainforest has existed for ten million years; it may not survive the next hundred.

The urban building environment is especially vulnerable to these climate extremes. Heat waves in particular have become more frequent, causing more frequent warm days and fewer cool days. The environmental baselines of cities have started to shift, to the point where cities are several degrees warmer than surrounding areas due to the urban heat island (UHI) effect [6]. There is also a reduction in evaporative cooling due to a lack of vegetation, as well as the production of waste heat.

ISSN: 2398-2640 (paper format), ISSN: 2398-2659 (online), http://www.witpress.com/journals
DOI: 10.2495/EI-V5-N4-350-361

Green infrastructure (GI) has emerged as a viable option to combat the effects of climate change. It is designed to imitate natural hydrology, incorporating porous surfaces which can absorb up to 90% of the stormwater runoff that reaches them. In absorbing this runoff, GI reduces the stress on sewer systems and mitigates risk of flooding. The quality of the runoff is filtered through processes such as adsorption, filtration and plant uptake. GI can also generate positive effects such as air quality improvement (by absorbing pollutants from the air) and preservation of ecological habitats (by reducing erosion-causing runoff). In the context of rising temperatures specifically [7], GI provides increased resilience against climate change by combating UHI effect and reducing temperatures through evaporative cooling, while absorbing potential floodwater [8].

One form of GI is the green roof. Green roofs are multi-level roofing layers on buildings, coated with vegetation. Research concerning the thermal performance of green roofs in urban [9,10] and suburban settings is relatively new. The majority of this work underscores the thermal benefits of green roofs over traditional black tar asphalt and gravel roofs [11,12]. Green roofs provide physical protection of the conventional roof from solar radiation and reduce both daily and seasonal variations in surface temperature. This buffering is accomplished through reflection, convection, vaporization and eventual transmission processes [13]. Green roofs typically have a higher albedo than traditional black roofs, and thus are able to reflect a larger fraction of the incident solar radiation away from the roof surface. Radiation that is not reflected away from the surface heats up the green roof elements (its vegetation, growing media and the moisture stored within it) [14,15].

Water quality is another important parameter to measure the effectiveness of green roofs. Water quality can be quantified through many values, one of which being the level of nitrates in runoff. The effects of nitrates were studied from a variety of sources. As with other salts, nitrates in soil increase osmotic pressure outside of the plant roots, reducing the amount of water they can take in against the concentration gradient. Excess nitrogen can be leached out of the soil by runoff water, which can enter aquatic systems and cause rapid algal growth. This process, known as eutrophication, can lead to reduced dissolved oxygen levels and limited penetration of sunlight into the water. Processes for soil remediation vary [16]. For nitrate remediation, usage of wood mulch to tie up excess nitrogen was seen to be an effective strategy [8].

2 EXPERIMENTATION

The results of the field and laboratory studies at Cooper Union are provided in this paper. A series of laboratory experiments were conducted both on-site at the Javits Green Roof, as well as off-site.

Two studies took place at the Javits Center Green Roof (JGR) in 2017 and 2018, complemented by green roof models. During the 2017 study, weather stations were set up at the JGR, equipped with an anemometer, a rainfall sensor, a humidity sensor, a radiation sensor, a FLIR T440 thermal imaging camera, and an infrared thermometer. These stations recorded the following parameters: wind speed/direction, rainfall, radiation, air temperature, humidity, and temperature of the air, exterior roof surface and interior ceiling surface. The IR cameras collected exterior surface temperatures, which were correlated with air temperatures from the closest weather stations, and interior surface temperatures were correlated with air temperatures inside the Javits Center collected by thermometers. The difference in temperature between the exterior and interior surface was used to quantify thermal buffering of the roof. These on-site studies were complemented by the construction of five physical models of the JGR in the Cooper Union laboratory, with lateral dimensions of 1.2 by 0.6 m. Results from

this study found that the JGR had a substantial impact on reducing heat transfer through the Javits roof [14]

Runoff observations at the JGR were compared with the results from a computer model, which predicted peak runoff rates and total event runoff within +25% to 15% and +10% to 20%, respectively. This study found that, on average, 96% of rainfall was retained for events less than 6.35 mm, while 27% was retained for events greater than 12.7 mm [17]. This study provided strong evidence for green roofs' capacity for stormwater retention.

One experimental study took place at the Cooper Union, and involved the construction of a two-part model roof; half of this area was an unvegetated control section, and the other half was coated with geomembrane, soil and sod to simulate a green roof. To act as a source of simulated rainfall, a 4' × 4' grid of PVC pipes was built, and placed above the roof model. The roof model is on a 2% slope, with holes at the bottom for runoff collection. A uniform level of precipitation was applied to both roofs over five trials. Figure 1 is a view of the lab model, showing the overhead rain maker.

The second experimental study for this paper also took place at Cooper Union, and examined a model green roof based on the JGR. The purpose of that study was to first investigate the effects of excess nitrogen on soil, and then to examine the effect of wood mulch on nitrate concentration in soil [8].

Two 2-foot by 4-foot boxes had holes drilled along one of the shorter ends. This end would be covered by a PVC pipe, to allow a path for runoff. These boxes were placed on a 3-degree incline and coated with felt to cover any cracks, after which they were both filled up to a height of 1 foot with soil. The upper layer of soil for Box A (the experimental box) was mixed with four quarts of wood mulch. Water mixed with soluble nitrates was poured over each box on the first trial date, and tap water was poured over each box on the second trial date. The parameters measured included nitrate concentration, pH and temperature for inflow/outflow, which were measured with nitrate test strips, pH test strips and a thermometer, respectively [8].

Figure 1: Roof model with asphalt shingles, root barrier and drainage map and thermistors [14].

3 RESULTS

To determine the behaviour of green roofs due to extreme heat conditions, the green roof and control roof were tested under a series of runoff and heat conditions (see section 2) For the runs tested the precipitation was varied as well as the rain and room temperatures. Table 1 shows the range of values for the runs considered and tested.

The following graph (Fig. 2) shows rain versus the green roof and control temperatures. Control has a larger slope (i.e., larger temperatures) compared to the green roof. The room temperature was held at 71°F.

Hydrographs were constructed for the green roof and control. One example of these hydrographs is shown in Fig. 3, with the graph data in Table 2. Each curve ends when the quantity of discharge accumulated during a given time interval is less than 100 ml. The accumulated percent retained and average lag time for each run was compared. These figures show hydrograph curves with best fit equations and R^2 values – all greater than 0.95 most over 0.99.

Table 1: Range of temperature values for all green roof and control runs.

Trial	Surface temp. (°F)	Rain (in/day)	Room temp. (°F)	Rain temp. (°F)	Control roof temp. (°F)	Green roof temp. (°F)
1	84	1.68	70.9	105	93.2	76.5
2	77	7.92	71.1	93	86.6	71.2
3	74	7.1	71.2	79.6	79.4	73
4	76	5.04	66.7	85.5	80.9	74
5	71	12.98	73.2	57.3	57.4	62.5
		6.16	73.8	58.5	57.8	61.6

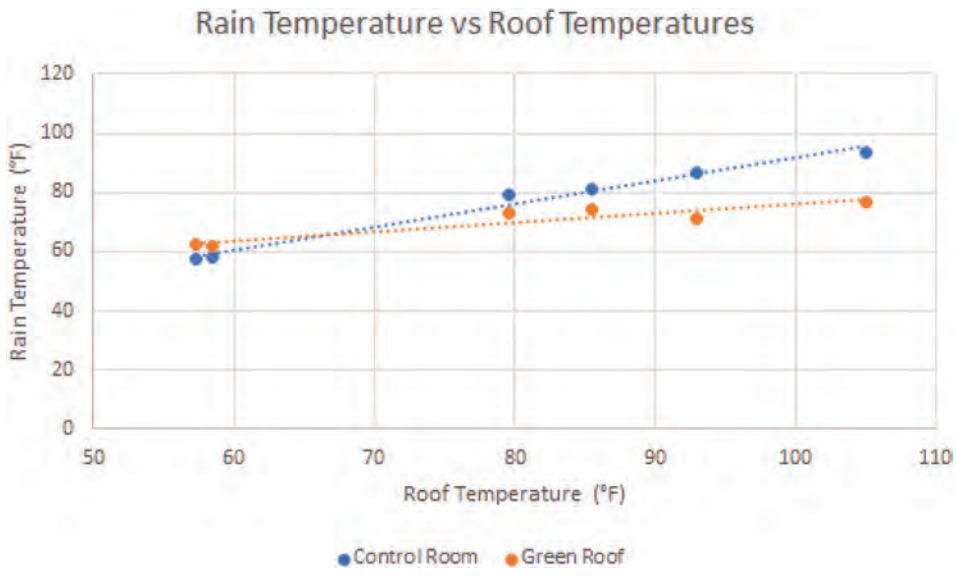

Figure 2: Rain temperature vs green roof and control roof temperatures.

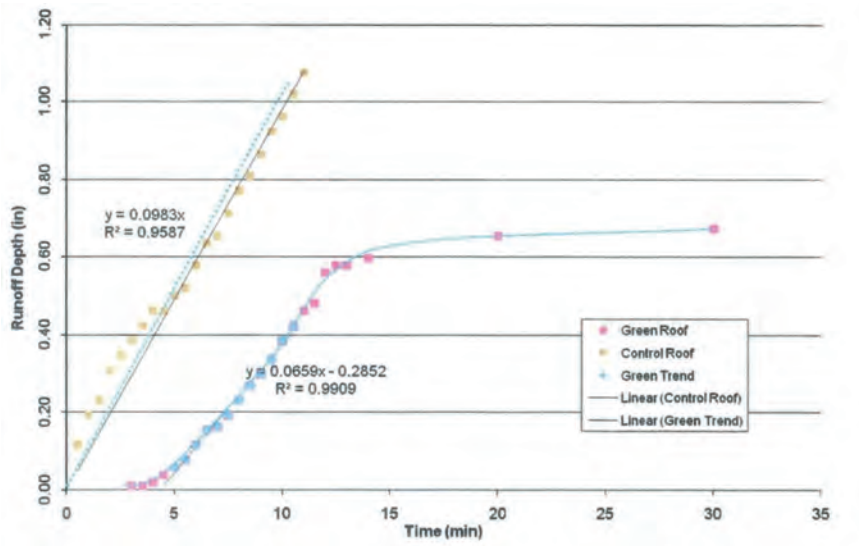

Figure 3: Hydrograph for an 11-minute storm.

Table 2: Hydrograph data for all trials.

	Hydrograph line of best fit: roof temperature vs rain temperature		R^2	
Trial number	**Control roof**	**Green roof**	**Control roof**	**Green roof**
1	$y = 0.133x$	$y = 0.1422x - 0.1703$	0.9966	0.9845
2	$y = 0.1226x$	$y = 0.0993x - 0.1413$	0.9907	0.9872
3	$y = 0.0983x$	$y = 0.0659x - 0.2852$	0.9587	0.9909
4	$y = 0.2162x$	$y = 0.1408x - 0.2617$	0.9556	0.9904
5	$y = 0.1054x - 0.9358$	$y = 0.0937x - 0.7677$	0.9936	0.9909

The percent retained by the green roof ranges from 2% to 22%. The lag time ranges from 2 to 11 minutes. Studies have found that the intensity of rainfall also significantly affects the ability of green roofs to control stormwater. Green roofs are generally more effective at retaining Rainwater from small storms. For the first two runs there was 100% retention to 6 and 9 minutes. For the remaining runs, full retention was measured about 1 1/2 minutes from the start of rain. The Green roof delays the onset of runoff, shown by the lack of cumulative runoff curve compared to the inflow curve and also extends the hydrograph which indicates that green roofs retain the precipitation for a long time. Table 2 shows the retention and average lag time for each trial, while Table 3 highlights the peak runoff rates.

As seen from Fig. 3 and Table 4, the green roof reduces the peak runoff, with the reduction ranging from 19% to 28%. The slope of the cumulative runoff for the green roof is less steep than the inflow, which indicates that the green roof is able to reduce the rate of drainage volume.

Table 3: Green roof retention and lag time

Run number	Total inflow (mL)	Cumulative runoff (mL)	% Retained	Average lag time (min)	Moisture Content
1	26,330 ± 2,630	20,656 ± 2,085	22%	11	49.0% ± 2.7%
2	35,083 ± 3,520	27,353 ± 2,755	22%	12	45.1% ± 4.7%
3	17,023 ± 800	16,661 ± 725	2%	2	56.2% ± 7.6%
4	18,110 ± 800	17,241 ± 725	5%	2	45.4% ± 19.6%
5	17,023 ± 800	15,212 ± 725	11%	3	48.6% ± 22.2%

Table 4: Peak runoff rates.

Run number	Peak inflow (mL/min)	Peak outflow, green roof (mL/min)	% Reduction
1	1,188	880	26%
2	2,250	1,730	23%
3	3,780	2,716	28%
4	3,343	2,717	19%
5	5,433	5,433	0% (discarded)

The nitrate experimental trials were carried out in the Cooper Union Fluids Laboratory. Table 4 shows data from the first trial date (with nitrogen-dissolved water), while Table 5 includes the measurements from the second trial date 2 weeks later, with tap water. From both tables, it is seen how runoff emerged in larger quantities from the box with wood mulch mixed in (due to the increased voids, and decreased retention capacity, caused by mixing the soil). The nitrate concentration in runoff decreased by 300 ppm in the wood mulch box, while it stayed similar to the initial value in the control box (shifting from 800 to 750 ppm). There were no significant changes in pH throughout the trials. During both weeks, the temperature of the runoff was 23°C, regardless of inflow temperature [8].

The infrared photo of the green roof and control model is shown in Fig. 4. The colour of the control roof on the right is red, with the temperatures in the mid-90s; this illustrates ponding of the heated water at the lower edge of the model. Ponding is when water pools, creating a "pond". The top of the control roof has lower temperatures (in the 80s), as there is no hot water ponding there. The green roof, in contrast shows green and blue colours, with temperatures in the mid-70s. There are a number of small red-yellow colours, indicating ponding of hotter water. The discharge overhead rain water pipe is at the top of the figure with temperatures in the mid-90s.

4 DISCUSSION

The three experiments conducted at the Cooper Union laboratory all provide information which can determine green roof parameters such as thermal buffering, runoff storage and nitrate remediation, on physical green roof models representative of the JGR. The models from the 2017 study examined the behaviour of a green roof in comparison to a control roof, and how conditions on the in-situ Javits roof were affected. The results were used as

Table 5: Flow data for Trial 1: nitrate water inflow into green roof [8].

Trial 1		Quantity (mL)	Nitrate concentration (ppm)	pH	Temperature
Wood mulch-mixed soil	Inflow	9,000	N/A	6.5	25 °C
	Runoff	1,850	1,300	6.5	23 °C
Only soil	Inflow	9,000	600	6.5	25 °C
	Runoff	1,300	800	6.5	23 °C

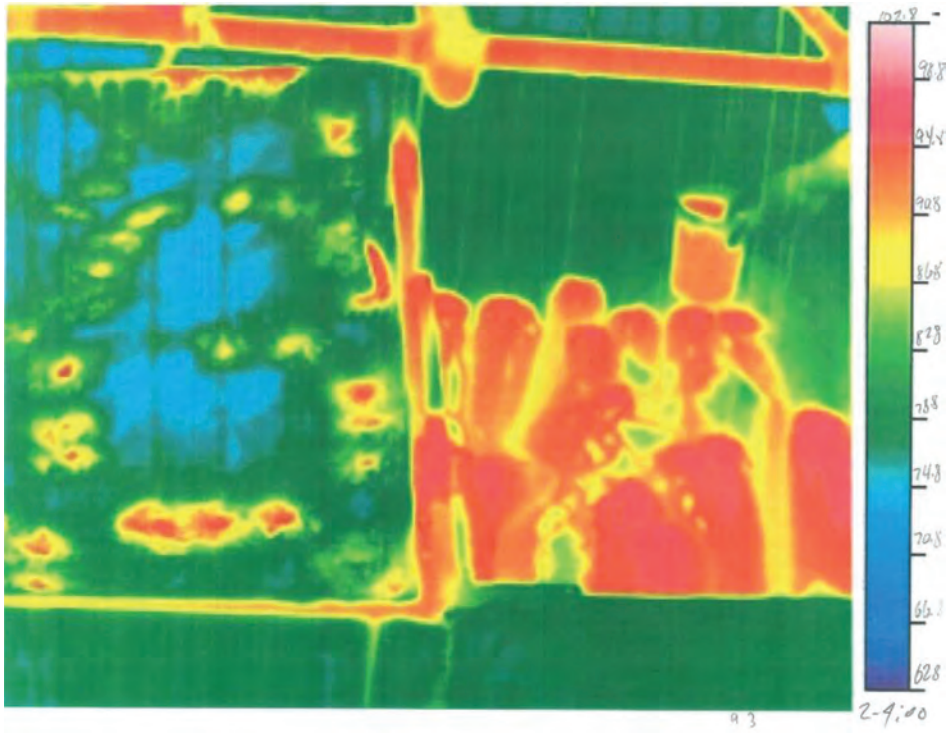

Figure 4: Infrared photo of green roof (left) and control roof (right) setup.

Table 6: Flow data for Trial 2: tap water inflow into green roof [8].

Quantity (mL)		Quantity (mL)	Nitrate concentration (ppm)	pH	Temperature
Wood mulch-mixed soil	Inflow	9,000	N/A	6.5	24 °C
	Runoff	2,360	1,000	6.5	23 °C
Only soil	Inflow	9,000	600	7.0	24 °C
	Runoff	1,460	750	6.5	23 °C

parameters for an error function mathematical model [14,17]. The second study elaborated further on runoff retention and thermal buffering. Furthermore, the proximity of the Javits Center to the Lincoln Tunnel was taken into account. As such, there will be a high nitrate loading. The tests in the Cooper Union laboratory showed that the green roof can be managed to reduce this loading. Coupled with the thermal buffering and rainfall storage tests, these experiments can be used as a predictive tool of green roof behaviour, applicable on a larger scale.

During the on-site studies, 55% of the cumulative precipitation that fell on the green roof during the monitoring period was retained, with an average of 75.4%–79.3% of precipitation retained per event. Tests on three roof models run by Carson et al. [18] found that vegetated roofs held 60.6% of rainfall, while media roofs retained 50.4% and gravel ballast roofs retained 27.2%. Additional research can focus on variation of substrate depth and climate conditions, as deeper substrates would hypothetically lead to increased retention. It is possible, however that during the colder seasons (when there is less evapotranspiration), substrates will naturally be wetter from condensation, and runoff may actually occur from the green roof surface at saturation. As the current studies were carried out during the summer, this could not be determined, but should additional studies prove this hypothesis correct, it would reduce the importance given to substrate depth for rainfall retention [14]. Empirical relationships suggested that the green roof's ability to store moisture is directly related with the duration of the event's preceding dry period.

Each run is about 10 minutes long, to simulate a ten-minute storm. Rainfall rates are high, ranging from 1.6 to 13 minutes per hour. The discharge draining from the green roof has a constant temperature for each run and for 20 minutes after the storm. Since there is no albedo and little evapotranspiration, the mechanism to account for this is the transfer of heat from the soil to the green roof (including geotextile and drainage systems). The green roof discharge water is at least 2.5 times more than the control roof for runs with higher rain temperatures than room temperatures. The temperatures for all six runs go through the room temperature.

From the hydrograph data in Fig. 3 and Table 2, there is a lag time between the control and green roof model runs. The control response to the rain is rapid since there is almost no overland flow time. The green roof has a delay, i.e., the time difference in time between the control and green roof at the beginning of the hydrograph from 2 to 12 min. The ratio between the slopes of the control roof line and the green roof line varies from 0.94 to 2.3. The equations of best fit and R2 values are given in Fig. 3 and Table 2. There is a linear fit between the peak flows and ln of the slope. Therefore, we have a method to find peak inflow [peak outflow] in a green roof from this equation. From the IR photos and isotherms, the control roof is as much as 25°F warmer than the green roof.

The mitigation of the heat due to the green roof can be seen in the IR photo in Fig. 4. The deep red colour [temperatures in the mid-90s] on more than half of the control roof contrast to the green blue colour [temperatures in the mid-70s] on most of the green roof. This buffering of up to 25°F effect of the green roof is an advantage in controlling and reducing heat waves an is a serious consideration in the design of buildings and gardens in an urban environment.

Several strategies exist for nitrate remediation in soil. One method is by planting non-legume plants, which absorb nitrates in soil effectively [19]. Leafy greens can be especially useful for this purpose, as they tend to absorb large amounts of nitrogen; examples include carrots, kale and lettuce [20]. A third strategy is wood mulch, which can tie up nitrogen in soil, preventing it from leaching into runoff. For this research, wood mulch was used, due to its ease of application for experimental studies.

The runoff from the boxes had to be diluted with 20 mL of deionized water per 5 mL of runoff. For Box A (with wood mulch), the average nitrate concentration of the runoff changed from 1,300 ppm on Trial Date 1 to 1,000 ppm on Trial Date 2, showing a significant decrease of 23.1%. For the control group in Box B, with no wood mulch, the Trial 1 average nitrate level of 800 ppm changed on Trial Date 2 to 750 ppm, a reduction of only 6.25%. No conclusions can be drawn from the pH, as there was no significant change across both trial dates. According to previous research, use of nitrate-based fertilizers (as was added to the inflow in this experiment) have no potential for acidification, and may actually have the opposite effect when plants release OH^- when absorbing hydrogen ions. However, this was not the case in the experiment, likely because there were no plants in the experimental setup, only soil [8]. The temperature of the runoff ending at 23°C for both boxes, despite the inflow temperature, shows that the soil temperature had an effect on the runoff temperature. There was a significant amount of inflow retention by both boxes, ranging from 74% to 85% [8].

The removal of excess nitrates from soil can be beneficial to improving soil health. By reducing the osmotic pressure, plants will be able to take in more nutrients, while also diverting less energy towards metabolizing nitrates. Eutrophication will also be mitigated, preventing excessive algal growth in the water and maintaining oxygen levels and sunlight penetration. Furthermore, nitrate leaching tends to also carry away other essential minerals such as sulphur – by preventing this outcome, the soil quality is maintained [8].

The error function mathematical model previously referenced is presented in the 2017 study, and used again as a predictive equation in the 2018 study [14,17]. It was first developed by Carslaw and Jaegar [23] and uses heat conduction principles. This model is a function of thermal conductivity, depth and heat exposure time. It is subjective to two boundary conditions. The temperature gradient in the sub-layers of the JGR was determined using this one-dimensional heat conduction model. This heat conduction model relies on the material properties of the roof. A sensitivity analysis was conducted by varying a number of green roof parameters such as depth, Javits Convention Center ambient temperatures, alpha values, and heat exposure times. There is little change in the ceiling temperature when these parameters were altered. The average change in the Javits Convention Center ceiling is less than 3%. When the ambient outside air temperature is less than inside of the convention centre, the roof acts as an insulator from cold air. A thicker foam layer makes for better insulation from heat source, but a larger change in depths of this results in a relatively smaller thermal change.

5 CONCLUSION

From the tests run on the Javits Green Roof, laboratory tests, and mathematical modelling the following conclusions are drawn:

- The surface of the green roof was 16°C cooler than the surface of the bitumen green roof, and also cooler than sidewalk surfaces by 5–10°C [14]
- From field observations, laboratory investigations and mathematical modelling, the cross section of the green roof is more effective for thermal buffering than the corresponding structural roof cross section (11.9°C vs. 9.0°C) [14]

These studies of the Javits Green Roof provide evidence for the claim that construction of green roofs can be seen as a win-win opportunity While the floor space inside the building is maximized for development, the rooftop can be used to simultaneously mitigate heavy rainfall and comply with the city's stormwater regulations. Some of these regulations are defined

under NYC Local Laws 92 and 94 of 2019, which require that any roofing constructions or expansions must incorporate sustainable roofing systems; this means either solar panels, green roofs, or a combination of both [21]. Green roofs also allow the city to be better prepared to combat climate change (reducing UHI effect), along with other social and aesthetic improvements brought about from their construction [14].

The observations, modelling and analysis of the Javits Green Roof suggests that for some, building green roofs represent a win-win opportunity. By utilizing the building's rooftop space to mitigate incident rainfall, building owners can maximize developable floor space inside the building, while minimizing the cost to comply with current stormwater management requirements in New York City. Simultaneously, this same strategy can help prepare the city for climate change, while enhancing the city with the other co-benefits of this rediscovered approach to urban storm water management [14].

The error function model was used to simulate 53 pairs of internal surface temperatures. On average the model predictions were within 3% of the measured values as recorded during the experimental procedures [14,17]. This validation indicates that the error function mathematical model is very accurate in predicting the ceiling temperatures of the Javits Center and the thermal heat diffusion profile through the green roof layers.

For the experimental models tested in the laboratory, the heat exchange between the rainwater and the green roof material takes place during the first few minutes of the storm. The front is defined by movement of the infiltrating rain, and diffuses upstream and downstream, spreading its heat. For the experiment conducted, 10- to-15-min storms were not long enough to raise the green roof model temperatures more than 7.3 °F above room temperature. There is no radiation and little evapotranspiration; therefore, the conductivity of the green roof can be examined independently.

The IR photo shows how the green roof mitigates the temperatures on a black control roof by as much as 25 °F. The ponding of the control roof, for rain storms larger than the capacity of the drain is shown in the infrared photo. The black roof model has almost all temperatures in the 90s. The vegetated roof shows green and blue colours, signifying temperatures in the mid-70s. From the slope of the control roof and green roof hydrographs, the peak flows can be determined with R^2 larger than 0.9.

According to the NYC Department of Environmental Protection, green roofs can remove 35% of the total nitrogen in its inflow [22]. This study showed that wood mulch, when mixed in with soil, can effectively reduce nitrogen levels in soil runoff by an additional 17%, This provides evidence for the theory that incorporation of wood mulch into green roofs increases their usefulness as a mechanism for water quality improvement. There was no evidence found for the effect on pH. However, support was provided for the concept that soil temperatures will influence runoff temperatures, as well as the idea that green roofs are highly effective for inflow retention.

REFERENCES

[1] Masters, J., July 2021 was Earth's warmest month in recorded history, says NOAA; Yale Climate Connections, https://yaleclimateconnections.org/2021/08/july-2021-was-earths-warmest-month-in-recorded-history-says-noaa/, Accessed on: 24 September 2021

[2] Plumer, B. & Fountain, H., A Hotter Future Is Certain, Climate Panel Warns. But How Hot Is Up to Us; NY Times, https://www.nytimes.com/2021/08/09/climate/climate-change-report-ipcc-un.html, Accessed on: 24 September 2021

[3] Global Climate Report – Annual 2020; National Centers for Environmental Information, https://www.ncdc.noaa.gov/sotc/global/202013, Accessed on: 24 September 2021
[4] Climate Impacts Along the Mississippi River Corridor; Climate Nexus, https://climatenexus.org/climate-change-us/climate-impacts-along-the-mississippi-river-corridor/, Accessed on: 24 September 2021
[5] Bernton, H., As Alaska permafrost melts, roads sink, bridges tilt and greenhouse gases escape; Anchorage Daily News https://www.adn.com/alaska-news/weather/2019/12/17/as-alaska-permafrost-melts-roads-sink-bridges-tilt-and-greenhouse-gases-escape/, Accessed on: 24 September 2021
[6] Oke, T.R., & Claughm H.A., Urban heat storage derived as energy balance residuals. *Boundary Layer Meteorology*, **39**, pp 233–245, 1987.
[7] da Silva, J., Kernaghan, S., & Luque, A., A systems approach to meeting the challenges of urban climate change. *International Journal of Urban Sustainable Development*, **4**(2), pp 125,145, 17 September 2012.
[8] Sanyal, H., Elborolosy, Y.Y. & Cataldo, J., Modeling the Behavior of Rain Gardens. *Sustainable Water Resources Management 2021*, pp. 143-154, 2021
[9] Rozenzweig, C., Solecki, W.D., Hammer, S.A. & Mehrotra, S., Climate Change and Cities: First Assessment Report of the Urban Climate Change Research Network, Cambridge University Press, 2011.
[10] Best, M.J., & Grimmond, C.S.B., Key Conclusions of the First International Urban Land Surface Model Comparison Project. *Bulletin of the American Meteorological Society*, **96**(5), pp. 805-819, 1 May 2015
[11] Rozenzweig, C., Gaffin, S. & Parshall, L., Green Roofs in the New York Metropolitan Region, Columbia University Center for Climate System Research, 2004.
[12] Liptan, T. Planning zoning & financial incentive for ecoroofs in Portland, Oregon. *Proceedings of 1st North American Green Roof Conference: Greening Rooftops for Sustainable Communities*, Chicago 29-30, 2003, pp 113-120, 2003
[13] Lankao P.R., Urban Areas & Climate Change: Review of Current Issues and Trends; Institute for the Study of Society and Environment, National Center for Atmospheric Research, https://citeseerx.ist.psu.edu/viewdoc/download?doi=10.1.1.448.9789&rep=rep1&type=pdf, Accessed on: 4 September 2015
[14] Alvizuri, J., Cataldo, J., Smalls-Mantey, L.A., Montalto & F.A., Green roof thermal buffering: insights derived from fixed and portable monitoring equipment. *Energy and Buildings, 151*, pp. 455-468, 2017.
[15] Solecki, W., Leichenko, R. & O'Brien, K., Climate change adaptation strategies and disaster risk reduction in cities: connections, contentions, and synergies. *Current Opinion in Environmental Sustainability*, **3**(3), pp 135-141, 2011.
[16] Pelling, M., O'Brien, K. & Matyas, D., Adaptation and transformation. *Climate Change*, **133**, pp. 113-127, 2015.
[17] Abualfaraj, N., Cataldo, J., Elborolosy, Y., Fagan, D., Woerdeman, S., Carson, T. & Montalto, F., Monitoring and Modeling the Long-Term Rainfall-Runoff Response of the Jacob K. Javits Center Green Roof. *Water 2018*, **10**(11), 2018.
[18] Carson T.B., Marasco D.E., Culligan P.J. & McGillis W.R., Hydrological performance of extensive green roofs in New York City: observations and multi-year modeling of three full-scale systems. *Environmental Research Letters*, **8**(2), 024036, 7 June 2013.
[19] Parnes, R., Chapter 10. Nitrogen, https://www.nofa.org/soil/html/nitrogen.php, Accessed on: 10 December 2020

[20] Tobias, M. Local Laws 92 and 94 of 2019: Mandatory Solar and Green Roofs in NYC. https://www.ny-engineers.com/blog/local-laws-92-and-94-of-2019, Accessed on: 1 October 2021
[21] MacDonald, M. Too Much Nitrogen. R https://www.westcoastseeds.com/blogs/garden-wisdom/too-much-nitrogen, Accessed on: 10 December 2020
[22] New York City Stormwater Design Manual; NYC Department of Environmental Protection, https://www1.nyc.gov/assets/dep/downloads/pdf/water/stormwater/ms4/stormwater-manual-final.pdf, Accessed on: 1 October 2021
[23] Carslaw, H.S. & Jaeger, J.C., *Conduction of Heat in Solids*, 2nd Edition, Clarendon, Oxford, 1959

SATELLITE DERIVED ESTIMATION OF CHLOROPHYLL-A ON HARMFUL ALGAL BLOOMS (HABS) IN SELECTED DAMS OF VHEMBE DISTRICT, LIMPOPO PROVINCE

LINTON F. MUNYAI[1*], FARAI DONDOFEMA[1], KAWAWA BANDA[2], MULALO I. MUTOTI[3] & JABULANI R. GUMBO[3]
[1]Aquatic Systems Research Group, Department of Geography and Environmental sciences, University of Venda, South Africa
[2]Integrated Water Resources Management Centre, C/O Department of Geology, University of Zambia, Zambia
[3]Department of Earth Sciences, University of Venda, South Africa

ABSTRACT
Satellite remote sensing techniques have been proved to be capable of quantifying chlorophyll-a (Chl-*a*) levels by estimating algal concentrations in water bodies. Harmful algal blooms (HABs) pose a significant threat to many water bodies in South Africa. This study aimed at using a remote sensing solution to estimate chlorophyll concentrations in water bodies of Vhembe District Municipality using Landsat 8 OLI. This study seeks to provide quantitative water quality information for the Vhembe region's water bodies from a time series of satellite remotely sensed data and in-situ laboratory data. The 30 meters spatial resolution multispectral Landsat 8 OLI for 2016, 2017 and 2018 were used to derive Chl-*a* estimate at three water bodies, namely, Nandoni, Albasini and Vondo reserviors. The Chl-*a* concentrations obtained from Landsat 8 (OLI) satellite were compared with the laboratory analysis using the Kappa coefficient statistical analysis. This study show that Landsat derived chl-*a* estimates have a high positive correlation of 80–90% accurate with field measurements. In all the reservoirs, it was detected that there is low content of HABs and thus the water bodies are in good condition since the chl-*a* concentrations were very low. In conclusion, it can be stated that Landsat 8 OLI sensor can be used to map and monitor inland water bodies dominated by algal blooms to a certain extent.
Keywords: chlorophyll-a, harmful algal blooms, L andsat 8-OLI, remote sensing, water quality.

1 INTRODUCTION

Anthropogenic activities progressively subject the freshwater ecosystems to stress, which significantly decreases the water quality, and this reduces chances for aquatic life (Rashid and Romshoo, 2013). Most of the freshwater resources are threatened by harmful algal blooms (HABs) which increases in severity within developing countries (Vilmi et al., 2015). These HABs often tend to alter aquatic habitats, through shading, reducing dissolved oxygen and can also pose adverse effects on various life stages of fish and other pelagic marine organisms (Stumpf and Tomlinson, 2007). Remote sensing has been used previously to monitor these phenomena (Winarso and Ishizaka, 2017). Previous studies conducted on assessing the Spatio-temporal distribution of HABs mostly were primarily done in larger reservoirs and marine systems (Carvalho et al., 2010; Kudela et al., 2015); however, with advancement, remote sensing can now utilize data sets and statistical regressions techniques to analyze reflectance from an inland water body (Diouf, and Seck, 2019; Hikosaka and Noda, 2019; De Souza et al., 2020). Within South Africa, HABs cause mass fatalities of fish and other aquatic species in aquatic systems (Botes et al., 2003). The Spatio-temporal distribution of HABs on inland aquaculture especially in Vhembe District, has not been studied. Furthermore, HABs are increasingly attracting the attention of water authorities, environmental agencies and government departments since they pose water quality and treatment problems (Kutser et al., 2006). This study evaluated the distribution extent of HABs along the water supply reservoirs

ISSN: 2398-2640 (paper format), ISSN: 2398-2659 (online), http://www.witpress.com/journals
DOI: 10.2495/EI-V5-N4-362-374

of the Vhembe region in the Limpopo Province. It estimated the chl-a concentration of the respective reservoirs.

Fish kills have occurred for many years, possibly from cyanobacteria toxins that have been ingested by fish while feeding on floating diets which are passively assimilated through gills during breathing (Dawood et al., 2015). Most algae species are considered helpful in food-fish production ponds (Zimba et al., 2001) They release oxygen as by-product of photo-synthesis process and remove toxic compounds from a water column such as ammonia and nitrates (Huang et al., 2018). Inland fisheries contribute to economic development, poverty alleviation and food security whereas on the other side they degrade the quality of water resources (McCafferty et al., 2012). According to Craig et al. (2017), fish feeds contribute to degradation of water quality in food-fish production ponds. The evidence suggest that eutrophic conditions lead to increasing dominance of HABs which pose threat to aquatic ecosystems through producing potentially lethal cyanotoxins (Paerl et al., 2016).

According to Trescott (2012), HABs in surface waters such as lakes and ponds results from the impacts of anthropogenic and natural activities. Nutrients loads in surface waters also contribute to the increased growth of HABs in our water bodies. It is essential to essentially blooms in freshwater systems to provide knowledge, indicators of degraded water quality in different areas, and different other alerts on the progression of HABs in our water resources (Adeleye et al., 2016). Since water treatment is expensive and costly in most rural areas, there is a cost-effective, to monitor the growth of HABs using remote sensing in the water for management purposes (Lawton and Robertson, 1999).

1.1 Harmful algal blooms, chlorophyll-A and remote Sensing

Remote sensing has widely been used in monitoring HABs in lakes, oceans and dams. However, few studies have focused on remote sensing monitoring cyanobacteria in inland aquaculture water bodies by extrapolating algae, phycocyanin and chl-a present. Remote sensing application for HABs detection requires satellite sensors with high spatial/temporal resolution and high radiometric sensitivity (Giardino et al., 2014). According to Shen et al. (2012), remote sensing of monitoring HABs requires knowledge, skills and a comprehensive understanding of remote sensing mechanisms. Caballero et al. (2020) suggest that monitoring of HABs using remote sensing as a tool is more complicated, however, satellite remote sensing of monitoring inland water bodies impacted with HABs is limited to larger water bodies/lakes and handheld sensors because there are few satellite sensors with high spatial resolution to map inland water bodies since they are small (Kutser, 2009).

Most studies focused on chl-a estimation in turbid water using different algorithms, models and laboratory analysis of chl-a concentration (Hansen et al., 2013; Hansen et al., 2015; Caballero et al., 2013). Several studies on detection and monitoring chl-a in water bodies are based on the empirical models of reflectance, radiance in narrow bands and chl-a (Devi et al., 2015). Researchers collected field data on chlorophyll through handheld satellite or sensors mounted on space to validate their models. This is a very good approach since satellites remote sensing data is calibrated or validated by field observation and ground truthing. Furthermore, the combination of all these methods makes the data more linked and as such, the results are reliable and conclusive.

One of the main objectives of aquaculture systems especially in rural area is to provide food security and alleviate poverty by provision of employment to people. Numerous studies reported fish mortality in aquaculture systems from cyanobacterial toxins and oxygen

competition (Zimba et al., 2001; Zi et al., 2018). Most fish farming is vulnerable to deterioration by HABs and this is influenced by different environmental factors (physical, biological and chemical) which are driven by anthropogenic activities. It is of paramount importance to reduce the impacts of HABs in fish farming hence this study intends to investigate the use of satellites and in-situ field data as a tool for monitoring the progression of HABs.

Remote Sensing can be used to determine chlorophyll and cyanobacteria contents in deep and shallow waters. The concentration of chl-a in water bodies has been determined using the empirical correlation between radiance and reflectance of algae in water bodies, thus few studies focused on narrow bands (Duab et al., 2012; Devi et al., 2015). Other studies developed models focusing on both empirical and semi-analytical algorithms for conducting in-situ spectral analysis (Ali et al., 2014; Mouw et al., 2015). Most of the field data which are collected in remote sensing studies are intended to validate models formulated, however some of the data is used to correlate the two sets of data (Satellite and in-situ data). It has been found that in-situ field measurements provide the water bodies spectrum and chl-a concentration through collection of water samples and analyzing spectral reflectance from Spectroradiometer. Several studies have been done in determination of chlorophyll and its derivatives with exceptions of pheophytin and phycocyanin in natural water systems by extracting the pigment from the plant material or the algal bloom (Gavrilović et al., 2012; Hynstova et al., 2018). Moreover, lot of methodology in determination of chlorophyll has been identified by researchers including the use of satellite remote sensing in extracting the green pigment found on algae by estimating chlorophyll content.

In detecting trophic status of chl-a, mathematical algorithms have been used with the application of top-atmosphere data from satellite especially MERIS (Gons et al., 2005; Odermatt et al., 2010; Zhang et al., 2019; Free et al., 2020). Matthews et al. (2012) used Maximum Height Peak (MPH) algorithm to detect cyanobacterial blooms, surface scums and chl-a by calculating the height of the dominant peak across the MERIS bands which are red and near infrared between 664 and 885nm wavelength. The idea of using both MERIS and in situ data was to allow models to cover a wide trophic water dominated by surface scums, where oligotrophic, hypertrophic and dry floating algae are differentiated based on the MPH variable magnitude (Matthews et al., 2012). Hence the current study applied Landsat 8-OLI in detecting the distribution of HABs at Nandoni, Albasini and Vondo dams. The present study aimed at (1) determining the spatial and temporal distribution of chl-a in Nandoni, Vondo and Albasini dam, (2) to compare the remote sensing data and in-situ data through applying the existing model of remote sensing on inland water bodies.

2 MATERIAL AND METHODS

2.1 Study area

Three reserviors, namely, Nandoni, Albasini and Vondo in Vhembe District Municipality (VDM) were considered for in-situ sampling of chl-a analysis using both Laboratory and Remotely sensed methods (Fig. 1). Two reserviors (Nandoni and Vondo) are located under Thulamela Local Municipality and Albasini Dam is located under Makhado Local Municipality. All these reserviors are the water suppliers of almost all communities in VDM and they provide habitat to most fish, invertebrates and other aquatic species. Nandoni reservior (Lat: −22.983324° and Long: 30.579191°) is the most reliable water supply reservoir and is situated at Ha-Budeli which is 30 km from Thohoyandou town. The reservoir supplies water

to different communities such as Thohoyandou, Sibasa, University of Venda and nearby communities. The reservoir has the total capacity of 164 million cubic meters and a catchment area of 1380 km^3 with the total surface area of 1570 hectares.

Vondo reservior (Lat: –22.946375° and Long: 30.336539°) is situated at the mountainous area under Vondo Tribal authority. The reservoir is a source of water to communities such as Thathe Vondo village, Gondeni, Maranzhe and Phiphidi and has the total capacity of 30 million cubic meters with 219 hectares of surface area. Whereas Albasini reservior (Lat: –23.107238° and Long: 30.117978°) is a source of water for communities such as Makhado town, Mpheni Village, Elim and Waterval. This reservoir has a total capacity of 25,200,000 cubic meters and a surface area of 350 hectares.

Sampling sites were selected to span the entire surface of each reservoir. Sampling station quantity was determined for them to provide enough representation of the entire water body including both deep and shallow areas (Randolph et al., 2008). The samples were collected along the water column at a range of 0.5–1.0 m in the morning at each site of the dam and stored on ice for analysis in the laboratory. Nineteen (19) samples were collected from Nandoni dam and eight (8) Samples were collected from Vondo dam whereas (nine) 9 samples were collected from Albasini dam using a boat. The number of collected samples in each dam depended on the size of the particular reservoir.

2.2 Chlorophyll-A analysis in water samples

Water samples were defrosted, homogenized in an electric homogenizer and filtered through a Whatman GF/F 0.7 µm glass fiber filter papers, and the volume of the filtered samples was recorded. A 90% ethanol solution was used to extract the chl-a and concentration in mg/m^3 were measures using the spectrophotometric method and converted to µg/L. Absorbance was measured at 665 and 750 nm using a spectrophotometer (Orion aquamate 700, VIS

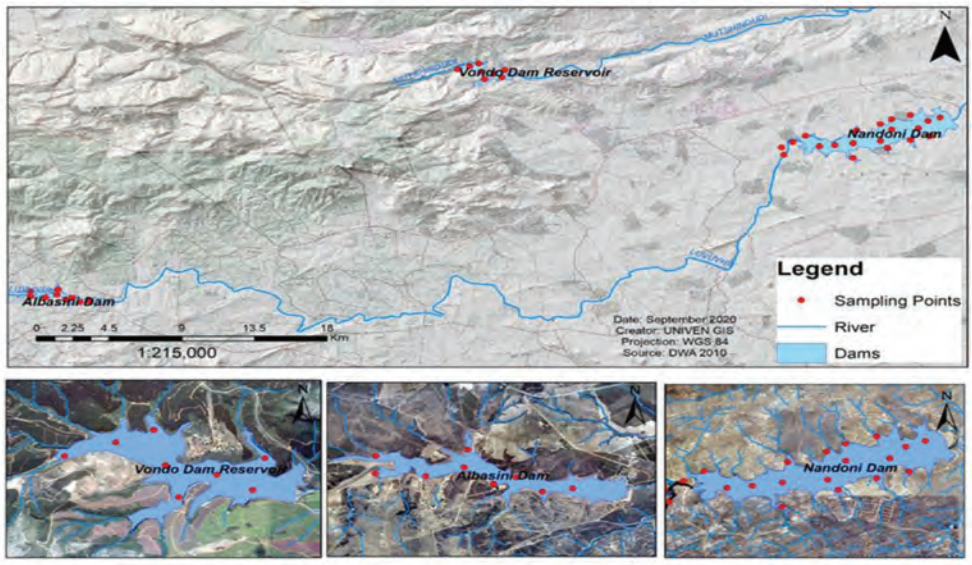

Figure 1: Map of the study area where Measurements of Chlorophyll-a in the dams for comparison with Satellite data were done.

spectrometer). Water samples that were collected during summer and winter were analyzed in the laboratory for chl-a concentration. Chl-a calculation was performed by subtracting absorbance 665a-750a = corrected 665a, absorbance 665b-750b = corrected 665b absorbance. In the present study, the Spectro-photometrical method was employed as described by Dalu et al. (2013) for analysis of chl-a in water samples. The equation 1 below was used to calculate the concentration of chl-a in water samples:

$$Chl-a = \frac{29.62\left(665a-665b\right)\times Ve}{Ve\times l} \quad (1)$$

Where: V_e = Volume of ethanol extract (ml)
Vs = Volume of water sample filtered (litres)
l = Path length of cuvette (cm)

2.3 Remote sensing data acquisition and pre-processing

Three medium spatial resolution (30 m) multispectral Landsat 8 Operational Land Imager (OLI) images freely acquired over Nandoni, Vondo and Albasini for the year 2016, 2017 and 2018 were used to derive chl-a estimates from the selected points in the reservoirs. In this study, all images with cloud cover greater that 75% were excluded to retrieve chl-a concentration accurately (Ndungu et al., 2013). The satellite images were acquired on the following dates (Table 1):

All Landsat images were downloaded from USGS and were in Digital number format (DN values). To derive chl-a from those images, the images were calibrated from DN values to Top-of-atmosphere spectral reflectance units (Wm-2 sr-1 μm-1) using the algorithm provided by the USGS for converting reflective band to top-of-atmosphere reflectance. The algorithm (2) is as follows:

$$\rho\lambda = M\rho Qcal + A\rho \quad (2)$$

Where: Mρ = Reflectance_Mult_Band
Aρ = Reflectance_Add_Band
Qcal = Quantized and calibrated standard product pixel values (DN)

All the variables presented on the above equation could be retrieved from the metadata file which was downloaded with the original images. Band math was also used to convert radiance to reflectance using ENVI 4.4 Software. The visible spectral bands of the Landsat OLI (Band 2 and 3) were used in order to retrieve chl-a over the Nandoni, Albasini and Vondo reservoirs (Dube, 2012; Dube et al., 2014).

Table1: Landsat acquisition information sourced from USGS ONLINE Archive (http://earthexplorer.usgs.gov/.).

Satellites images	Date of acquisitions	Landsat scene ID	
2016	26 August 2016	LC81690762016223LGN01	**Path= 169**
2017	26 August 2017	LC81690762017241LGN00	**Row= 76**
2018	26 August 2018	LC81690762018228LGN01	

In estimating chl-a concentrations from reflectance values, spectral bands at 445 and 556nm are very important because that is where chl-a absorption is at peak while the lowest chl-a absorption is normally found at 520 and 550 nm (Dube, 2012; Dube et al., 2014). Based on this knowledge, this study employed the most popular chl-a estimation expression (Yadav et al., 2019; Buditama et al., 2017) to derive estimates over Nandoni, Albasini and Vondo dam from atmospherically corrected Landsat OLI images. The following function (3) was used to computes chl-a concentration:

$$\text{Log Chl-a} = (2.41*\text{B4/B3}) + 0.187 \tag{3}$$

2.4 Data validation

The chl-a in-situ data that were measured in the field on the 07 September 2017 was used to validate the Landsat 8 OLI which was acquired on the 26 of August 2017. The data was validated by comparing the concentrations of chl-a of two different dates in all reservoirs. The concentrations of chl-a for both field measurements and remotely sensed data were exported from ESRI ArcGIS 10x attribute table to Microsoft excel spreadsheet.

Kappa coefficient statistic method was used for validating the field measurements and the pixel values retrieved from Landsat 8. Kappa measured inter-raster agreement for the two data sets collected and K value was computed using Microsoft excel. Equation 4 below was used to determine the significance of two variables which had a strong relationship. After deploying the above index, an output was created on ENVI software 4.4 with a Logarithm spectral reflectance value, therefore an anti-log was calculated.

$$K = \frac{\text{Po} - \text{Pc}}{1 - \text{Pc}} \tag{4}$$

Where, Po = Field measurements
Pc = Remotely sensed values (Derived from anti-log expression)
K= Agreement Coefficient Value

3 RESULTS AND DISCUSSION

3.1 Remote sensing and in-situ measurements

Figure 2 shows the maps of chlorophyll-*a* concentration estimated by the model where red and green band ratios were used. On this study, we had shown the potential of estimating chlorophyll-*a* concentration in dams with the positive pixel values. The pixels were not represented in the maps, but the classes represented on the images were derived from the empirical model used by Buditama et al. (2017).

From the image classes shown on Fig. 2, 2016 Images in all reservoirs showed very low concentration of chl-*a*, however Landsat 8 OLI was able to map algal blooms in the respective reservoirs. In the reservoirs, distribution of chl-*a* varies spatially and temporally. It can simply be observed that during summer 2016, the concentration of chl-*a* was very low as compared to summer 2018 at Nandoni reservoir. However, the algal abundance was remotely sensed at the edges of the dam. From the observation of the images in Fig. 2, spatial distribution of low algal content was observed in the middle of the Nandoni reservoir in the year

2018 while in 2016 there were no algal blooms detected. Vondo reservoir revealed no algal bloom content from 2016 to 2018. This shows that Vondo reservoir has not been impacted by cyanobacterial blooms for the period of 3 years. The concentration of chl-*a* in Vondo reservoir ranged from 0.0 to 0.3 mg m^{-3}.

In Nandoni and Albasini reservoirs, the chl-*a* had higher values on the area near the dam wall and reservoir edges while getting lower in the middle of the reservoir. This statement is based on sample data P9, P11, P17 and P19 which are nearest samples to the edges and in the middle of the reservoir. The dominance of chl-*a* is mainly caused by the few nutrients which are washed from agriculture, mining and other industries and deposited on the edges of the reservoirs. This results in a rapid growth of algae where there is high accumulation of nutrients (at the edges of the dams). The temporal variations of chl-*a* concentrations are mainly caused by rainfall which tempers with runoff as the main supplier of algal blooms (Buditama et al., 2017).

From Fig. 2, it was also observed that besides detection of algal blooms in water, during classification, vegetation adjacent to the reservoir was detected as algae since plants contains the chlorophyll pigment, however, the present study only accounts for chl-*a* detected within the water body as attested by the field measurements.

Overall, from the results obtained from the remotely sensed and the In-situ measurements, it can be concluded that the three reservoirs have not been affected by high concentration of chlorophyll between the year 2016 and 2018. Since all the data discussed in this study was acquired during summer periods with low rainfall, this maybe the reason for low chlorophyll concentration in the dams because of low rainfall which normally carry nutrients to the water bodies which facilitate algal growth.

From the remotely sensed and Laboratory analysis, we have observed a strong correlation of pixel values derived from chl-*a* estimates and chl-*a* values analyzed in the laboratory (Tables 2 to 4). The correlation is positive because the increase in one value of chlorophyll estimates from Landsat is an increase in the Lab data while decrease of Landsat pixel value is also a decrease in Chlorophyll lab results. This study demonstrated the potential of Landsat 8

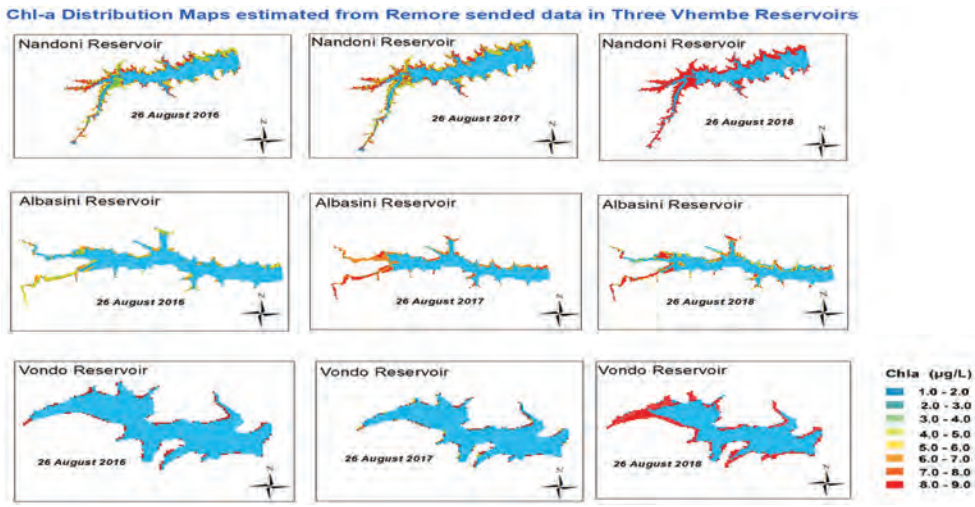

Figure 2: Showing chlorophyll-a distribution map in the Nandoni, Albasini and Vondo dams in Vhembe district, Limpopo province.

Table 2: Mean Concentrations of chlorophyll-a for Laboratory analysis, remotely sensed data and KAPPA Index Value in Nandoni dam for three years (2016, 2017 and 2018.).

Sample number (Nandoni Dam)	Field measurements. Chlorophyll-a concentration (mg m^{-3})	Remotely sensed (Anti-Log extracted values)	KAPPA Index value
P1	0.8	0.2	0.75 (75%)
P2	0.8	0.2	0.75 (75%)
P3	0.9	0.5	0.80 (80%)
P4	0.7	0.1	0.67 (67%)
P5	0.8	0.5	0.60 (60%)
P6	0.3	0.2	0.13 (13%)
P7	0.8	0.3	0.71 (71%)
P8	0.9	0.1	0.89 (89%)
P9	0.8	0.3	0.71 (71%)
P10	0.7	0.1	0.67 (67%)
P11	0.8	0.2	0.75 (75%)
P12	0.7	0.1	0.67 (67%)
P13	0.7	0.1	0.67 (67%)
P14	0.6	0.5	0.20 (20%)
P15	0.9	0.5	0.80 (80%)
P16	0.8	0.2	0.75 (75%)
P17	0.9	0.5	0.80 (80%)
P18	0.7	0.1	0.67 (67%)
P19	0.8	0.6	0.50 (50%)

Table 3: Mean Concentrations of chlorophyll-a for Laboratory analysis, remotely sensed data and KAPPA Index Value in Vondo dam for three years (2016, 2017 and 2018.).

Sample number (Vondo Dam)	Field measurements. Chlorophyll-a concentration (mg m^{-3})	Remotely sensed (Anti-Log extracted values)	KAPPA Index value
V1	0.9	0.1	0.89 (89%)
V2	0.9	0	0.90 (90%)
V3	0.8	0	0.80 (80%)
V4	0.8	0.2	0.75 (75%)
V5	0.7	0.1	0.67 (67%)
V6	0.8	0	0.80 (80%)
V7	0.9	0.5	0.80 (80%)
V8	0.9	0.4	0.83 (83%)
V9	0.7	0.2	0.63 (63%)

Table 4: Mean Concentrations of chlorophyll-a for Laboratory analysis, remotely sensed data and KAPPA Index Value in Albasini dam for three years (2016, 2017 and 2018.).

Sample number (Albasini Dam)	Field measurements. Chlorophyll-a concentration (mg m^{-3})	Remotely sensed (Anti-Log extracted values)	KAPPA-Index value
A1	0.9	0.5	0.80 (80%)
A2	0.8	0.1	0.78 (78%)
A3	0.8	0.2	0.75 (75%)
A4	0.9	0.5	0.80 (80%)
A5	0.7	0.1	0.67 (67%)
A6	0.6	0.4	0.33 (33%)
A7	0.9	0.1	0.89 (89%)
A8	0.9	0.4	0.83 (83%)
A9	0.9	0.2	0.88 (88%)

OLI images on mapping areas with high and low concentration of chl-*a*. The spatio-temporal variation in the concentration of Chl-*a* within the dams likely reflects the yearly and physicochemical factors influences. Chlorophyll estimates of all dams derived from Landsat OLI images were very low for most part of the dams which is attributed to decreased water level in the Nandoni, Vondo and Albasini dam (Dalu et al., 2015).

4 CONCLUSION

Based on the derived and measured total chl-a concentrations across all the reservoir i.e. Nandoni, Vondo and Albasini, it can be concluded that the dams possess low concentrations. The algorithm employed in the images to derive chl-a worked successfully on the Landsat OLI images. It can be concluded that Landsat OLI is suitable for real time monitoring of HABs in water bodies and can accurately map areas where cyanobacterial blooms are abundant. This was also attested by the Kappa coefficient analysis which determined the level of agreements between two or more data sets. 80–90% of K values were observed across all the sites which showed high level of agreement of correlation of field chl-a concentration and satellite remotely sensed variables.

ACKNOWLEDGEMENTS

This research was funded by National Research Foundation of South Africa "NRF Innovation Master's scholarship", project UID 106618 and University of Venda Post graduate research funds: Grant number SES/07/ERM/01. We wish to acknowledge Dr Sam Kaheru for providing a working space for conducting experiments in the School of Education, Physical Science Laboratory, University of Venda.

REFERENCES

[1] Adeleye, A.S., Conway, J.R., Garner, K., Huang, Y., Su, Y. & Keller, A.A., Engineered nanomaterials for water treatment and remediation: costs, benefits, and applicability. *Chemical Engineering Journal*, **286**, pp. 640-662, 2016.

[2] Ali, K., Witter, D. and Ortiz, J., Application of empirical and semi-analytical algorithms to MERIS data for estimating chlorophyll a in Case 2 waters of Lake Erie. *Environmental Earth Sciences*, **71(9)**, pp. 4209-4220, 2014.

[3] Botes, L., Smit, A.J. and Cook, P.A., The potential threat of algal blooms to the abalone (Haliotis midae) mariculture industry situated around the South African coast. Harmful Algae, **2(4)**, pp. 247-259, 2003.

[4] Buditama, G., Damayanti, A. and Pin, T.G., December. Identifying Distribution of Chlorophyll-a Concentration Using Landsat 8 OLI on Marine Waters Area of Cirebon. In *IOP Conference Series: Earth and Environmental Science* (Vol. 98, No. 1, p. 012040), 2017. IOP Publishing.

[5] Caballero, I., Fernández, R., Escalante, O.M., Mamán, L. and Navarro, G., New capabilities of Sentinel-2A/B satellites combined with in situ data for monitoring small harmful algal blooms in complex coastal waters. *Scientific Reports*, **10(1)**, pp. 1-14, 2020.

[6] Carvalho, G.A., Minnett, P.J., Fleming, L.E., Banzon, V.F. and Baringer, W., Satellite remote sensing of harmful algal blooms: A new multi-algorithm method for detecting the Florida Red Tide (Karenia brevis). Harmful algae, **9(5)**, pp. 440-448, 2010.

[7] Craig, S., Helfrich, L.A., Kuhn, D. and Schwarz, M.H., Understanding fish nutrition, feeds, and feeding. 2017.

[8] Dalu, T., Clegg, B. and Nhiwatiwa, T., Temporal variation of the plankton communities in a small tropical reservoir (Malilangwe, Zimbabwe). *Transactions of the Royal Society of South Africa*, **68(2)**, pp. 85-96, 2013.

[9] Dalu, T., Dube, T., Froneman, P.W., Sachikonye, M.T., Clegg, B.W. and Nhiwatiwa, T., An assessment of chlorophyll-a concentration spatio-temporal variation using Landsat satellite data, in a small tropical reservoir. *Geocarto International*, **30(10)**, pp. 1130-1143, 2015.

[10] Dawood, M.A., Koshio, S., Ishikawa, M. and Yokoyama, S., Effects of partial substitution of fish meal by soybean meal with or without heat-killed Lactobacillus plantarum (LP20) on growth performance, digestibility, and immune response of amberjack, Seriola dumerili juveniles. *BioMed research international*, 2015, 2015.

[11] De Souza, R., Grasso, R., Peña-Fleitas, M.T., Gallardo, M., Thompson, R.B. and Padilla, F.M., Effect of Cultivar on Chlorophyll Meter and Canopy Reflectance Measurements in Cucumber. *Sensors*, **20(2)**, pp. 509, 2020.

[12] Devi, L. & Ohno, M., Effects of BACE1 haploinsufficiency on APP processing and Aβ concentrations in male and female 5XFAD Alzheimer mice at different disease stages. Neuroscience, **307**, pp. 128-137, 2015.

[13] Diouf, D. and Seck, D., Modeling the Chlorophyll-a from Sea Surface Reflectance in West Africa by Deep Learning Methods: A Comparison of Multiple Algorithms. arXiv preprint arXiv:1912.03216, 2019.

[14] Duan, H., Ma, R., Xu, J., Zhang, Y. and Zhang, B., Comparison of different semi-empirical algorithms to estimate chlorophyll-a concentration in inland lake water. *Environmental monitoring and assessment*, **170(1)**, pp. 231-244, 2010.

[15] Dube, T., Primary productivity of intertidal mudflats in the Wadden Sea: a remote sensing method. [Msc Thesis] University of Twente Faculty of Geo-Information and Earth Observation (ITC), 2012.

[16] Dube, T., Gumindoga, W. & Chawira, M., Detection of land cover changes around Lake Mutirikwi, Zimbabwe, based on traditional remote sensing image classification techniques. *African Journal of Aquatic Science*, **39(1)**, pp. 89-95, 2014.

[17] Free, G., Bresciani, M., Pinardi, M., Ghirardi, N., Luciani, G., Caroni, R. and Giardino, C., A regional evaluation of the influence of climate change on long term trends in chlorophyll-a in large Italian lakes from satellite data. *Earth System Dynamics Discussions*, pp. 1-19, 2020.

[18] Gavrilović, B., Popović, S., Ćirić, M., Subakov–Simić, G., Krizmanić, J. and Vidović, M., Qualitative and quantitative composition of the algal community in the water column of the Grlište reservoir (Eastern Serbia). *Botanica Serbica*, **40(2)**, pp. 129-135, 2016.

[19] Giardino, P.P., Karnnike, K., Masina, I,. Raidal, M & Strumia, A. The universal Higgs fit. Journal of High Energy Physics. Springer Berlin Heidelberg, 2014.

[20] Gons, H.J., Rijkeboer, M. and Ruddick, K.G., Effect of a waveband shift on chlorophyll retrieval from MERIS imagery of inland and coastal waters. *Journal of Plankton research*, **27(1)**, pp. 125-127, 2005.

[21] Hansen, C., Swain, N., Munson, K., Adjei, Z., Williams, G. P. & Miller, W., Development of sub-seasonal remote sensing chlorophyll-a detection Models. American Journal of Plant Sciences, 2013, 2013.

[22] Hansen, C.H., Williams, G.P. & Adjei, Z., Long-Term Application of Remote Sensing Chlorophyll Detection Models: Jordanelle Reservoir Case Study. *Natural Resources*, **6**, pp. 123-129, 2015.

[23] Hikosaka, K. and Noda, H.M., Modeling leaf CO2 assimilation and Photosystem II photochemistry from chlorophyll fluorescence and the photochemical reflectance index. *Plant, cell & environment*, **42(2)**, pp. 730-739, 2019.

[24] Huang, J., Zhang, Y., Huang, Q. and Gao, J., When and where to reduce nutrient for controlling harmful algal blooms in large eutrophic lake Chaohu, China?. *Ecological Indicators*, **89**, pp. 808-817, 2018.

[25] Hynstova, V., Sterbova, D., Klejdus, B., Hedbavny, J., Huska, D. and Adam, V., Separation, identification and quantification of carotenoids and chlorophylls in dietary supplements containing Chlorella vulgaris and Spirulina platensis using high performance thin layer chromatography. *Journal of pharmaceutical and biomedical analysis,* **148**, pp. 108-118, 2018.

[26] Kudela, R.M., Palacios, S.L., Austerberry, D.C., Accorsi, E.K., Guild, L.S. and Torres-Perez, J., 2015. Application of hyperspectral remote sensing to cyanobacterial blooms in inland waters. *Remote Sensing of Environment*, **167**, pp. 196-205.

[27] Kutser, T., Metsamaa, L., Strömbeck, N. and Vahtmäe, E., Monitoring cyanobacterial blooms by satellite remote sensing. Estuarine, *Coastal and Shelf Science*, **67(1-2)**, pp. 303-312, 2006.

[28] Kutser, T., Passive optical remote sensing of cyanobacteria and other intense phytoplankton blooms in coastal and inland waters. *International Journal of Remote Sensing*, **30(17)**, pp. 4401-4425, 2009.

[29] Lawton, L.A. & Robertson, P.K.J., Physico-chemical treatment methods for the removal of microcystins (cyanobacterial hepatotoxins) from potable waters. School of Applied Sciences, The Robert Gordon University, St Andrew Street, Aberdeen, UK. *Chemical Society Reviews*, **28**, pp. 217–224, 1999.

[30] Matthews, M.W., Bernard, S. and Robertson, L., An algorithm for detecting trophic status (chlorophyll-a), cyanobacterial-dominance, surface scums and floating vegetation in inland and coastal waters. *Remote Sensing of Environment*, **124**, pp. 637-652, 2012.

[31] McCafferty, J.R., Ellender, B.R., Weyl, O.L.F. and Britz, P.J., The use of water resources for inland fisheries in South Africa. *Water SA*, **38(2)**, pp. 327-344, 2012.

[32] Mouw, C.B., Greb, S., Aurin, D., DiGiacomo, P.M., Lee, Z., Twardowski, M., Binding, C., Hu, C., Ma, R., Moore, T. and Moses, W., Aquatic color radiometry remote sensing of coastal and inland waters: Challenges and recommendations for future satellite missions. *Remote sensing of environment*, **160**, pp. 15-30, 2015.

[33] Ndungu, J., Monger, B.C., Augustijn, D.C., Hulscher, S.J., Kitaka, N. & Mathooko, J. M., Evaluation of spatio-temporal variations in chlorophyll-a in Lake Naivasha, Kenya: remote-sensing approach. *International journal of remote sensing*, **34(22)**, pp. 8142-8155, 2013.

[34] Odermatt, D., Giardino, C. and Heege, T., Chlorophyll retrieval with MERIS Case-2-Regional in perialpine lakes. *Remote Sensing of Environment*, **114(3)**, pp. 607-617, 2010.

[35] Paerl, H.W., Gardner, W.S., Havens, K.E., Joyner, A.R., McCarthy, M.J., Newell, S.E., Qin, B. and Scott, J.T., Mitigating cyanobacterial harmful algal blooms in aquatic ecosystems impacted by climate change and anthropogenic nutrients. *Harmful Algae*, **54**, pp. 213-222, 2016.

[36] Randolph, K., Wilson, J., Tedesco, L., Li, L., Pascual, D.L. and Soyeux, E., Hyperspectral remote sensing of cyanobacteria in turbid productive water using optically active pigments, chlorophyll-a and phycocyanin. *Remote Sensing of Environment*, **112(11)**, pp. 4009-4019, 2008.

[37] Rashid, I. and Romshoo, S.A., Impact of anthropogenic activities on water quality of Lidder River in Kashmir Himalayas. *Environmental monitoring and assessment*, **185(6)**, pp. 4705-4719, 2013.

[38] Shen, L., Xu, H. & Guo, X. Satellite remote sensing of harmful algal blooms (HABs) and a potential synthesized framework. *Sensors*, **12(6)**, pp. 7778-7803, 2012.

[39] Stumpf, R.P. and Tomlinson, M.C., *Remote sensing of harmful algal blooms. In Remote sensing of coastal aquatic environments*, Springer: Dordrecht, pp. 277-296, 2007.

[40] Trescott, A., Remote Sensing Models of Algal Blooms and Cyanobacteria in Lake Champlain. Environmental & Water Resources Engineering Masters Projects. University of Massachusetts Amherst. Paper 48., 2012.

[41] Vilmi, A., Karjalainen, S.M., Landeiro, V.L. and Heino, J., Freshwater diatoms as environmental indicators: evaluating the effects of eutrophication using species morphology and biological indices. *Environmental monitoring and assessment*, **187(5)**, pp. 243, 2015.

[42] Winarso, G. and Ishizaka, J., Validation of cochlodinium polykrikoides red tide detection using seawifs-derived chlorophyll-a data with nfrdi red tide map in south east korean waters. *International Journal of Remote Sensing and Earth Sciences (IJReSES)*, **14(1)**, pp. 19-26, 2017.

[43] Yadav, S., Yamashiki, Y., Susaki, J., Yamashita, Y. and Ishikawa, K., Chlorophyll estimation of lake water and coastal water using landsat-8 and sentinel-2a satellite. International Archives of the Photogrammetry, Remote Sensing & Spatial Information Sciences, 2019.

[44] Zi, J., Pan, X., MacIsaac, H.J., Yang, J., Xu, R., Chen, S. & Chang, X. Cyanobacteria blooms induce embryonic heart failure in an endangered fish species. Aquatic Toxicology, **194**, pp. 78-85, 2018.

[45] Zimba, P.V., Khoo, L., Gaunt, P.S., Brittain, S. and Carmichael, W.W., Confirmation of catfish, Ictalurus punctatus (Rafinesque), mortality from Microcystis toxins. *Journal of Fish Diseases*, **24(1)**, pp. 41-47, 2001.

[46] Zhang, F., Li, J., Shen, Q., Zhang, B., Tian, L., Ye, H., Wang, S. and Lu, Z., A soft-classification-based chlorophyll-a estimation method using MERIS data in the highly turbid and eutrophic Taihu Lake. *International Journal of Applied Earth Observation and Geoinformation*, **74**, pp. 138-149, 2019.

AIR AND WATER POLLUTION 2022

OVERVIEW

With the main objective to preserve our delegates' wellbeing, but also with the belief that the international contacts among the scientific community should not be stopped, WIT decided that this conference should not take place as scheduled in Milan, Italy, but take place as an online event instead.

The conference was organised by the Wessex Institute, UK, represented by Professor Stefano Mambretti, a member of WIT Board of Directors, the Polytechnic of Milan, Italy and the University of the West of England, UK.

This conference was the merging of two successful events organised by the Wessex Institute, the International Conference on Modelling, Monitoring and Management of Air Pollution which started in Mexico in 1993; and the International Conference on Monitoring, Modelling and Management of Water Pollution which originated in Southampton, UK in 1991.

The meetings in the Air Pollution series have discussed and considered many important air pollution issues and the international nature of the attendees has ensured that the conference findings and conclusions enjoy wide and rapid dissemination amongst the air pollution science and policy communities.

The Water Pollution conference series has provided a forum for discussion amongst scientists, managers and academics from different areas of water contamination.

OPENING OF THE CONFERENCE

The conference was opened by Professor Stefano Mambretti, a member of the WIT Board of Directors, who welcomed the delegates to the event.

INVITED SPEAKERS

There were a series of invited lectures on advanced topics of research and applications, as follows:

"Estimation of atmospheric boundary layer values in the context of the daily prediction of PM10 air pollution" P. A. Kowalski, M. Kusy, M. Szwagrzyk & J. Izodorczyk

"Assessment of cumulus parameterization schemes in modeling meteorology associated with an air pollution event in the Andean region of Ecuador" R. Parra

"Comparison of Gaussian and Lagrangian puff dispersion models for the risk assessment of receptors nearby a contaminated site" M. Ravina, I. Verginelli, R. Baciocchi & M. Zanetti

"Diffusion of innovation - implementation of constructed wetlands in the Kathmandu Valley, Nepal" Z. Boukalova, J. Tesitel & B. D. Gurung

"Hydrochemical and radiometric study of groundwaters from Serra Negra spa, São Paulo State, Brazil" P. D. Avona & D. M. Bonotto

"Public perceptions of the role and competency of government to deal with water-related issues over a 34-year period in the Pacific Northwest, USA" Robert L. Mahler

"Evolution of the activates sludge community of a WWTP with industrial discharges" A. Baeza-Serrano, F. Sempere, N. Oliver, P. Gutierrez & G. Fayos

CONFERENCE SESSIONS

The papers presented during the conference were classified under the following headings:

- Atmospheric modelling and forecasting
- Health risk assessment
- Global, regional and local studies
- Water treatment

PRIGOGINE AWARD CEREMONIES

During the conference, live presentations of the last three year's Prigogine Award medal took place, as the ceremonies in 2020 and 2021 had to be postponed due to COVID-19.

The 2020 Medal was awarded to Professor Diederik Aerts from Belgium, who gave a Special Prigogine Lecture "A Quantum Quest. From operational quantum axiomatics to quantum conceptuality, or how to unveil meaning in reality".

The 2021 Medal was awarded to Professor Simone Bastianoni, University of Siena, Italy who gave a Special Prigogine Lecture "A Sustainability Viewpoint for a Post Covid-19 Pandemic Society".

The 2022 Medal was awarded to Professor Robert Gilmore, Drexel University, USA who gave a Special Prigogine Lecture "ThermoDynamics and EcoDynamics".

More information on the Prigogine Award Ceremonies can be found at: https://www.wessex.ac.uk/prigogine-award

Q&A LIVE ZOOM SESSIONS

Conference delegates were invited to participate in two Q&A live zoom sessions which took place on 6th and 7th July 2022. These friendly sessions were a great opportunity for participants to interact with each other and put questions to authors about their papers.

CONFERENCE PUBLICATION

Papers presented at this conference are published in Volume 259 of the WIT Transactions on Ecology and the Environment (Electronic ISSN: 1743-3541). Papers presented at the meeting are available Open Access in the eLibrary of the Wessex Institute (https://www.witpress.com/elibrary) from where they can be freely downloaded by any interested parties.

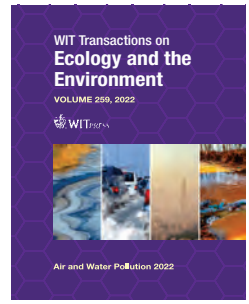

CLOSING OF THE CONFERENCE

We are very sorry that we were not able to meet our delegates in person this time, but hope that we will be able to do so at a future event.

Air and Water Pollution XXX

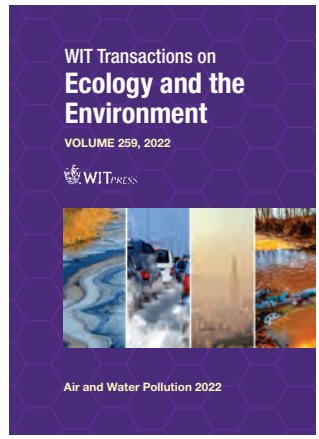

***EDITORS: S. MAMBRETTI**, Polytechnic of Milan, Italy and Member of WIT Board of Directors and **J. LONGHURST & J BARNES,** University of the West of England, UK*

The merger of two successful events to form the 30th International Conference on Modelling, Monitoring and Management of Air and Water Pollution provided the papers that are published in this volume.

Many important air pollution issues are discussed, demonstrating the widespread nature of the air pollution phenomena and the in-depth exploration required to address their impacts on human health and the environment.

The scientific knowledge derived from well-designed studies needs to be allied with further technical and economic studies in order to ensure cost-effective and efficient mitigation. In turn, the science, technology and economic outcomes are necessary but not sufficient. The outcome of such research needs to be contextualised within well-formulated communication strategies that help policymakers and citizens to understand and appreciate the risks and rewards arising from air pollution management.

In addition, the topic of Water Pollution is discussed in a number of contexts across different areas of water contamination.

The environmental problems caused by the increase of pollutant loads discharged into natural water bodies requires the formation of a framework for regulation and control. This framework needs to be based on scientific results that relate pollutant discharge with changes in water quality. The results of these studies allow the industry to apply more efficient methods of controlling and treating waste loads, and water authorities to enforce appropriate regulations regarding this matter.

Environmental problems are essentially interdisciplinary. Engineers and scientists working in this field must be familiar with a wide range of issues including the physical processes of mixing and dilution, chemical and biological processes, mathematical modelling, data acquisition and measurement, to name but a few. In view of the scarcity of available data, it is important that experiences are shared on an international basis. Thus, a continuous exchange of information between scientists from different countries is essential.

WIT Transactions on Ecology and the Environment, 259

ISBN: 978-1-78466-467-1 **eISBN: 978-1-78466-468-8** **Published 2022 / 174pp**

Subscription Order Form

Subscribe to receive your 2023 quarterly issues of the **International Journal of Environmental Impacts,** or purchase individual copies in printed format.

Complete this form, or alternatively visit: **www.witpress.com/journals**.

❑ Subscription - This journal is issued quarterly at the subscription rate of **US$950.00**

❑ Purchase individual copies at **US$300 each** (free P&P). Please send me the following:

Volume:..... Issue: ..... Quantity:..... Total: .....

Method of payment

❑ I am enclosing a **cheque** for:..... (Payable to 'WIT Press Ltd')

❑ I am making a **direct transfer** to Natwest Bank plc.,
Bank Account Name: Computational Mechanics International Ltd
BIC/Swift Code: NWB KGB 2L Bank Sort Code: 53-81-23.
Account: $ US Dollar 140-02-10366067
IBAN: GB83NWBK60730110366067

❑ I wish to pay by **credit card** ❑Mastercard ❑Visa ❑American Express

Card Number:..... Expiry Date: .....

Credit Card Security Code: (3 digit number printed on card signature strip):.....

Signature: ..... Date: .....

Your Details

Please quote your VAT number (EC Countries only): .....

Name: .....

.....

Position: .....

Organisation: .....

Address: .....

.....

RETURN ADDRESS

Please return this form to: **Lorraine Carter**, WIT Press, Ashurst Lodge, Ashurst, Southampton, SO40 7AA, UK. Tel: +44 (0) 238 029 3223 Fax: +44 (0) 238 029 2853
E-mail: lcarter@witpress.com

Customers in the USA, Canada and Mexico please return your order form to:
Linda Ouellette, Customer Service Manager, WIT Press, 25 Bridge Street, Billerica, MA 01821, USA. Tel: +1 978 667 5841 Fax: +1 978 667 7582 E-mail: infoUSA@witpress.com

THE KNOWLEDGE CENTRE
of The Wessex Institute of Technology
The essential gateway to the latest scientific research

The Knowledge Centre of the Wessex Institute of Technology provides information on the latest scientific and technological research through a series of locations detailed below.

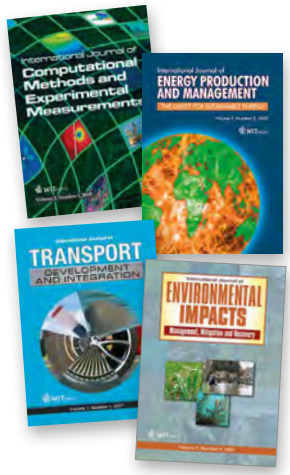

International Journals www.witpress.com/journals

The following journals are published by WIT Press:

- International Journal of Computational Methods and Experimental Measurements
- International Journal of Energy Production and Management
- International Journal of Transport Development and Integration
- International Journal of Environmental Impacts

All papers are archived in the above site where they can be accessed by the community.

Transactions of the Wessex Institute
www.witpress.com/elibrary

With nearly 30,000 papers available online, the Transactions of Wessex Institute collection offers a rapid and efficient way for researchers and academics to access the material delivered at the Institute's prestigious conferences.

International Conference Programme
www.wessex.ac.uk/conferences

This site contains information on past and forthcoming international conferences organised by the Wessex Institute of Technology and other associated institutions in many different locations around the world. The meetings provide friendly and congenial means to achieve a high level of interaction amongst the participants. The emphasis is on high quality presentations which are afterwards published in the Transactions of Wessex Institute.

WIT Press Book Store www.witpress.com

This contains books published by WIT Press and written and edited by leading specialists which enable researchers, engineers, scientists and manages to be aware of the latest developments in the field.

The **International Journal of Environmental Impacts** is published by:
WIT Press, Ashurst Lodge, Ashurst, Southampton, SO40 7AA, UK
Tel: 44 (0) 238 029 3223; Fax: 44 (0) 238 029 2853; E-Mail: witpress@witpress.com, http://www.witpress.com
For USA, Canada and Mexico
WIT Press International, 25 Bridge Street, Billerica, MA 01821, USA
Tel: 978 667 5841; Fax: 978 667 7582; E-Mail: infousa@witpress.com, http://www.witpress.com
ISSN: 2398-2659 (on line) and ISSN: 2398-2640 (paper format)

University of Venda
Creating Future Leaders

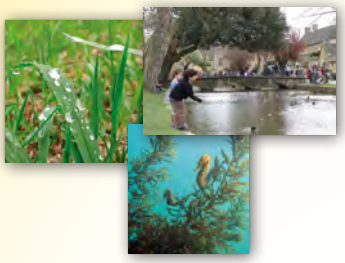

International Journal of
ENVIRONMENTAL IMPACTS
Management, Mitigation and Recovery

CONTENTS: Volume 5, Number 4, 2022

ISSN: 2398-2640 (print)
ISSN: 2398-2659 (online)
Email: witpress@witpress.com
www.witpress.com